2013

Detection of Microorganisms using MALDI and ion mobility mass spectrometry

Juaneka Monet Hayes

Louisiana State University and Agricultural and Mechanical College

Follow this and additional works at: https://digitalcommons.lsu.edu/gradschool_dissertations

Part of the Chemistry Commons

DETECTION OF MICROORGANISMS USING MALDI AND ION MOBILITY MASS SPECTROMETRY

A Dissertation

Submitted to the Graduate Faculty of the
Louisiana State University and
Agricultural and Mechanical College
in partial fulfillment of the
requirements for the degree of
Doctor of Philosophy
in
The Department Chemistry

by
Juaneka Monet Hayes
B.S., Florida A&M University, 2002
M.S., Florida A&M University, 2005
May 2013

ACKNOWLEDGEMENTS

First and foremost, I give glory to God. Without Him, none of this would have been possible. Often times, we set out on a journey and we are met with challenges that are not anticipated. I must say that it is God's will that has gotten my through some of my darkest hours by making a way out of no way. I also thank God for giving me the where with all to embrace who I am, and not be afraid to make mistakes, but, at the same time, know that I will continue to grow throughout this journey called life.

To my husband, Evan, thank you for being you. Your support and words of encouragement have been invaluable during this journey. I look forward to many more years of us growing individually, building a stronger bond together, and adding to our family. Our union has really been blessed and God has blessed us with the most precious gift of all-a healthy and beautiful child. Aven Brielle, you are the most perfect daughter and the best thing to ever happen to me. You are the air that I breathe. From the moment our eyes met, I knew that I would never be the same. You have a personality and sense of humor that is unmatched and every day you show me how to love and teach me so many new things. You are my world and I can't wait to see the woman that you will become. To my mom, Dorothy Starks you have always been my biggest cheerleader, standing on the sideline cheering me on in your special way. There have been so many situations where there may not have been a bridge, but you had the strength and determination to build one. I love watching and listening to the grandmother (Gi-Gi) in you; you are a wonderful grandmother. Now it is my turn to encourage you on this new journey you have decided to undertake. Remember that I am always here for you, no matter what. To my second mom, Aunt Alma, I would like to say a very special thank you for taking me under your wing. Your encouragement, wisdom, and listening ear without judgement have been indispensable. To my siblings: James, Nate, Teka, Tefa, Neal, Tasha, Babycakes, and Sherman your love and encouragement has helped me to become who I am. Teka, we shared a special bond from the beginning and you have always been my protector. Thank you for always being there for me and

TABLE OF CONTENTS

LIST OF TABLES

LIST OF FIGURES

viii

LIST OF ABBREVIATIONS

μL	microliters
μm	micrometers
ATOFMS	Aerosol Time-of-Flight Mass Spectrometer
BIDS	Biological Integrated Detection System
BWs	biological weapons
CDC	Centers for Disease Control
CHCA	α-cyano-4-hydroxycinnamic acid
CID	collision induced dissociation
CMR	Comprehensive Microbial Resource
CNL	constant neutral loss
DART	direct analysis in real-time
DE	delayed extraction
DESI	Desorption electrospray ionization
DTIM	drift-time ion mobility
EI	electron ionization
ELISA	enzyme-linked immunosorbent assay

ESI	electrospray ionization
ESP	electrostatic precipitation
F_2	molecular fluorine
FAB	fast atom bombardment
FAME	fatty acid methyl esters
FCM	flow cytometry
FTIR	Fourier transform infrared
FTMS	Fourier transform mass spectrometer
FWHM	full width at half maximum
GC	gas chromatography
HHA	hand-held immunoassays
IE	ionization energy
IMMS	ion mobility mass spectrometry
IMS	ion mobility spectrometry
IR	infrared
JBPDS	Joint Biological Point Detection System
LAL	*Limulus* amoebocyte assay
LAPS	light-addressable potentiometric pH sensor

LAST	laser ablation sample transfer
LDI	laser desorption ionization
LPS	lipopolysaccharides
LRBSDS	Long-Range Biological Standoff Detection System
LTOF MS	linear time-of-flight mass spectrometer
m/z	mass-to-charge ratio
MALDI	matrix assisted laser desorption ionization
MALDI IM-TOF MS	matrix-assisted laser desorption ionization ion
MB	MALDI Biotyper
MS	mass spectrometry
MS/MS	tandem mass spectrometry
NALDI	nano-structured assisted laser desorption ionization
OPO	optical parametric oscillator
o-TOF	orthogonal time-of-flight
PALMS	Particle Analysis by Laser Mass Spectrometry
PCA	principal component analysis
PCR	polymerase chain reaction
PE	phosphatidylethanolamine

PG	phospatidylglycerol
PLMS	post lift metastable suppressor
PSD	post-source decay
Py-GC-IMS	pyrolysis gas chromatography ion mobility mass spectrometry
PYMS	pyrolysis mass spectrometry
RMIDb	Rapid Microorganisms Identification Database
SEM	Scanning electron microscopy
TIS	timed ion selector
TMAH	tetramethylammonium hydroxide
TMH	thermal hydrolysis methylation
TOF	time-of-flight
TWIMS	traveling wave ion mobility separation
UV	ultraviolet
VBNC	viable but non-culturable
VUV	vacuum ultraviolet

ABSTRACT

Matrix-assisted laser ablation desorption ionization (MALDI) and ion mobility (IM) MALDI mass spectrometry (MS) were used for the detection and identification of microorganisms. MALDI MS is an analytical tool that separates ions by their mass-to-charge ratio (m/z) and is routinely used for bioanalysis because of its sensitivity, selectivity, general applicability, and tolerance to impurities. Ion mobility is a gas phase technique that separates ions based on their charge and collision cross-section. In this research, MALDI-TOF MS and MALDI-IM-TOF MS analysis were conducted in parallel to assess the effectiveness of MALDI-IM-TOF MS for microorganism identification. Whole cell bacteria *Escherichia coli* and *Bacillus subtilis* were prepared and analyzed using both MALDI-TOF MS and MALDI-IM-TOF MS. The signals from both analysis methods were identified using a microbial database. Vacuum ultraviolet (VUV) post-ionization MALDI-IM-TOF MS was also used and additional peaks that could not be detected using MALDI-TOF MS and MALDI-IM-TOF MS were observed from *B. subtilis*. MALDI MS was used in combination with mass spectral fingerprinting software for the identification of whole cell bacteria in the presence of potential environmental interferents. Whole bacteria were analyzed in the presence of fumed silica, bentonite, and pollen from *Juglans nigra* (black walnut) at various mass ratios. The effect of the interferents on the identifications of bacteria at the genus and species level was evaluated using the bacteria fingerprinting software MB. The results showed that correct species identification for *E. coli*, could be determined with fumed silica, bentonite, and pollen at a mass ratio of 1:1; whereas, at the same mass ratio, with diesel particulate, only genus identification could be made. Species identification for *E. aerogenes* with fumed silica and pollen at a mass ratio of 1:1 was achieved. Genus identification was determined for *E.aerogenes* with bentonite and diesel particulate. As the mass ratio of the interferent increased, the likelihood of species identification decreased with the exception of *E. aerogenes* with fumed silica and pollen. Under ambient conditions, laser ablation sample transfer using a mid-infrared laser at 2.94 μm

was used to ablate gram-negative and gram-positive *B. cereus* bacterial colony particulate into a solvent droplet suspended above the Petri dish. The solvent droplet containing the captured material was then transferred to a nanostructured-assisted laser desorption ionization (NALDI) target for analysis. Several peaks that were observed in the NALDI spectra of both gram-negative and gram-positive correspond to phospholipid classes, phosphatidylethanolamine (PE) and phosphatidylglycerol (PG). Additional phospholipids diglycosyldiglyceride (DGDG), triacylglyceride (TAG) and a lipopeptide, which are typically found in gram-positive bacteria were observed in the NALDI spectrum of *B. cereus.* Using LAST-NALDI, phospholipids could be identified from both bacterial species without any sample pretreatment.

CHAPTER 1. INTRODUCTION

Microorganism detection, identification, and characterization are of the utmost importance because of their potential adverse effects on human health.[2] Moreover, a major concern is the deliberate use of microorganisms as biological weapons (BWs) especially when dispersed as aerosol particles.[3] The release of anthrax letters in 2001 through the United States Postal Service to media outlets and United States senators increased the awareness of this threat.[4, 5] These incidents exposed our nation's unpreparedness to deal with biological terrorism. As a result, there has been renewed interest in preparedness and the development of detection measures for biological agents. Technologies for this purpose must be capable of rapid detection and identification.

Conventional identification of microorganisms is based on phenotypic or genotypic testing. Phenotypic testing includes culture and growth characteristics, gram-staining, behavior and biochemical patterns.[6] These properties are sometimes unreliable because of variability in culture conditions such as temperature, media, and pH. Genotypic methods are approaches that probe the genetic makeup of the cell including methods such as PCR or any bioassay that requires DNA amplification. Whether genotypic or phenotypic tests are employed, often no single test can be used for an accurate identification. Therefore, a combination of tests must be used for identification confirmation.[7] These methods of identification are time-consuming and laborious and, in some cases, may take several days. This time delay from initial analysis to identification can pose a threat for scenarios ranging from clinical diagnosis to biological attacks. To reduce the risk to human health, rapid and reliable methods of identification are needed.

Matrix assisted laser desorption ionization mass spectrometry (MALDI MS) is an analytical technique that has been used in the detection of high molecular weight molecules.[8] Its speed, sensitivity, and general applicability make it a powerful analytical tool. The use of MALDI MS to characterize biomolecules has been adapted to the characterization of microorganisms for classification

and identification,[9, 10, 11, 12] which can augment phenotypic and genotypic identification methods.[13] MALDI MS is applicable to whole cell or lysed bacteria. MALDI results generated from bacteria are typically free of interferences that may occur from growth medium or contaminants, and are typically dominated by high abundant ribosomal proteins.[9, 14]

There are two general approaches that can be used for bacterial biomarker identification in MALDI: mass fingerprinting and proteomic-based identification. The mass fingerprinting approach compares peaks in experimental mass spectra to a library of reference spectra for a possible identification.[11] Fingerprint libraries have been developed and are fairly simple to use but can be limited by spectral reproducibility. For example, spectra variation can be caused by choice of instrument, matrix, matrix to sample ratio, culture medium, growth conditions, and growth stage.[12] The use of pattern matching algorithms help to minimize the effect of spectral variation associated with fingerprinting and improve identification. In the proteomic approach, proteins are identified and matched to proteins in a database to determine identification.[9, 15]

Although these approaches for the identification of bacterial biomarkers have been demonstrated, the detection of biological agents dispersed as aerosol particles presents several additional challenges.[16, 17, 18] The low concentration of pathogenic material present in a bioaerosol in an ambient environment requires analysis methods that are highly sensitive.[19] Also, bioaerosols are not present as pure samples in the environment: naturally occurring and anthropogenic background aerosols and other biological material may also be present.[17, 18, 20] These issues present a challenge for rapid analysis and positive identification in the presence of complex a background. Field analysis also requires portable or transportable instrumentation that can be operated in harsh environments.

The goal of the research described in this dissertation was to develop methods for microorganism detection and identification that are applicable to analysis of bacteria and collected

bioaerosols using MALDI coupled with time-of-flight mass spectrometry (TOF MS) and ion mobility (IM) orthogonal TOF MS. Microorganisms in this work were selected based on their use as pathogen simulants and because they are well studied by mass spectrometry. This chapter provides an overview of mass spectrometry and methods of ionization. Traditional methods of microorganism analysis and mass spectrometry of microorganisms are also discussed.

1.1 Microorganisms

Microorganisms are single-celled organisms that include fungi, algae, protozoa, and bacteria. Bacteria are the simplest cells and are about one-hundredth the size of a human cell.[21] Bacteria, which are typically a few micrometers (µm) in length, can be found throughout the environment. Typically, they are found in large groups because of their ability to multiply quickly. They have three basic morphologies, such as spirillum (plural, spirilla), rods called bacillus (plural, bacilli), and spheres called coccus (plural, cocci),[21] as shown Figure 1.1.

Bacterial cells are classified as gram-positive or gram-negative based upon their cell wall structure. Both gram-positive and gram-negative bacteria contain peptidoglycan; however, gram-positive bacteria have a cell wall thickness of approximately 20–80 nm compared to 10 nm for gram-negative bacteria.[21] The difference in thickness is due to repeated cross-linking of the glycan strands that encompass the cell of gram-positive bacteria, while gram-negative bacteria are alternately cross-linked. Another important component of the cell of gram-positive bacteria are techoic acids that interlace the peptidoglycan layers, helping to stabilize the cell wall and make it stronger. The exterior cell membrane of gram-negative bacteria is a lipid bilayer that contains lipids, proteins, and lipopolysaccharides (LPS). The LPS consists of lipid A and a polysaccharide chain. Structural
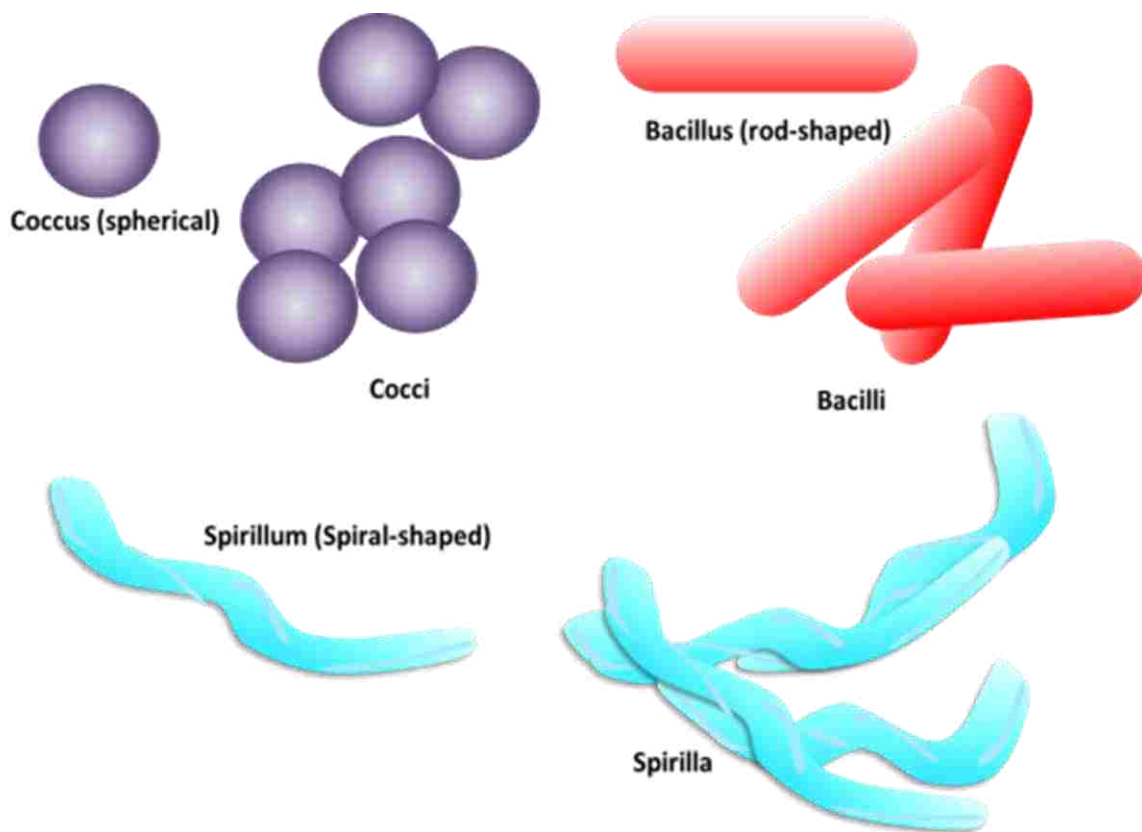
Figure 1.1. Illustration of different shapes of bacteria.

differences in the cell walls in gram-positive and gram-negative bacteria can be easily seen using a microscope and gram-staining dyes.[22] The thicker external cellular wall of gram-positive bacteria retain the primary dye, crystal violet and safranin stains, and gram-negative bacteria shows the counterstain safranin dye.[22] An illustration of gram-positive and gram-negative cells walls is shown in Figure 1.2 (a) and Figure 1.2 (b), respectively.
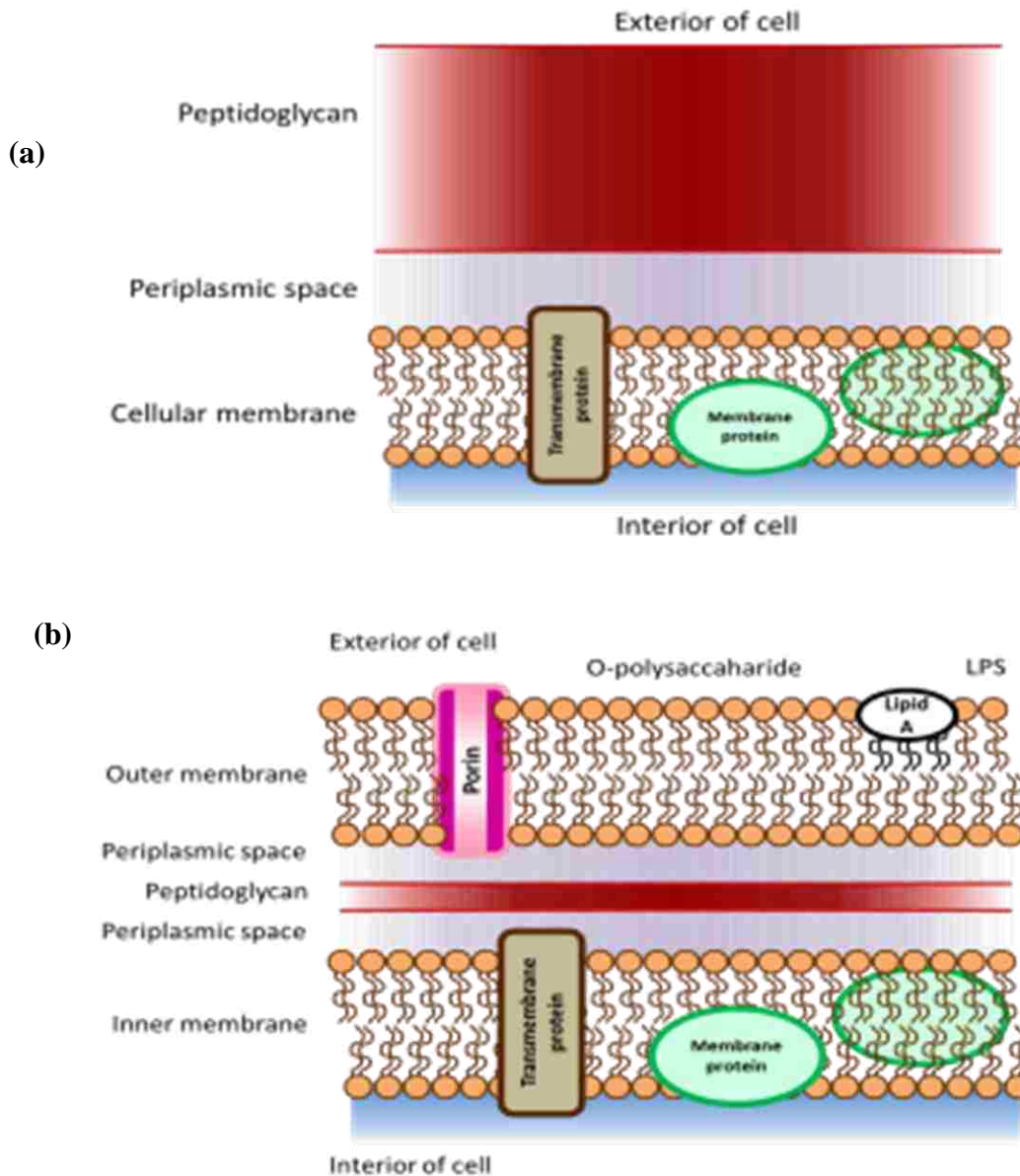
Figure 1.2. Cell of wall of (a) gram-positive bacteria and (b) gram-negative bacteria.

Gram-positive bacteria, including *Bacillus* and *Clostridium,* when in unfavorable environments, undergo a process called sporulation. This process forms spores within the cell (called endospores) as a form of protection.[23] Through this process, the bacterium is able to replicate its genetic material and surround it with a thick coating.[23] In this sporulated form, water is released and metabolism no longer takes place. While in this state, bacteria can survive harsh temperatures, radiation, lack of air, water,

and nutrients for extended periods of time.[23, 24] When conditions become favorable the spore reactivates and returns to its original vegetative state.[24]

Biological Weapons

Microorganisms have been used throughout history as weapons because they are readily available in nature and self-replicating.[25, 26] The military use of biological weapons has been recorded throughout history.[26, 27] For example, in 1495 A. D., Spanish forces contaminated the wine of their French adversaries with blood from leprosy patients.[26] More recently, in Sverdlovsk, a city east of Moscow, at least 100 individuals died from exposure to anthrax spores in 1979.[28] The government of the former Soviet Union blamed the cause of the outbreak on contaminated meat. However, there was considerable skepticism for this explanation. Later in the early 90's, investigations revealed that the anthrax related deaths were the result of an unintentional release from a military facility in Sverdlovsk that was covered-up by the government to keep their bioweapons program a secret. The total number of deaths is unknown, but, based on wind patterns on the particular day of the release, the reported deaths could be traced to where the victims lived relative to the military facility. This event has become known as the Sverdlovsk anthrax leak.

Microorganisms can be dispersed as a bioaerosol, defined as an aerosol of biological origin ranging in size from 0.2 μm to greater than 100 μm.[29, 30] Harmful bioaerosols contain bacteria, bacterial endotoxins, or viruses, and can be used as a biological weapon. These biological agents can be dispersed with aerosol sprayers, pressurized gases, and sometimes with explosives. For greater efficiency, aircraft outfitted with spray tanks, missiles, drones, and small rotary wing vehicles can be used for dispersal. Aerosol dissemination is the most common method because it allows particle size and density to be controlled, which determines an agents effectiveness.[32] Extreme conditions of temperature and pressure associated with explosives can reduce the activity of an agent.[33]

The Centers for Disease Control (CDC) have defined and categorized biological weapons based on their ease of dissemination, transmission and mortality rate, and divided them into categories: A, B and C.[34] Agents in Category A pose the highest threat and are listed in Table 1-1. *Bacillus anthracis* is one of the best-known pathogen on the list. The name *B. anthracis* is derived from the Greek word for coal, *anthrakis*, because of the black skin lesions it causes. In 1876, Robert Koch isolated *B. anthracis*, a pathogenic bacterium, and proved that it was the cause of anthrax acute disease.[35, 36] It is a gram-positive, spore forming bacteria that ranges from 1 μm to 9 μm in length, with a spore size of about 1 μm, and can remain dormant in the environment for several years before being activated.[37, 38]

Table 1-1. CDC Category A Biological Weapons.[1]

Agent	Incubation period	Mortality	Dissemination method
Anthrax (*Bacillus anthracis*)	1-4 days	25-100%	Aerosol
Botulism (*Clostridium botulinum* toxin)	1-3 days	8-50%	Aerosol
Smallpox (*Variola major*)	2-3 days	50-100%	Aerosol
Plague (*Yersinia pestis*)	7-17 days	30-90%	Aerosol
Tularemia (*Francisella tularensis*)	1-10 days	30-40%	Aerosol
Viral Hemorrhage Fevers (Ebola, Marburg, Lass, etc.)	4-21 days	40-90%	Aerosol

The effectiveness and lethality of biological weapons is dependent upon their ability to remain as an aerosol in the environment until inhaled.[39] The size of the biological agent must also be optimized and for maximum dispersion is in the range of 1 μm to 10 μm. To enhance the effectiveness of aerosolized microorganisms, additives called "weaponizing agents" such as fumed silica or bentonite are used.[40] Fumed silica can absorb moisture and easily attach to the surface of larger particles (see Figure 1.3). Bentonite is an absorbent clay that contains aluminum and a high percentage of fine particulate silica. These weaponizing additives attach to the surface of biological agents and inhibit Van der Waals forces and electrostatic interactions, preventing the particles from aggregating which allows them to remain airborne for an extended period of time.
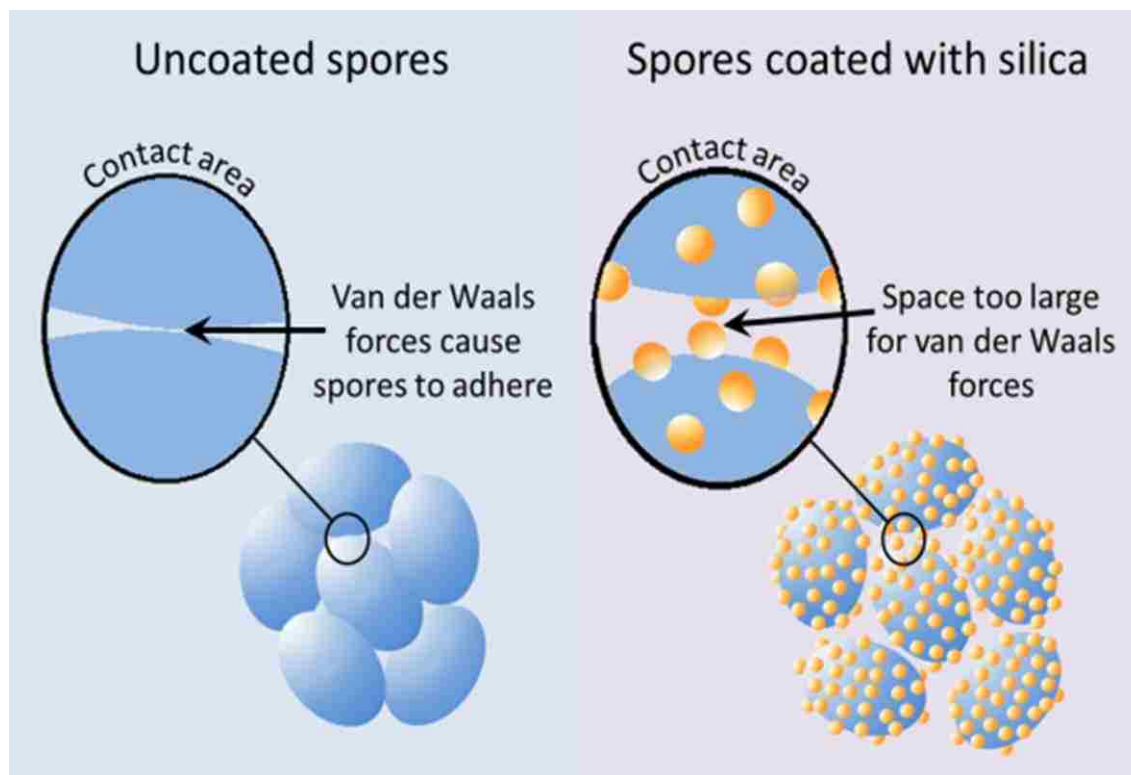
Figure 1.3. Illustration of the effect of van der Waals forces on uncoated particles and particles coated with silica nanoparticles.

8

Currently, the United States Armed Forces use a number of systems that can monitor, detect, and identify pathogenic microorganisms as a network of systems or as independent systems. An early warning system for biological detection is known as the Long-Range Biological Standoff Detection System (LRBSDS) is used to detect and track aerosol clouds.[41, 42] It operates by using an IR laser system mounted in a helicopter for long range detection.[42] The LRBSDS can discriminate between naturally occurring and man-made clouds and can continuously detect the concentration of an aerosol cloud, its location, its size, and path at a distance of up to 50 km.[41, 42] However, it cannot determine the identity of the aerosol in the cloud. The LRBSDS early warning system triggers other biodetection systems such as the Biological Integrated Detection System (BIDS) or the Joint Biological Point Detection System (JBPDS).[41]

BIDS is a mobile biochemistry lab that uses a number of assay methods including immunoassays. It is capable of detecting different types of biological agents in less than 10 min and can simultaneously identify 8 pre-selected agents in less than 30 min.[42] BIDS is composed of a ultraviolet (UV) particle sizer, a liquid sampler, a flow cytometer, and ELISA assays, allowing it operate independently of other biodetection systems. When the particle sizer detects particles in the range of 1 to 10 μm, the sampling device is triggered for collection. The collected sample is then analyzed using luminescence detection with a UV light, ELISA, flow cytometry, and a light-addressable potentiometric pH sensor (LAPS) immunoassay, which uses light to probe the surface of a sample.[42]

The JBPDS is a transportable system that can monitor and identify microorganisms independently in less than 15 minutes.[41, 42] It is similar to the BIDS system but is more automated. It is composed of a cyclone collector/concentrator that collects aerosols in an aqueous solution; a fluid control system that transfers the collected samples between reservoirs, the collector, identification assays, and confirmation sample vials. The system has a biological agent warning system that uses a

9

UV laser to measure elastic scattering and fluorescence to distinguish biological particulate from inorganic particulate. There are identification assays with 10 antibody-antigen reactions for detection and identification of biological warfare agents that can be automatically inoculated and read simultaneously.[42, 43]

The Portal Shield is a point detector that uses disposable, automated hand-held immunoassays (HHA) for biodetection and is typically deployed at airports and ports.[41] The system can simultaneously identify up to 8 biological agents in 20 minutes.[41, 42] Samples are collected and concentrated and deposited on a card that contains immunoreagents on a solid support. If there is a positive response, a red line appears that is read by a laser scanner. However, HHAs have a lower sensitivity and a higher limit of detection when compared to traditional immunoassays, which means that a low concentration biological agent may not be detected. These limitations show the need for further analysis from other biodetection detection systems such as the BIDS and the JBPDS.

1.2 Methods for Detecting Microorganisms

Culture-Based Methods

Traditional methods for microbe identification focus on culturing and morphological studies, enumeration, and biochemical testing.[10, 44]

Culture-based methods are the traditional approach to microorganism identification.[45] Microorganism samples are collected directly from the air, soil, liquid suspensions, filters, biological fluids, or manmade items, and then cultured in growth media under optimum conditions such as temperature, oxygen, and growth time.[29] To characterize bacterial colonies in terms of morphology and number of colony forming units, cultures must be grown on solid or liquid media for 24 hours or more.

Cultures or smears can be directly visualized using optical microscopy. The colonies are inspected under the microscope to examine characteristics in terms of morphology and size. Bacterial smears can be obtained from colonies grown on solid media or from liquid cultures that have been applied to a glass slide and treated with histological stains to be viewed under the microscope.

Scanning electron microscopy (SEM) can also be used to determine shape and surface structures of microorganisms.[46, 47] In SEM, a focused electron beam is directed at the sample and secondary electrons and are used to generate an image as the electron beam is rastered across the surface of the sample[48] to generate an image with a high depth of field and a spatial resolution of a few nanometers.[46, 47]

Although culturing bacteria can be done with relative ease, it has a number of limitations. First, it is important to consider whether the microorganisms of interest are viable or culturable. Here, viable is defined as the ability to grow,[49] whereas, culturable is the ability to produce a population, at a minimum a single colony.[50] Culturable cells are viable but not all viable cells are culturable: those that are not culturable are termed viable but non-culturable (VBNC) because they will not grow to colonies on growth media but are nonetheless alive.[51] It is thought that cells enter the VBNC state as a survival mechanism in response to stimuli such as stress, nutrient deficiency, inappropriate oxygen concentration, and osmotic shock.[51, 52] Pathogenic microbes that can enter a VBNC state include *E. coli*, *Salmonella typhuimurium*, *Francisella tularensis*, *Enterobacter aerogenes, Listeria monocytogenes*, and *Mycobacterium tuberculosis*.[51] Cells in the VBNC state can be revived when conditions become favorable.[51, 52]

Culturing provides enumeration information and is only effective if the microorganisms are viable and culturable under specific growth conditions. It has been reported that fewer than 10% of all microorganisms found in both indoor and outdoor environments are culturable.[53]

11

Non-culture Based Methods

Non-culture based approaches are important because they provide the ability to obtain a true representation of all the microorganisms present in a collected sample. The advances in instrumentation and bioanalytical techniques that allow for direct and indirect analyses of microorganisms are based upon microscopy, flow cytometry, immuonnoassays, polymerase chain reaction and spectroscopic techniques.[29]

Flow cytometry (FCM) is an analytical technique used to count, sort, and measure the physical and chemical properties of cells based upon light scattering and fluorescence.[54] Cells in a fluid stream are irradiated with a laser, causing the cells to scatter light, which is subsequently collected by an array of detectors. Cells can be separated from the total population and sorted for subsequent analysis. FCM can be used to analyze human cells as well as bacterial cells; furthermore, FCM can separate a heterogeneous population of cells. Cells can be analyzed with or without a fluorescent dye. Properties such as cell size, shape and internal complexity can be determined from the intensity of scattered light without fluorescent staining.[54, 55] However, fluorescent dyes or fluorescent probes are needed to differentiate gram negative and gram positive bacteria,[56] identify intracellular and extracellular biomolecules of the cell,[54] determine biological from non-biological material,[54] and separate living cells from dead cells.[57, 58] Typically, 1 mL of the cultured cells is incubated with a fluorescent dye, in some cases up to an hour before analysis.[58] The sample is excited at the UV wavelength at which the fluorescent dye absorbs and is monitored at its emission wavelength. The major advantage of FCM is its ability to analyze thousands of cells within a matter of seconds.[54] Nevertheless, aggregates and debris can give false positives.

Immunoassays are rapid, sensitive, and highly specific and can be used to detect and quantify analytes through antigen-antibody interactions.[59, 60] The detection can be radioactive, colorimetric, or

12

fluorescent.[29] The enzyme-linked immunosorbent assay (ELISA) is a commonly used antibody-based detection method, designed to bind specific antigens.[59, 60] ELISA has been used to target a number of bacterial pathogens including *E. coli:* O157,[61] *Listeria monocytogenes*,[19-21] and *Salmonella*.[62, 63] Although ELISA is sensitive, it is selective, which means there must an antibody with specificity for the antigen for successful analysis.

Polymerase chain reaction (PCR) is a technique that is used to amplify DNA.[64] This technique is conducted by allowing a reaction mixture containing cell lysate, DNA polymerase, nucleotides, and microorganism specific primers (strands of nucleic acid that initiate DNA synthesis) to undergo a number of heating and cooling cycles. During the heating and cooling cycles, the primers anneal to complementary sequences in the DNA of the microbial species. At an optimum temperature, the polymerase enzyme catalyzes the extension of the annealed primer by adding more nucleotides, resulting in a copy of the microbial DNA. Following this step, the cycle of heating and cooling is initiated again, and as the process continues, more copies of DNA are generated. This can be accomplished in 20-80 minutes using commercial PCR systems. There are a number of companies that sell PCR kits for microorganism detection. In particular, the BAX detection system has been developed by Dupont Qualicon for the detection of microbial pathogens such as *Listeria*, *Salmonella*, and *E. coli*: O157.[65] Nevertheless, because of the sensitivity of PCR, false-positives can occur from contamination of DNA from previous PCR and amplification of dead cells.[66]

Raman and Fourier transform infrared (FTIR) spectroscopy can be used to detect and identify whole cell microorganisms and cell isolates.[67, 68, 69, 70] Raman studies provide structural information obtained from vibrations associated with chemical bonds (e.g. carbon backbone), while structural information from IR studies is achieved from vibrational absorption of functional groups (e.g. those of amino acids); the two techniques, thus, can provide complimentary information.[71] FTIR has the ability to probe molecular structure and molecular environment of microbial cells. A sample is irradiated with

an infrared source and functional groups in the molecule absorb the radiation, resulting in different vibrational motions such as stretching, torsion, and bending at specific frequencies. FTIR spectra are obtained by detecting changes in absorption band vibrational energy as a function of frequency. The peaks are broad due to contributions from all molecules in the bacteria cell. The wavenumber of the absorbance peaks, peak intensities, and peak width can be used to identify functional groups and cell components.[70] Some of the most common peaks observed from functional group vibrations are attributed to biomolecules such as proteins, fatty acids, nucleic acids, and carbohydrates.[69] However, bands are attributed to biomolecules as well as specific conformational and structural changes, which are difficult to interpret,[55,72] and often require detailed analysis.[70]

When the sample is irradiated in Raman studies, the light is scattered.[73] Unlike IR absorption analysis, Raman spectra typically have narrow peaks that are well separated and are not affected by interference from water, water vapor or carbon dioxide; water is a weak Raman scatterer and gases do not scatter well.[74] This simplifies sample preparation because aqueous samples can be analyzed as well as solvents that may contain carbon. Using IR and Raman techniques in tandem, microbial cells can be classified and identified by the spectroscopic fingerprint of their intracellular components.[69] Although both techniques require minimal sample preparation, the preparation methods must be followed for reproducible results because the results can be affected by impurities.[69]

Mass spectrometry (MS)[9, 10] and ion mobility (IM)[75, 76] spectrometry are general gas phase techniques that have been used to investigate biomolecules. Both techniques are sensitive and have low detection limits and their generality makes them easily applicable for the detection, identification, and characterization of microorganisms. The results of these techniques are spectra with a number of different peaks that can be attributed to biomolecules. The application of MS and IM for the analysis of microorganisms is the focus of this work. A review of both techniques for microorganism analysis is given below.

1.3 Mass Spectrometry for the Analysis of Microorganisms

Mass spectrometry is an analytical technique that has the ability to separate ions based on their mass-to-charge ratio (*m/z*),[77] which can be used to determine the molecular weight and provide structural information for chemical and biological compounds. It is applicable to nearly all analytes: volatile, nonvolatile, polar, nonpolar, solid, liquids, and gases. MS has become routine for bioanalysis because of its sensitivity, high mass accuracy, and high-throughput capabilities. It is an effective tool for biomolecule identification, elucidating structure and function relationships, and revealing biological pathways and processes.

In an early study of microorganisms by mass spectrometry, Meuzelaar and Kistemaker utilized curie point pyrolysis in combination with electron ionization (EI) and a scanning quadrupole mass spectrometer to demonstrate a rapid and reproducible method for microorganism fingerprinting.[78] Their investigation showed the reproducibility of two successive experiments using *Neisserria sicca*. A total of 30 peaks in range of 12 *m/z* to 48 *m/z* were observed. The results showed that the peak ratios deviated by less than 4% and it was also determined that peaks at *m/e* 18, 28, and 44 were background. A further analysis was conducted with *Neisserria meinigitides* (group C) and *Leptospira* to show that different bacterial strains show different spectral fingerprints. However, the researchers did acknowledge the limitations of this technique were due to the fragmentation caused by EI.

Initially, most MS methods for microbial analysis employed heating of whole cell microorganisms or extracts for sample introduction. Since then the use of mass spectrometry for the analysis of microorganisms has continued to grow, using a number of different approaches for sample preparation, ionization, and mass analysis. The following sections describe different approaches to MS analysis of microorganisms and include detailed discussions of MALDI MS and IMMS.

Pyrolysis Mass Spectrometry

In pyrolysis mass spectrometry (PYMS), samples undergo rapid thermal degradation (pyrolysis) prior to mass separation.[79] Samples are typically heated in a quartz sample tube or direct contact with a platinum wire. The weakest bonds in molecules break due to pyrolysis, producing smaller fragments (pyrolyzates) that give the structural information that can be obtained from the mass spectrum. The pyrolysate expands into a heated chamber and then diffuses into the ionization region of the mass spectrometer and is ionized by chemical or electron ionization.[11, 80]

PYMS is commonly used to identify the lipid profile of fatty acid methyl esters (FAME) of microorganisms.[81] The plasma membrane of microorganisms is composed of phospholipids, which have polar head groups and hydrophobic tails. Extraction with methanol and acid is used to separate the membrane from other cellular material. The phospholipid head groups and fatty acid tails are then separated from one another by esterification before mass analysis. In an example of this approach, Voorhees and co-workers used PYMS to detect four whole cell bacterial pathogens.[82] An *in situ* thermal hydrolysis methylation (TMH) technique was used by mixing the bacterial cells with a methylating reagent, tetramethylammonium (TMAH), on the pyrolysis element (wire, coil, foil, or frit). The mixture was pyrolyzed at temperatures from 200 to 300 °C. The lipid profiles of the four pathogenic bacteria were generated and compared to PYMS and gas chromatography (GC) analysis of FAME extracts from bacterial cells from previous studies.[81, 83] The advantage of PYMS with *in situ* TMH is a sample preparation time of less than a minute, whereas, sample preparation time for methylation prior MS and GC is one hour.

PyMS can be used as an off-line or on-line technique that can be coupled with various separation methods and detectors.[84, 85] Online methods using PyMS can be used to analyze bioaerosols containing a single bacterium.[84] GC coupled with PyMS has been used for the identification of

16

biomarkers of viruses, protozoa, bacteria, algae, and fungi.[80] Lipid and protein biomarkers were observed from the *Brucella noetomae* species when investigated using high resolution MS and tandem MS with pyrolysis.[86] The differentiation of potential bioterror agents from benign substances has also been demonstrated using PyMS.[87] Most recently, a pyrolysis gas chromatography ion mobility mass spectrometry system (Py-GC-IMS) was used to detect and classify bacteria, viruses, and proteins generated during field analysis exercises.[85] PyMS has a number of advantages such as high temporal and spatial resolution, small sample quantities, and rapid analysis.[88]

Fast Atom Bombardment Ionization

Fast atom bombardment (FAB), a desorption ionization method, was introduced in the early 1980s by Barber and co-workers.[89] This technique can provide molecular weight and structural information of organic, inorganic, and small biological molecules. In FAB, the analyte is prepared by dissolving in a polar, inert liquid matrix.[90] This mixture is then bombarded with a high-energy beam (2 – 10 keV) of Xe atoms or Cs^+ ions. The ionization mechanism for this method is thought to occur from ions formed in the liquid matrix and subsequent acid-base and electrochemical reactions. Ion fragmentation is typically species specific, and also driven by association and dissociation reactions with the matrix ions. Fenselau and coworkers were able to differentiate three gram-positive and three gram-negative bacteria species using positive and negative mode FAB MS.[91] Lipids were extracted from each species using a mixture of methanol and chloroform. The extracted lipid suspensions were then mixed with liquid matrices diethanolamine and thioglycerol and analyzed using a magnetic sector mass spectrometer. Phospholipids and other polar lipids were observed and identified. Phosphatidylethanolamine (PE) and phospatidylglycerol (PG) are dominant lipid species in gram-negative and gram-positive bacteria and this was reflected in the mass spectra.

Later, Fenselau and coworkers used positive and negative mode FAB with tandem MS with constant neutral loss (CNL) for the analysis of lysed bacterial cells to determine if greater selectivity for polar lipids and specificity for particular phospholipids classes could be achieved.[92] CNL is a scanning technique that can determine precursor ions by detection of the product ions corresponding to a particular neutral loss. Here, PE and PG dominated the spectra of both gram-negative and gram-positive bacteria. Results showed that bacterial species could be determined using CNL scans with positive mode FAB and suggested that the CNL approach also increased the specificity for phospholipid classes.

Laser Desorption Ionization

Laser desorption ionization (LDI) uses a pulsed laser to rapidly heat a sample deposited onto a surface and generate ions.[90] Typically, a UV laser is used but IR lasers can be used as well. Quadrupole, magnetic sector, time-of-flight (TOF), and Fourier transform mass spectrometer (FTMS) mass analyzers all have been used for LDI; however, the TOF is the best suited because the laser pulse serves as a convenient start for the ion flight time. In general, samples are prepared from about 10^{-6} to 10^{-3} M solutions and are allowed to either air dry on the target or samples can be electrosprayed onto the target and analyzed.[93] LDI has a number of advantages including good spatial resolution and low sample consumption; however, this technique is generally limited to small molecules with masses of less than a few thousand Da.[94, 95, 96]

Microorganisms have been detected in the presence of background aerosols using UV and IR LDI with TOF MS.[97] A custom made IR optical parametric oscillator (OPO) was used in the range of 3.05 μm to 3.08 μm to study spores from four closely related bacillus species: *B. subtilis, B. niger, B. cereus,* and *B. thuringiensis*. The wavelength dependent study showed that 3.05 μm gave the best

results in signal intensity. Based on the spectra of each species, it was determined that *B. subtilis* and *B. niger* spores are closely related *and B. cereus* and *B. thuringiensis* spores are closely related. However, the four species of *Bacillus* could be differentiated by different lipopeptides observed near 1000 *m/z*, which appear to be species specific.[97] Background aerosols, such as Arizona road dust and pollen, that are typically encountered when sampling aerosolized microorganisms were also investigated to determine whether *B. subtilis* could be differentiated from background particulate. The spectra of the background aerosols did not show any spectral similarities to *B. subtilis*, which makes it easy to differentiate the background aerosols from *B. subtilis*.

Phospholipids have also been detected from lyophilized and extractions of *E. coli* cells using LDI with an IR CO_2 laser.[98] Results from this work showed that this technique is selective for phospholipids and can be used to determine phospholipid profiles of bacterial species.

Matrix-assisted Laser Desorption Ionization

The development of soft ionization methods such as MALDI MS allows the analysis of intact biomolecules. MALDI methods used for the analysis of biomolecules have been tailored for microbial analysis and have been demonstrated by a number of groups.[9, 99, 100, 101] It is attractive because of its low detection limit and tolerance of impurities. Mass spectra generated from microbial samples are easy to interpret and peaks are typically attributed to proteins, unless extraction methods or enzymatic digestion methods are employed. When investigating whole cell bacteria, the focus for bacterial protein biomarkers is in the 4,000 to 20,000 *m/z* range.[102,9, 10] In this mass range, most identifications are based on highly abundant ribosomal proteins and other abundant proteins, which tend to dominate bacterial mass spectra.[9, 10] The masses obtained from MALDI spectra are compared to a reference library for identification in what is called the fingerprint approach. Reproducibility of spectra of intact

microorganisms can be influenced by growth media, growth time, choice of matrix and sample preparation methods including, choice of solvents, and sampled deposition methods, which can make identification difficult.[103]

The challenge of analysis has been met through the use of algorithms that can perform peak matching analysis based on m/z and intensity,[104] and by spectral libraries that account for spectral reproducibility.[105, 106] The use of database searches for microbial identification was first reported by Reilly and co-workers and shortly thereafter by Wahl and co-workers.[104, 107] In these approaches, microorganisms are cultured using different conditions and analyzed on different days. Several spectra are collected for each microorganism and for each culturing condition. These spectra are then averaged to give a representative spectrum and are added to the reference library. Unknown spectra are compared to spectra in the reference library using a pattern-matching algorithm. For example, Jarman *et al.* performed this type of analysis with 3 three microorganisms by collecting a total of 60 mass spectra of each microorganism grown on different culture media on different days.[105] Peak tables were constructed for each growth condition and peaks with a m/z within a given standard deviation were calculated to give an average m/z. Peaks that were observed in more than 70% of the 60 collected spectra were included. Unknown spectra were compared to the reference library and 100% of the unknowns were identified, despite the use of different culture media.

Another approach to bacterial identification is the use of sequence databases to match observed protein or peptide masses that can be related to known proteins.[9, 108] Proteomic tools, such as bioinformatic databases, are used with algorithms to compare and rank the m/z of the experimentally obtained peaks to protein and peptide masses in the database,[109, 110] which has the advantage of being independent of ionization methods, mass analyzer used, and growth conditions.[111, 112, 113, 114] A given m/z within a given error range, determined by the user, must be input. Demirev *et al.* were the first to report the use of bioinformatic databases for the identification of microorganism biomarkers.[111] A

SwissProt/TrEMBL database was used to match 16 observed protein masses from a MALDI TOF MS spectrum of a mixture of *E. coli* and *B. subtilis*. The error range for the search, determined by the user, was ± 3 to ± 5 *m/z* and was limited to bacterial species only. It was found that 6 peaks were assigned to *E. coli,* 4 peaks were as assigned to *B. subtilis,* and 5 peaks were attributed to both species.

A commercial database, MALDI Biotyper (MB), is a microbial database that was developed for bacteria identification.[14] MB uses a mass spectrum pattern-matching algorithm. MALDI TOF MS with MB was designed as a routine diagnostic tool in clinical laboratories[100, 115, 116, 117] and can be run in parallel with conventional phenotypic methods.[116, 118] It serves as a rapid tool for the diagnosis of bacterial infections. Szabados and co-workers evaluated MB by testing more than 600 antibiotic-resistant and antibiotic-susceptible *Staphylococcus aureus* strains and a collection of over 400 other staphylococci.[101] Prior to MALDI analysis, isolates were first identified using colony morphology, agglutination test (bacteria cells clumping together in the presence of an antibody), and PCR for the *mecA* gene or a commercially available kit that uses substrate binding for identification. All *Staphylococcus aureus* strains were identified correctly at the species level. On average, 180 identifications were obtained in 22 minutes using MB, whereas PCR results and commercial kits took an average of 2.5 hours. It was concluded that MALDI-TOF MS with Biotyper is faster than conventional molecular methods, but was more time-consuming than agglutination testing. However, the authors stated that in their laboratory, MB would likely be used as a secondary identification tool when results are inconclusive.

Not all studies yield a high identification rate when using MS. For instance, 109 isolates of the *Acinetobacter* species, a well-known gram-negative bacteria that causes hospital acquired infections, was investigated using MALDI-TOF MS with MB and PCR for rpoB gene sequence molecular identification.[100] PCR was used as a conformation tool for the identification results. At the genus level, all of the isolates were identified correctly, but 31 samples were misidentified at the species level using

MB. The authors attributed most of these errors to the limited number of *Acinetobacter* species present in the database.

Ambient Ionization

Ambient ionization is the formation of ions external to the mass spectrometer in an ambient environment with minimum or no sample treatment.[119] Ions are introduced or extracted into the mass spectrometer. Mass spectrometers can easily be modified by attaching an external source to generate ions to be extracted into the mass spectrometer.

Desorption electrospray ionization (DESI) is an ambient ionization technique that is applicable to small organic compounds and large biomolecules that can be solids, liquid samples and even frozen solutions.[120-] In DESI, an electrospray of solvent charged droplets hits the surface of a sample, the solvent extracts the sample molecules, and the impinging pneumatic spray shears off charged droplets that go on to form ions by evaporation of the solvent.[121] Spectra recorded using DESI, are similar to ESI spectra.[122, 123] DESI has been used for a wide range of application including tissue imaging,[124, 125] environmental monitoring,[126, 127] thin layer chromatography,[128, 129] polymers,[130] and microorganism analysis.[130]

Direct analysis in real-time (DART), another ambient ionization technique, was introduced shortly after reports of DESI.[131] Ionization occurs by directing a heated plasma of excited-state ions at the sample that ionizes low molecular weight molecules.[123] DART is limited to small molecules because it is based on chemical ionization.[122, 123] It has wide applicability in forensics,[132] drug discovery,[133] and microorganism analysis.[134]

Recently, both DESI and DART have been added to the range of MS techniques to detect microorganisms.[134, 135, 136, 137, 138] DESI and DART allow microorganisms to be detected from a surface

with no sample pretreatment, which is ideal for a rapid detection and identification tool, especially for field analysis.[136] Using DESI, individual 1 mL suspensions of cultured cells of three strains of *Escherichia coli* and two strains of *Salmonella typhimurium* were deposited on a glass slide.[136] A mixture of methanol and water was electrosprayed onto the glass slide to extract the sample into the mass spectrometer. Mass spectra were reproducible and lipids observed from both *Escherichia coli* and *Salmonella typhimurium* were identified as phosphatidylethanolamine (PE).[136] The two species could be distinguished by the presence of three peaks observed in the spectra of S. *typhimurium* that were not present in the spectra of *E coli.* Differences in the strains of *E. coli* and *S. typhimurium* could not be observed by evaluating their mass spectra directly but was realized with the use of principal component analysis (PCA).

DART has been used with TOF MS to observe fatty acid methyl ester (FAME) mass spectra generated from hydrolized and methylated suspensions of whole cell bacteria of *E. coli*, *Coxiella burnetii*, and *Streptococcus pyogenes*.[134] The fatty acids were all detected as protonated methyl esters with a total analysis time of 9 minutes. Similar results were observed for the spectra of *E. coli* and *Coxiella burnetii,* both with FAME series of fatty acid moieties with 9 carbons and no double bonds (C9:0) to 19 carbons with 1 double bond (C19:1). However, distinguishing features such as C19:0 were only present in *E. coli* and C11:1 was only found in *S. pyogenes.* The two strains of *C. burnetii* were distinguishable by differences in their mass spectra.

1.4 Methods for the Detection of Bioaerosols

A number of techniques and methods have been developed for the detection and analysis of bioaerosols. The ideal sampling device for harmful bioaerosols will be transportable and capable of measuring 10^4 particles per cubic meter at a rate of hundreds of particles per minute.[139] Nevertheless,

there are a number of sampling methods for bioaerosols such as impaction, liquid collection, filtration, and electrostatic precipitation that are well established and are routinely used for collection. Several mass spectrometry methods can be used to analyze bioaerosols without collection.

Impaction is one of the most commonly used collection methods.[139, 140] This method uses inertial forces to collect particles from the air. Air is drawn through the impaction sampler and forced to change direction; particles whose inertia exceeds a certain value are collected on the surface of the impaction plate.[30, 140] An impaction sampler can be used with multiple impaction plates or a single impaction plate for collection using a number of different targets including solid targets, glass slides, metal targets, and agar growth media.[29, 30] Using agar plates as a collection medium in the sampling device has the advantage of allowing culturing and counting the microorganisms without further sample transfer.[141] However, the drawback of collecting microorganisms on the growth medium is the possibility of the plates becoming overloaded with microorganisms, which can result in colony aggregation, making it difficult to determine the number of colony forming units collected.

An impinger functions on the same principle as an impactor, except particles are collected into a liquid, for example, an isotonic or buffered solution.[29, 139] Single and multi-stage impinger samplers can be used.[29] Although, impinging is an inexpensive and effective sampling method, the liquid can evaporate when sampling for an extended time.[139] Unlike impaction, this method requires further sample processing if the number of microorganisms is to be determined as well as identified.

Filtration is a simple and inexpensive method used in the collection of microorganisms from bioaerosols through a porous membrane filter.[29, 140] The collection efficiency of this method depends on the physical properties of the filter and the particles, as well as the air flow rate.[29] Upon collection, only one filter is used which makes determining the total number of particles and the particle size distribution difficult.[29, 139] Much like the impaction sampler, during filtration the filter can become overloaded with microorganisms, making enumeration difficult.[142] After collection, the material is

usually desiccated or undergoes ultrasonication to retrieve the cells. The recovery efficiency is often poor, especially for vegetative bacterial cells.[142] Filtration is typically used when qualitative information is needed.

An electrostatic precipitation (ESP) sampler electrically charges particles as they enter the sampler, causing them to collect on a solid or liquid surface in the sampler.[139] Solid substrates, such as filters, have the highest recovery efficiency. This sampler causes less physical stress on microbial cells when compared to impaction and impingement, and for this reason recovery efficiencies are higher.

After bioaerosol collection, characterization of bioaerosols can range from simple techniques, such as culturing and microscopy to advanced biochemical and instrumental techniques. With proper sample handling, a number of other techniques used for microorganism detection such as culturing, microscopy, DNA amplification, ELISA, FCM, and MS are applicable to bioaerosol detection.

A commonly used bioaerosol assay is the *Limulus* amoebocyte assay (LAL), which determines the activity of endotoxins, which are only present in the cell wall of gram-negative bacteria.[143] An extract of blood cells taken from the horseshoe crab, *Limulus polyphemus*, reacts with bacterial endotoxins lipopolysaccharide from gram negative bacteria, activating an enzyme in the LAL extract that reacts with a clotting protein to form a gel or a clot (positive reaction) that can be visualized with the naked eye.[143, 144] If gram-positive bacteria are present or any bacteria that cannot produce endotoxins, a clot will not form. Endotoxins have different levels of toxicity, so experimentally measured toxicity levels are compared with the activity of standard endotoxin, *E. coli*.[142] The LAL assay has been used to analyze collected bioaerosols, using a filter and an impinger from a sewage treatment plant to monitor endotoxin exposure of employees.[145] It was found that endotoxin exposure was minimal, but the samples from the filter showed higher concentrations of endotoxins when compared with samples from the impinger.[145] Results from the LAL assays were compared with GC

MS data of collected bioaerosol samples taken from a sewage treatment plant. The level of toxicity found in both investigations was comparable.[145]

Laser Desorption Single Particle Analysis

The ideal aerosol instrument, as defined by McMurry,[146] has continuous measurement of the complete chemistry of single particles, continuous size and time resolution, including particle concentrations, size distributions, morphologies, chemical compositions, densities, refractive indices, and volatilities. Although there is no technique that can perform this task, it has long been realized that MS is ideal for aerosol particle analysis because of its general applicability and high sensitivity.[77] Single aerosol particle analysis using laser desorption ionization was first reported by Sinha in 1984.[147] Particles were irradiated with a Nd:YAG laser and the resulting ions were analyzed with a quadrupole mass spectrometer. The hardware for an aerosol mass spectrometer consists of an aerosol inlet, optional particle detection and sizing, and a mass spectrometer. The first aerosol TOF mass spectrometer instrument was reported by Mckeown and coworkers.[148]

Based on the LDI-TOFMS for single particle analysis, particle mass spectrometers, such as the PALMS (Particle Analysis by Laser Mass Spectrometry) and the ATOFMS (Aerosol Time-of-Flight Mass Spectrometer) were developed.[149] Aerosol particles of oleic acid, NaCl, KCl, NH_4Cl, $(NH_4)SO_4$ and ZnSO4 were irradiated using an excimer laser at 193 nm and mass analyzed in a TOF.[148] However, only particles of a certain size could be analyzed,[150-121] revealing there were a number of limitations in particle sizing that needed to be overcome.[148] Prather and co-workers developed an ATOF MS for on-line analysis of particles from 0.2 to 3.0 μm in diameter.[151] The system utilized a CO_2 laser at 10.6 μm and/or a Nd:YAG laser at 355 nm or 266 nm (third harmonic and fourth harmonic, respectively) for desorption and a reflectron TOF analyzer for mass separation. As proof of concept, initial studies

focused on the aerodynamic velocity of single particles of NaCl, KCl, and Na_2SO_4 as a function of their size. It was noted that the aerodynamic velocity results were comparable to particle studies previously conducted by Sinha.[147, 151] NaCl, KCl, and Na_2SO_4 particles were combined to form a single particle for analysis to determine its aerodynamic velocity.[151]

MALDI MS Bioaerosol Single Particle Analysis

The concept of aerosol analysis has also been applied to bioaerosol analysis because LDI does not provide sufficient information for bacterial identification due to its limited mass range.[84, 152, 153, 154] With the introduction of matrices,[155] aerosolized particles containing large biomolecules could be analyzed by irradiation.[156, 157] Murray and Russell demonstrated the use of MALDI-TOF MS for aerosols of gramicidin S and lysozyme mixed with the matrix 4-nitroaniline.[156] The aerosols were irradiated with a 355 frequency tripled Nd:YAG laser and separated in a linear TOF. Molecular ions of both analytes were detected.[156] Murray and co-workers later demonstrated a 10-fold increase in resolution of aerosolized peptides by utilizing a reflectron TOF and a higher laser pulse energy.[157] Molecular ion peaks and post-source decay (PSD) fragments were observed for bradykinin, angiotensin II, and gramicidin D, while the molecular ion peak of vitamin B_{12} was detected with the loss of CN and a PSD fragment.[157] The resolution of these peptides ranged from 300 to 400,[157] which was subsequently improved with a resolution greater than for 400 for bradykinin, angiotensin II, gramicidin S, gramicidin D and vitamin B_{12}.[158] The maximum molecular weight reported for an aerosol reflectron MALDI-TOF MS was 5734 for bovine insulin.[159] Using a dual polarity linear TOF with a focusing wire to guide higher masses to the detector, a cytochrome c monomer, dimer, and trimer at 12 kDa, 24 kDa, and 36 kDa *m/z*, respectively, were observed from an average of 27 aerosol particles.[160]

Condensation matrix addition MALDI MS was introduced by Stowers *et al.* for the analysis of aerosolized gramicidin S, erythromycin, and *Bacillus subtilis var niger* generated using a Collison nebulizer with matrix added by condensation in a heated saturator.[161] Protonated peaks of gramicidin S and erythromycin were observed while a peak at *m/z* 1224 was observed for the bacterial spores. Tandem electrospray ionization MS was used to further confirm the bacterial spore signal at *m/z* 1224, which is assigned as a fragment of the peptidoglycan layer of the cell. Jackson and Murray compared condensation matrix addition coated aerosolized peptides of gramicidin S and gramicidin D with liquid matrix 3-nitrobenzyl alcohol and without the addition of matrix.[34] It was observed that matrix addition increased the molecular ion peak and resulted in less fragmentation compared to recorded spectra of the peptides that did not employ a matrix. Ion trap mass spectrometry analysis of aerosolized bradykinin, leucine enkephalin, and substance P particles coated with 3-nitrobenzyl alcohol and picolinic acid matrices has also been reported.[22] Each peptide was coated with different size matrix particles. Particle size did not affect signal intensity of the spectra but showed that the sensitivity of this technique increases with smaller particle size. From these investigations, it was determined that the on-line addition of matrix to aerosolized particles, while in-flight, allows real-time analysis of aerodynamically-sized, individual aerosol particles. Analysis of collected particles can lead to loss of particle information due to chemical reactions and evaporation as well as slow analysis times.[162]

Fergenson *et al.* used a dual polarity aerosol TOF MS in real-time to differentiate aerosolized *B. thuringiensis*, and *B. atrophaeus*.[163] Experiments were also conducted to detect these species in the presence of other aerosolized biological material that could potentially be present in the environment, background aerosols (diesel, smoke, dust) and non-biological material such as white powders that could be present in a hoax situation. The ATOF MS spectra of *B. thuringiensis*, and *B. atrophaeus* were identical with the exception of the intensity differences of sodium and potassium peaks in the

spectra. However, *Bacillus* spores were detected in the presence of background aerosols and aerosolized biological and non-biological materials.

1.5 Ion Mobility Spectrometry

Ion mobility mass spectrometry (IMS) is a gas phase ion separation technique based upon the size and shape of ions. Ions are separated in a gas cell in the presence of a weak electric field.[75, 164] The drift velocity is proportional to the collision cross-section, Ω, of the ion in the inert gas.[75] Collisions with the inert gas slows down the ions: those with a large collision cross section encounter more collisions and spend more time in the drift cell.[165, 166] IMS can be used at atmospheric pressure as well as partial vacuum.[75] During its early development, IMS was coupled to analytical separation techniques such as gas chromatography,[167] supercritical fluid chromatography,[168, 169] and liquid chromatography,[170, 171] primarily as a detector for the analysis of volatile compounds.[164, 172, 173, 174, 175, 176, 177, 178, 179] With advances in electronics, it was found that this technique could be used to detect trace impurities.[179] The U. S. military has developed IMS as a hand-held device for chemical warfare agent detection.[179]

Snyder and coworkers used a hand-held IMS detector for the analysis of bacteria.[180] The bacteria was mixed with (o-nitrophenyl)galactopyranoside (ONPG) of its high vapor pressure. Suspensions of *E. coli* cells ranging from 200 to 2000 cells and ONPG were added to the filter paper inside of a sterilized vial and allowed to incubate for 10-30 min at 40-42 °C. The vial was sampled at the IMS inlet and the IMS peak intensities were correlated with the number of bacterial cells. An IMS, with a thermal desorber heated to 300 °C or less, was also used for the analysis of whole cell bacteria.[181] A number of experimental conditions were varied including, temperature and time spent on the thermal desorber and growth media. The spectra varied with experimental conditions, and it was

unclear if peaks in the spectra were the result of intact cells or products of cell decomposition from heating.

Coupling Ion Mobility with Mass Spectrometry

Ion mobility spectrometry combined with mass spectrometry (IMMS) is a useful tool for investigating complex mixtures because of its ability to separate different molecular classes.[75, 182] Coupling IMS with MS is beneficial because a mass analyzer can acquire a mass spectrum in a single scan.[183] ESI and MALDI are ionization sources routinely used for IMMS in bioanalysis; whereas, radioactive ionization, corona discharge ionization, photoionization, and secondary electrospray ionization sources are used for gas phase samples.[75] Mass analyzers routinely coupled to IM cells include quadrupole, ion trap, FTICR, and TOF mass spectrometers.[76] An IMMS instrument is capable of sample introduction, ionization, ion mobility separation, mass separation, and ion detection.[75]

The typical IM cell has two apertures: the first aperture is the entrance aperture where ions are formed in the presence of a background gas (He, N_2, Ar, CH_4) at 1-10 Torr,[183] and the second aperture is the exit of the IM cell, which allows ions to leave the IM cell and enter the mass spectrometer.[75, 183] Ions are first separated by size-to-charge in the drift cell and then separated by m/z in the second dimension. However, IM drift cells suffer from poor sensitivity due to a low duty cycle from ion loss between the sampling aperture and mobility cell due to radial diffusion as well as the IM cell and the mass analyzer.[184] The combination of ion funnels before and after the mobility drift cell has been shown to prevent the loss of ions during transmission.[165, 185, 186] The first funnel is used to accumulate ions and pulse them into the drift cell and the second ion funnel is used to focus radially diffused ions that have been separated in the drift cell.[165, 187]

Detection of Bacteria using Ion Mobility Mass Spectrometry

Recently, Dwivedi and coworkers investigated metabolites from *E. coli* strain W3110 extracts using IMMS with ESI.[188] A total of 500 peaks were found in the mass range of 60 to 600 *m/z* of the IMMS spectrum of *E. coli* strain W3110 extract. To identify metabolites, *m/z* values were correlated with metabolites listed in the *EcoCyc database*, a bioinformatics model database for the bacterium *E. coli* K-12. Using the database, 186 metabolites in the mass range of 70 to 600 *m/z* were assigned. Their work demonstrated that IMMS with ESI can be used for low *m/z* metabolomics studies. This study was followed by the use of MALDI as ion source with IMMS for metabolite studies.[189] Fewer metabolites were detected in the *m/z* range of *m/z* 300 to 1500.

1.6 Research Objectives

The objective of the work presented in this dissertation was to develop methods to detect microorganisms using matrix-assisted laser desorption ionization mass spectrometry (MALDI MS) and ion mobility spectrometry mass spectrometry (IMMS). First, bacterial species were analyzed in parallel using MALDI MS and IMMS. Resulting *m/z* values were correlated with proteins listed in the Rapid Microorganism Identification Database for identification. Bacterial species were also analyzed in the presence of environmental interferents and weaponizing agents. Spectra from these studies were then searched against the Bruker MALDI Biotyper database to determine whether characteristic biomarkers could be identified in the presence of the interferents. Lastly, bacterial cultures were grown and ablated using IR laser absorption sample transfer (LAST) and analyzed using a nano-structured assisted laser desorption ionization (NALDI) target for matrix-free LDI MS.

CHAPTER 2. EXPERIMENTAL

This work was performed using matrix assisted laser desorption ionization (MALDI) coupled with time-of-flight mass spectrometry (TOF MS) and ion mobility mass spectrometry (IMMS) and laser ablation sample transfer coupled with nano-assisted laser desorption ionization (NALDI). A detailed description of each instrument, experimental setup, and databases used for microorganism identification is also presented.

2.1 Mass Spectrometry

Mass spectrometry is an analytical technique that has the ability to separate ions based upon their mass-to-charge ratio (m/z),[77] which can be used to determine the molecular weight and structure of chemical and biological compounds. A mass spectrometer has three basic components: ion source, mass analyzer, and detector as shown in the schematic diagram in Figure 2.1. In the ion source, analyte molecules are converted to gas-phase ions. The ions are separated according to their m/z ratio and are detected. A mass spectrum is a plot of the relative abundances as a function of their m/z.
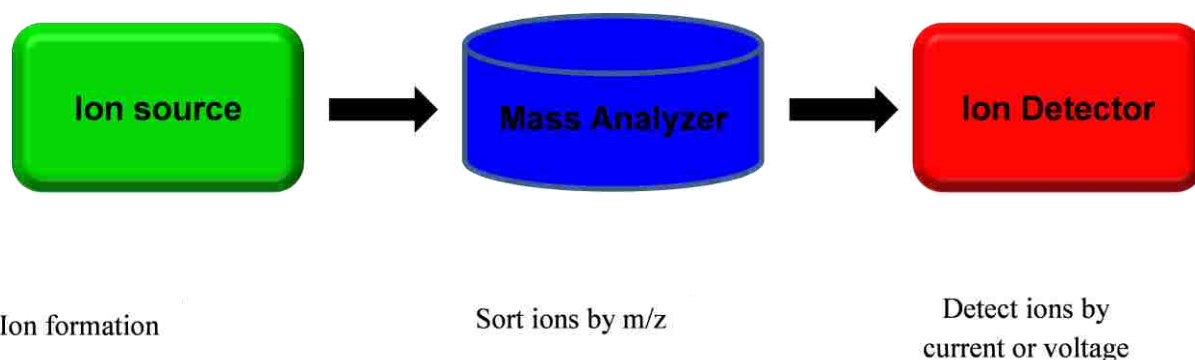
Figure 2.1. Schematic of a mass spectrometer.

2.2 Time-of-Flight Mass Spectrometry

A time-of-flight mass spectrometer is composed of an ion source, an acceleration region, a field-free drift region (also called the flight tube) and detector. The flight time of an ion begins at the point of ionization in the ion source. Ions are formed in the source and are then accelerated in an electric field into a field-free drift region towards the mass analyzer. The acceleration potential, which gives all of the ions the same kinetic energy, propels the ions at different velocities according to their mass and charge. In TOF systems, ion extraction can be axial or orthogonal. In axial extraction, the flight tube is on the same axis as the ion propagation direction and for orthogonal extraction, ions are extracted into a flight tube that is perpendicular to their initial direction of motion.

The time it takes for ions to traverse the field-free drift region can be correlated to the *m/z* of the ions. Because all of the ions with the same charge have the same kinetic energy, low mass ions travel faster than larger mass ions and arrive at the detector first.[90, 190] The length of the flight tube dictates the extent of ion separation. The arrival time of the ions at the detector is dependent upon their mass, *m*, in Equation (1)

$$E_{KE} = \frac{1}{2}mv^2 = zeV, \tag{1}$$

where E_{KE} is the kinetic energy, *v* is the velocity of the ion, *z* is the charge number of the ion, *e* is the electron charge, and *V* is the acceleration voltage. Note that this simple treatment neglects the time spent in the ion source and post-acceleration at the detector. Equation (1) can be rearranged to solve for the velocity of a singly charged ion ($z = 1$) as shown in Equation 2.

$$v = \left[\frac{2eV}{m}\right]^{\frac{1}{2}} \tag{2}$$

Equation (2) can be rearranged to solve for flight time (*t*): where *d* is the length of the field-free drift region of the flight tube, as shown in Equation (3).

$$t = \left[\frac{m}{2eV}\right]^{\frac{1}{2}} d \tag{3}$$

Equation 3 forms the basis of the mass calibration equation

$$m = A \cdot m^{1/2} + B \tag{4}$$

where A and B are empirically determined constants. The functional form of Equation 4 holds when acceleration and post-acceleration are taken into account.[191]

In TOF MS, mass resolution *(R)*, as given by Equation (5),[192]

$$R = \frac{m}{\Delta m} = \frac{t}{2\Delta t} \tag{5}$$

where *m* is the mass of the ion and *t* is the flight time; Δm and Δt are at the full width at half maximum (FWHM) of the mass and time peaks, respectively.

A schematic of a linear TOF MS system is shown in Figure 2.2. In TOF MS, ions are typically accelerated by voltages in the range of 3 kV to 30 kV.[193] The time for ions to reach the detector is a function of mass and is typically in the range of μs. When used with MALDI ionization in axial mode, linear TOF is used for high mass analytes of 10 kDa and greater with applied potentials of 20 kV to 30 kV.[194] The use of high acceleration voltages limits the contribution of the initial ion kinetic energy spread that can decrease resolution.
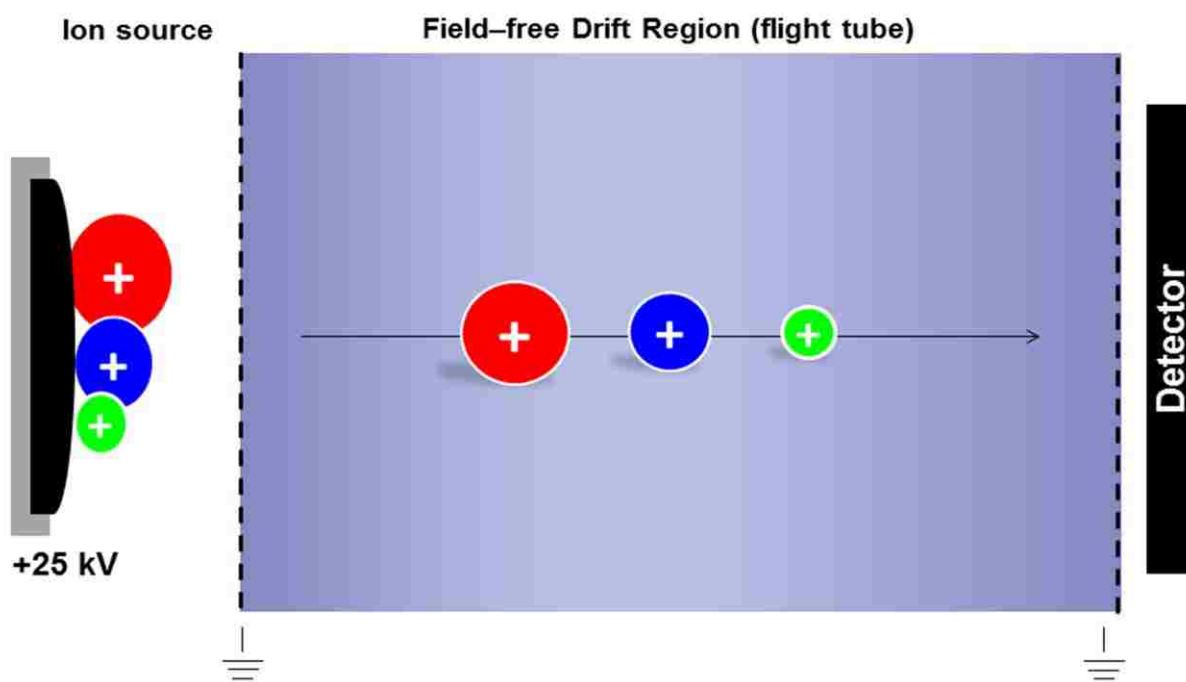
Figure 2.2. Linear time-of-flight mass spectrometer diagram**.**

The resolution of linear TOF MS is affected by the conditions of the ions at the point of ionization such as temporal distribution, spatial distribution, and initial kinetic energy distribution.[193] A spread in temporal distribution arises from ions that have the same mass but are formed at different

times and travel through the drift region at a constant difference in space and time, as seen in Figure 2.3 (a). Spatial distribution occurs when ions of the same mass are formed simultaneously and both have the same initial kinetic energy, but are formed in different locations, as shown in Figure 2.3 (b). Lastly, ions that have different initial kinetic energies have different velocities, and will reach the detector at different times, see Figure 2.3 (c).
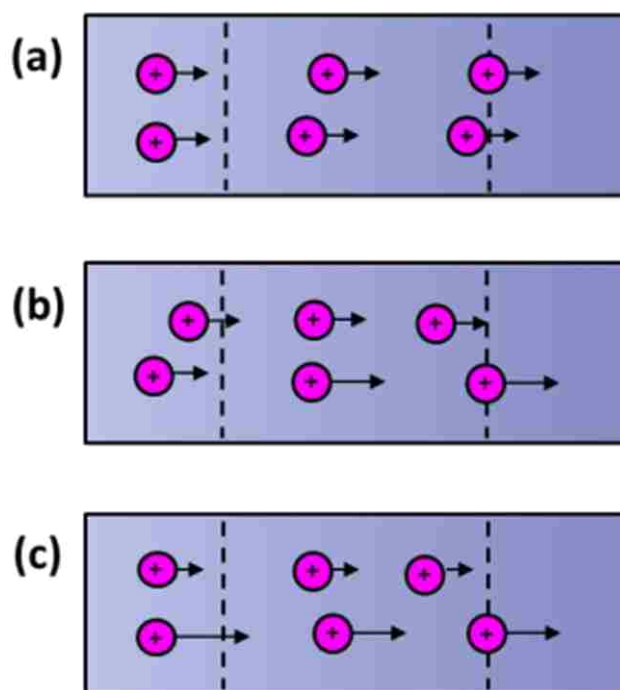
Figure 2.3. Initial ion formation effects. (a) Two ions that have the same mass and initial kinetic energy but formed at different times. (b) Two ions formed at different locations in the extraction field. (c) Two ions with the same mass formed in the same location but different initial kinetic energies.

To improve resolution, delayed extraction (DE) can be used. In DE, once ionization occurs there is a time delay of a few hundred nanoseconds before the acceleration potential is applied.[195, 196, 197] At this point, ions with a higher initial velocity are farther from the target. Whereas, slower ions are closer to the target when the extraction potential is applied, so they are accelerated at a greater

potential than ions with higher velocities. This allows the initially slower ions to catch up to the faster ions, as shown in Figure 2.4. With the proper extraction delay, ions of the same *m/z* reach the detector at the same time. This process compensates for the initial velocity spread and has been shown to dramatically improve resolution.[196, 198, 199, 200]

Ion source   **Field–free Drift Region (flight tube)**

Slow ion

Fast ion

+25V

Detector
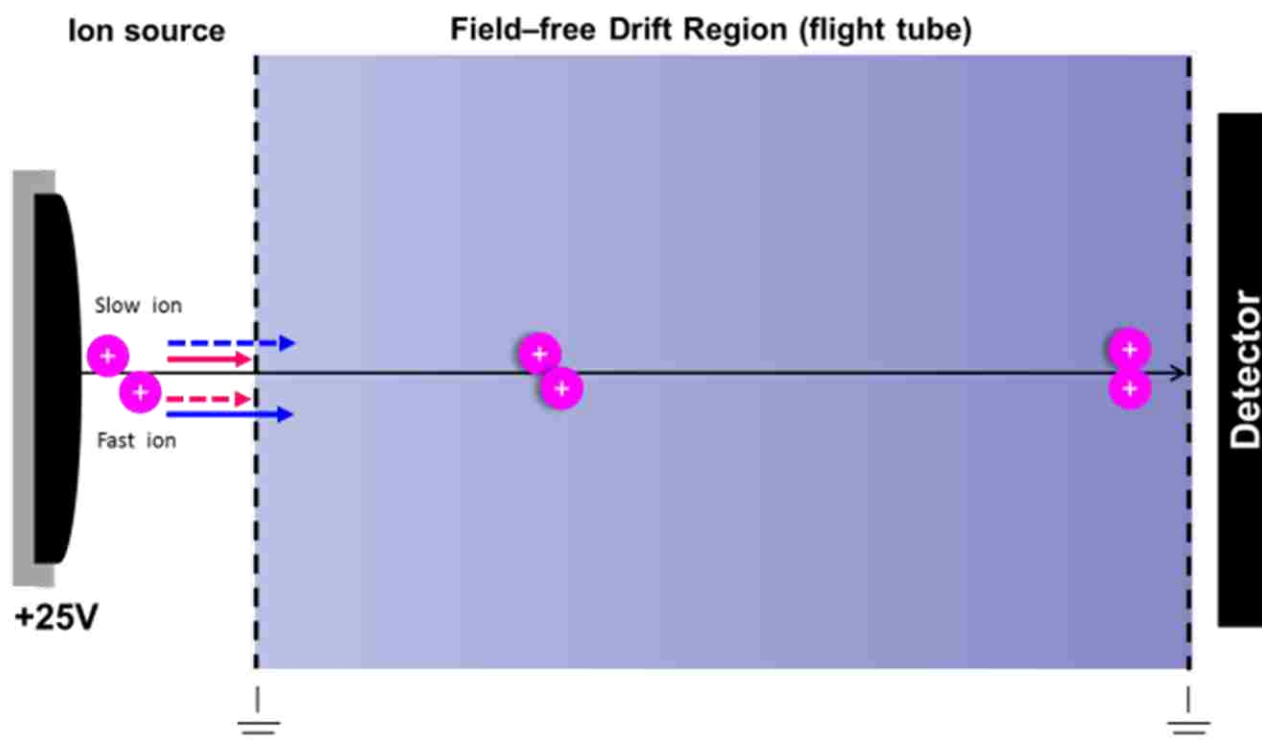
Figure 2.4. Diagram of delayed extraction MALDI TOF MS.

Reflectron Time-of-Flight

To improve mass resolution, a reflectron can be used to compensate for an initial kinetic energy spread.[193] A reflectron is composed of a series of ring electrodes to which a gradient voltage is applied.

The reflectron can be tilted at a small angle with respect to the flight axis, with an off-axis detector or not tilted with an on-axis detector. The electrostatic field slows the ions to a stop and accelerates them toward a detector. Ions with the same *m/z* with higher kinetic energies penetrate deeper into the reflectron and therefore, have a longer flight path, as shown in Figure 2.5. Ions with lower kinetic

Ion source

Field–free Drift Region (flight tube)

Fast ion

Slow ion

Detector

+25 kV
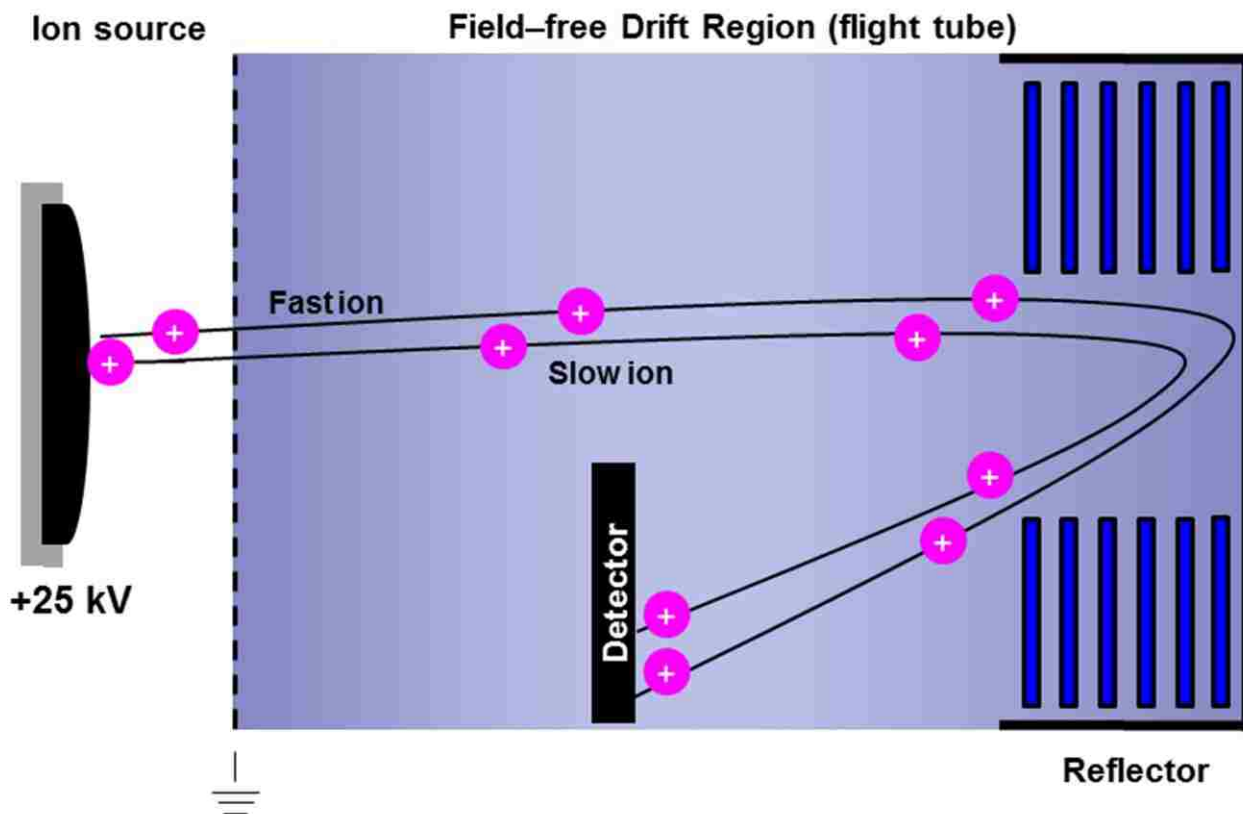
Reflector

Figure 2.5. Reflectron time-of-flight mass spectrometer diagram.

energy do not penetrate as far into the reflectron but are not accelerated to as great a velocity upon exiting. The detector is placed at the point where the faster ions catch up to the slower ions and thus compensates for the kinetic energy spread.

A reflectron can be single-stage, a double-stage, or a curved-field.[193] The single stage reflectron has a single linear potential, shown in Figure 2.5. The purpose of each reflectron is to compensate for the initial kinetic energy distributions but each differs in design and the type of electrostatic static field being employed. The single-stage reflectron, which has the simplest design, has an entrance and equally spaced grid electrodes, with linearly increasing voltages, shown in Figure 2.5. The use of a double-stage reflectron corrects for the initial spatial distribution of ions in the ion source.[194] The double-stage reflectron has two separate retarding fields of different potential gradients and an additional grid is employed,[197] which is used to separate the two retarding fields. The first region of the double-stage reflectron is short and has a high retarding field; whereas the second region is longer.[193, 194] In the first stage, the ions penetrate the first grid, which has the same potential as the flight tube (typically ground).[193] The kinetic energy of the ions is reduced to one-third of its initial value. In the second stage, the ions are reflected. However, ions tend to collide with the grids causing ion scattering, which reduces transmission efficiency and sensitivity. A curved-field reflectron (CFR) is a device that has a non-linear increasing retarding field and has the ability to energy focus ions formed after their initial acceleration, including product ions and metastable decay products.[201] Its design is similar to the single-stage reflectron, with the exception of non-linear voltages. The CFR decreases the depth of penetration for heavier ions, which reduces the dispersion of focal points of fragment ions of different masses.[202] It can focus ions over a broad mass range and collect a spectrum from a single laser shot.[201] In CFR, all ions are energy focused to the same spot, which is near the exit of the reflectron, while ions are focused to different focal lengths that are proportional to the mass of the fragment in linear-field reflectrons. For ions of different masses the CFR provides energy focusing and time dispersion.

Orthogonal Extraction Time-of-Flight

Orthogonal extraction is a method used to couple a continuous beam of ions to a TOF MS. For orthogonal extraction, ions are focused into a beam and extracted into the TOF that is orthogonal to the ion beam propagation direction, which is achieved using pulsed acceleration, as shown in Figure 2.6. With a sufficiently high pulse-out rate, a large fraction of the ions in the beam are directed into the TOF.[203] Typically, the duty cycle of an o-TOF is in the range of 3% to 30%, depending on the *m/z* range being analyzed.[197]
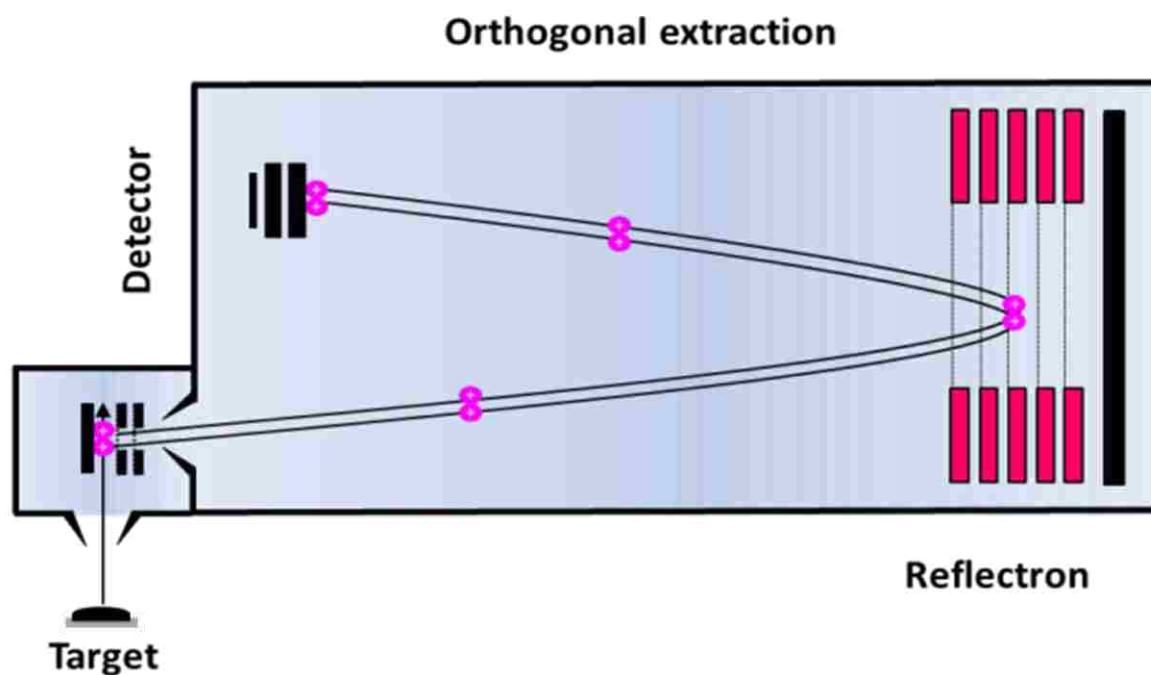
Figure 2.6. Orthogonal time-of-flight mass spectrometer. Ions from a continuous ion source are extracted into the field free region by a high voltage pulse.

Tandem Mass Spectrometry

Tandem mass spectrometry (MS/MS) is the coupling of two stages of mass spectrometry in space or time.[204] A tandem system can be two of the same mass analyzers (e.g. two quadrupole mass

40

analyzers) or two different mass analyzers (a quadrupole and a TOF). For MS/MS, the process of events of mass selection, fragmentation, and mass analysis occur consecutively. Fragmentation can be caused by collisions with an inert gas, a surface, electron capture, electron transfer, photon absorption, heat, or with reactive neutral molecules.[90, 204] Tandem in space means that mass analysis and precursor ion selection are performed in one section of the instrument, dissociated in an intermediate region, followed by mass analysis of product ions (fragments of precursor ions) in the second section of the instrument. Devices that are tandem in space includes sectors, tandem TOF, triple quadrupole and quadrupole time of flight[205] Only one mass analyzer is used in the tandem in time approach. The ions are consecutively selected, activated, and mass analyzed in one analyzer. Mass analyzers that use the tandem in time approach are traps such as a Paul ion trap or FT-ICR.

In TOF MS/MS, a specific mass selected (precursor ion) using a such as a Bradbury-Nielsen gate after the first TOF stage.[204] Ions that are less than the m/z of the precursor ion are electrostatically deflected, then the deflector is turned off to let the precursor ion pass, and the high voltage is switched on again to deflect heavier ions. A Bradbury-Nielsen gate is an ion gate constructed of closely spaced parallel wires.[206] The gate deflects ions when a potential of opposite sign is applied to each adjacent wire. When the potential between the wires is zero the ions pass. The gate closes by applying a potential of opposite sign to adjacent wires creating an electric field perpendicular to the ion path that deflects the ions. At approximately the middle of the MS/MS system, the precursor ion is fragmented by colliding with a neutral gas, such as He, N_2, or Ar; this is known as collision induced dissociation (CID).[204] The product ions are then mass analyzed in the second MS stage.[206]

Bruker UltrafleXtreme Tandem Time-of- Flight Mass Spectrometer

MALDI TOF MS analysis was carried out using a Bruker UltrafleXtreme MALDI-TOF/TOF mass spectrometer fitted with a cell for tandem mass spectrometry and a linear and reflectron detector. This system has a 4 GHz digitizer, a resolution of 40,000 from 700 to 5000 Da, and a 1 ppm and 5 ppm accuracy for internal and external calibration, respectively. This system employs a 1 kHz diode-pumped, frequency tripled Nd:YAG 355 nm solid-state laser with a homogenized modulated beam (Smartbeam II) laser[207] with a computer controlled laser spot size in the range of 10-100 μm.

The MALDI ion source accepts several targets or adapter plates of the same size and shape. The MALDI target most commonly used with the MALDI-TOF/TOF has 384 possible deposition spots for high-throughput analysis.[208] The MALDI-TOF/TOF instrument has nano-assisted laser desorption ionization (NALDI) targets that do not require a matrix, so there is no interference from matrix background. Adapter plates for imaging slides, NALDI targets,[209, 210] and pre-spotted anchor chips with α-cyano-4-hydroxycinnamic acid matrix and calibrations spots can also be used. Each plate or adapter plate has an integrated target transponder that is specific to each target and is read by the mass spectrometer upon insertion. Targets are introduced into the instrument automatically.

For MALDI MS, the MALDI-TOF/TOF operates at a maximum acceleration potential of 25 kV, as shown in Figure 2.7. All the ions have the same kinetic energy and the flight time depends on the mass of the analyte. Ions and fragment ions formed in the source are detected. Data can be obtained for positive ions and negative ions in both linear and reflectron mode. Further details about the components of the Bruker MALDI-TOF/TOF are discussed in the following section.
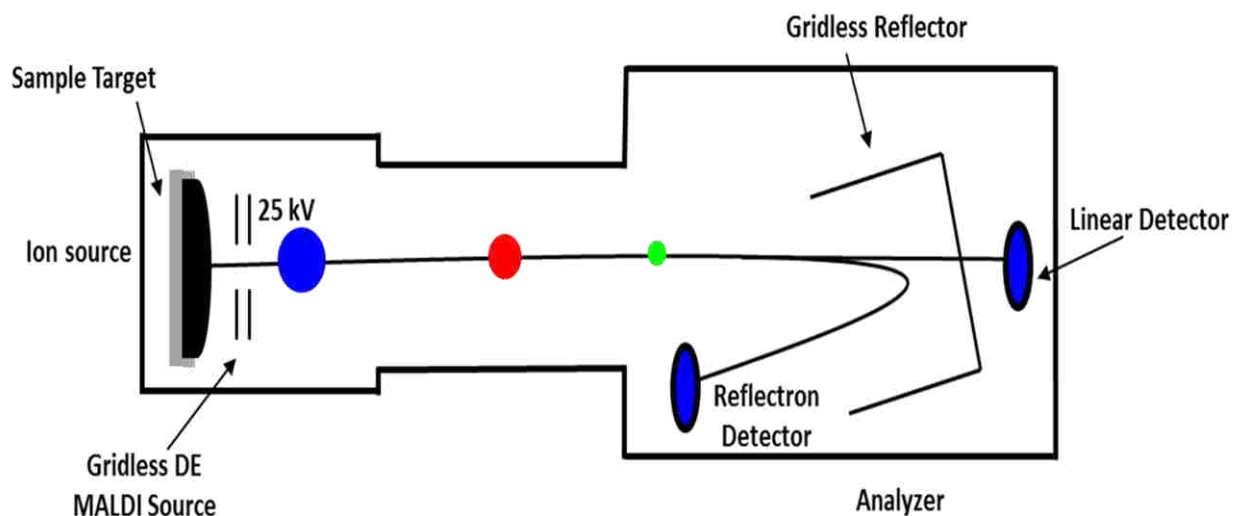
Figure 2.7. Diagram of the Bruker UltrafleXtreme MALDI TOF/TOF Mass Spectrometer for standard MALDI MS.

The collision cell for tandem mass spectrometry is called the LIFT cell. The TOF/TOF is composed of (1) a gridless MALDI ion source with delayed extraction (DE), (2) a timed ion selector (TIS) Bradbury Nielson gate to allow ions of a specific mass to pass, (3) a collision cell (LIFT cell) to raise the potential energy of both parent and fragment ions, (4) a velocity focusing stage for post-acceleration of fragment ions, (5) a post lift metastable suppressor (PLMS), which is located between the collision cell and the reflectron, that deflects precursor ions and unwanted fragment ions after post-acceleration by operating at a raised potential, so that only ions formed between the source and LIFT are detected, and (6) a gridless ion reflector, and (7) detectors for linear and reflectron modes,[208, 211] as illustrated in Figure 2.8.
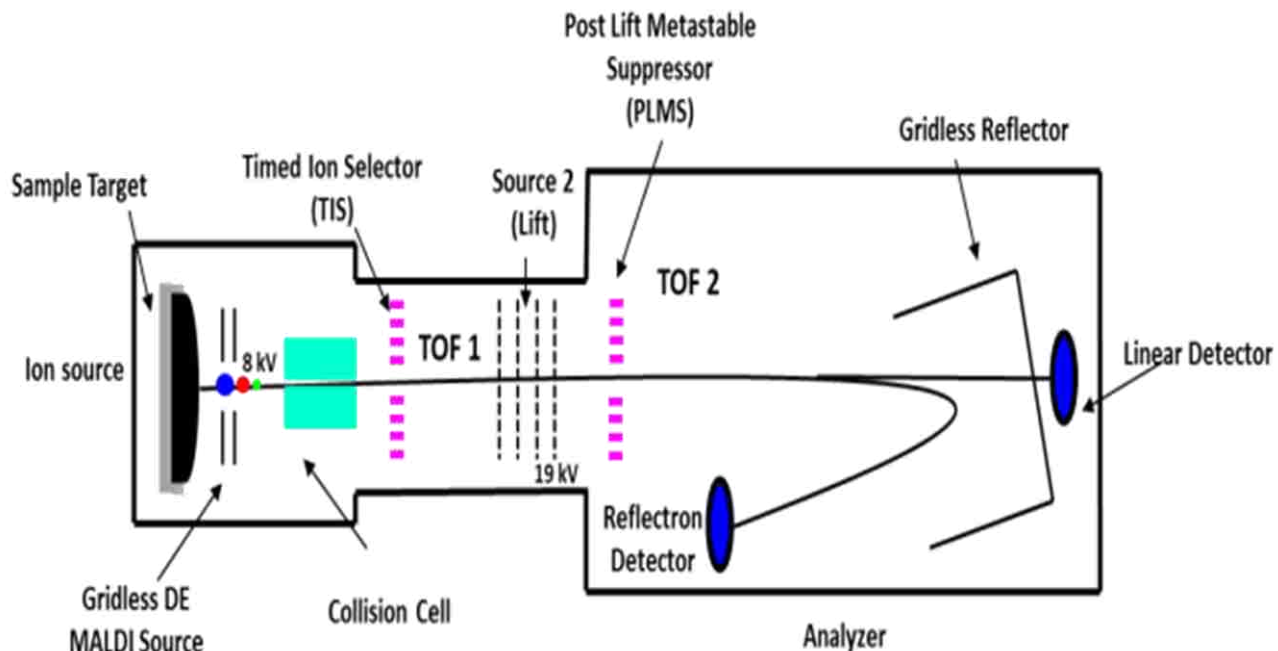
Figure 2.8. Diagram of Bruker UltrafleXtreme MALDI TOF/TOF Mass Spectrometer in MS/MS mode. Ions leave ion source 1 with an energy of 8 kV. Precursor ions are selected in TIS and the precursor ions along with their product ions travel to the LIFT cell where they are further accelerated by an addition 19 kV for a total kinetic energy of 27 kV in the LIFT cell. After the precursor ions and their product ions traverse the collision cell they are then focused onto the detector.

2.3 MALDI Ion Mobility Mass Spectrometry

Ion mobility spectrometry (IMS) is a fast gas phase technique that separates ions based on their charge and collision cross-section.[75] The sample to be investigated is ionized and the ions enter the mobility drift tube. In the drift tube, ions are exposed to a weak electric field (E) and a buffer gas at a pressure of a few Torr, and are separated by their drift velocities (v_d).

Larger ions with greater collision cross-sections collide more frequently with the buffer gas than the smaller ions, and traverse the drift cell more slowly. This means that ions of the same mass and charge but different size can be separated. The drift velocity of an ion is given by

44

$$v_d = KE \tag{6}$$

where K is the mobility of the ion and E is the applied electric field. K is typically represented as reduced mobility, K_o, which is the mobility of the ion at standard temperature and pressure, and is given by

$$K_0 = K \left(\frac{p}{760} \right) \left(\frac{273}{T} \right) \tag{7}$$

where P and T are pressure and temperature, respectively.

The mobility of an ion in a buffer gas depends on a number of factors, including the ion charge, q, the number density of the drift gas, N, the reduced mass of the ion, μ, temperature of the drift gas, T, and the collision cross-section of the ion, Ω_D. From Equation (8), it can be seen that K is inversely proportional to Ω_D:

$$K = \frac{3}{16} \times \frac{q}{N} \times \left(\frac{1}{\mu} \times \frac{2\pi}{k_b T} \right)^{\frac{1}{2}} \times \frac{1}{\Omega_D} \tag{8}$$

Ion Mobility Mass Spectrometry

Ion mobility mass spectrometry (IMMS) is the combination of ion mobility and mass spectrometry. An IMMS instrument performs five functions, which are sample introduction, ionization, ion mobility separation, mass separation, and detection.[75] In this two-dimensional separation technique, ions are separated by their size/charge, while colliding with a buffer gas, in the first dimension and are separated in the second dimension, according to their m/z.

There are four types of ion mobility drift cells that are coupled with mass spectrometers: drift-time, aspiration, field asymmetric (also known as differential mobility), and traveling wave mobility. These ion mobility cells are routinely coupled with a number of different mass analyzers: quadrupole, ion trap, FTICR and TOF.[76] The use of TOF and orthogonal-acceleration (OA) TOF mass analyzers is advantageous because of their high duty cycle.[75] In an aspiration ion mobility cell a buffer gas is introduced into the cell perpendicular to the electric field, which continuously directs ions onto the electrodes for detection. Field asymmetric ion mobility cells use an alternating high and low electric field is applied to two parallel or concentric electrodes. Ions are separated by their mobility difference in the two fields. A voltage is applied to one electrode to focus the ions through the electrodes and into the mass spectrometer. Another approach that has been used for the separation of ions in drift cells is traveling wave ion mobility separation (TWIMS) that operates at a reduced pressure with a radio frequency ion guide. The mobility cell comprises a series of electrodes with a high electric field that is applied sequentially from one electrode to another, in the same direction as ions migrate through the mobility cell.[75, 165,212] The traveling wave separates the ions as they traverse the cell.[75, 165] A drift-time ion mobility (DTIM) cell, which was used for a portion of the work in this dissertation, is a commonly used ion mobility cell and is referred to as an IMS cell.[24] DTIM cells are the only ion mobility cells in which the drift time can be used to directly calculate the collision cross-section of an ion.

Data recorded from this two-dimensional technique can be represented as a contour plot of ion signal as a function of mobility drift time and *m/z*. The correlation of mobility drift time and *m/z* is observed on trend lines of mass plotted as a function of drift. Ions with similar structures fall on the same trend line and ions that are structurally different are observed as outliers from the trend line.[213] Different classes of molecules such as peptides, lipids, carbohydrates, and nucleic acids that can be present in complex biological mixtures can often be distinguished by their ion mobility trend lines.[214,

[215] Sometimes ions of the same class can deviate from the trend line and, in some cases, this deviation is greater than 10%.[75]

Ion mobility spectrometry combined with mass spectrometry (IMMS) is a useful tool for investigating complex mixtures because of its ability to separate different molecular classes.[75, 182] Ions are first separated by size-to-charge in the drift cell and then separated by *m/z* in the second dimension. Samples can be introduced into these devices by a number of techniques and ionized by a variety of methods as well. IMMS has been used for bioanalytical investigations using ESI and MALDIfor peptides,[216, 217] trace explosives,[218, 219] peptide-peptide interactions,[220] and complex peptide mixtures.[165, 166, 183, 214, 221, 222, 223, 224, 225, 226, 227, 228, 229]

Both electrospray ionization (ESI) and MALDI have been used for analyte introduction for IMMS. ESI is susceptible to impurities and produces multiply-charged ions. When using continuous ion sources like ESI and low duty cycle extraction, the sample is not used efficiently.[75] Ion funnels have been used after the mobility cell to improve ion transmission.[184, 230] On the other hand, MALDI is tolerant of impurities. When using MALDI as ionization source, each laser pulse creates an ion packet that can be introduced for mobility separation. In addition, MALDI produces singly-charged ions, which makes spectra easy to interpret even at relatively low mass resolution.

Ionwerks Ion Mobility Time-of-flight Mass Spectrometer

A matrix-assisted laser desorption ionization ion mobility time-of-flight mass spectrometer (MALDI IM-TOF MS) developed by Ionwerks Inc. (Houston, TX) was used for the work reported in Chapter 3. A schematic of the MALDI IM-TOF MS system is shown in Figure 2.9. In this system, analytes can be ionized by a UV or IR laser. The system is equipped with a diode pumped Q-switched, 349 nm (third harmonic) Nd:YLF laser (Crystalaser, Reno, NV) used at a repetition rate of 200 Hz

(maximum repetition rate of 1 kHz). The beam is focused using a 15 cm focal length quartz lens that produces a spot size of approximately 60 μm.
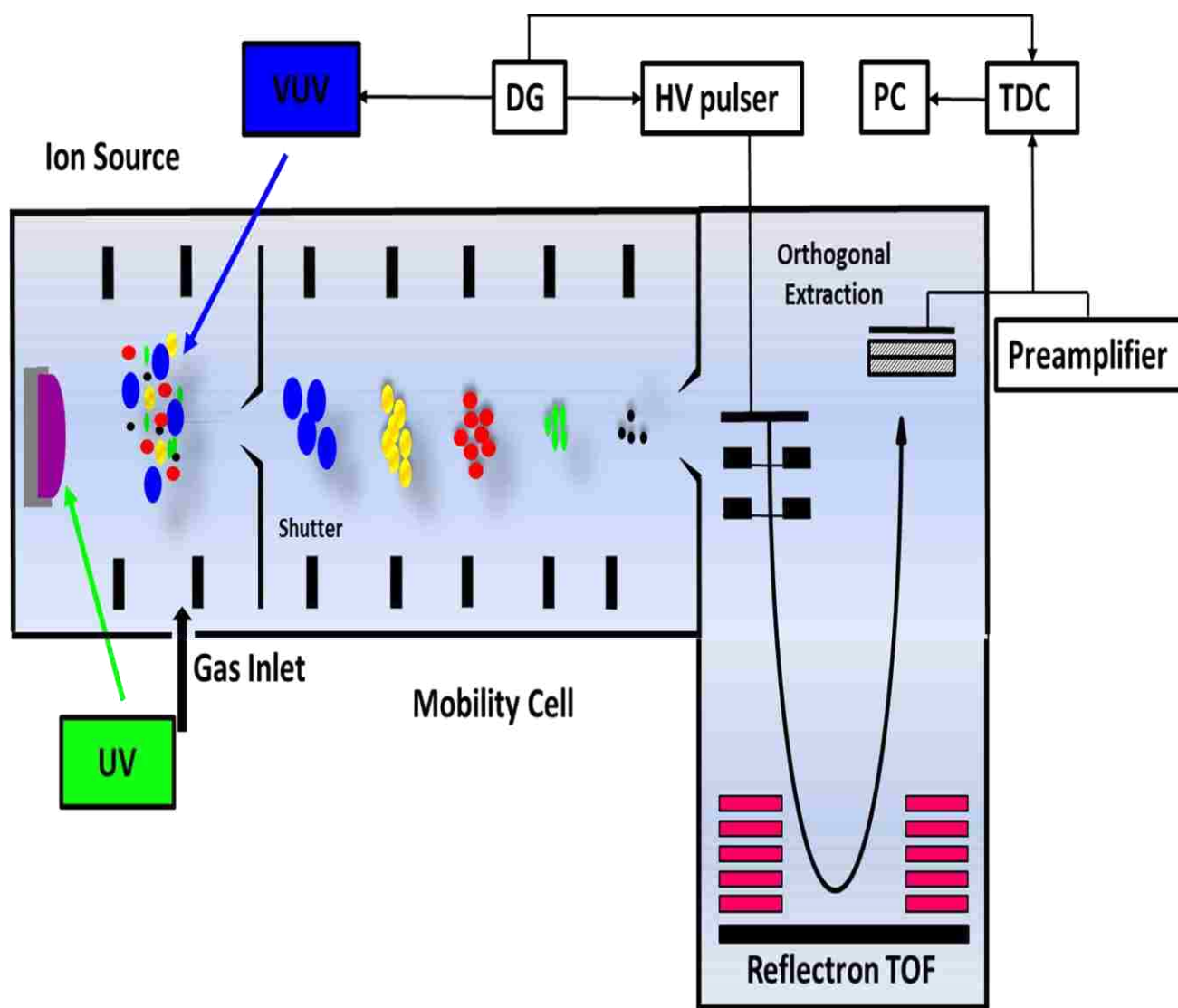
Figure 2.9. Diagram of the ion mobility time-of-flight mass spectrometer with a MALDI ion source. The ultraviolet (UV) laser is used to ionize the sample and the vacuum ultraviolet (VUV) laser is triggered by the delay generator (DG) and is used to post-ionize neutrals in the MALDI plume. The high voltage (HV) pulser and the time-to-digital converter (TDC) are also triggered by DG. The signal from the reflectron detector is amplified and transferred to the TDC and computer (PC).

The sample target is at ground potential, which allows the high voltage bias to pull the ions through the He gas. The bias voltage can be changed to allow both positive and negative ions to be analyzed. A flight tube liner is floated at this bias voltage. Ions desorbed by the laser drift for 15 cm under a

48

constant electric field in the mobility cell that is maintained at a pressure of 3 Torr He. The interaction of the ions with the buffer gas separates them according to their size-to-charge.

After each laser pulse, the ions drift to the end of the mobility cell, which is biased by 1900 V that is applied to a resistor divider network connected between the sample plate and the exit of the mobility cell. At the end of the mobility cell, ions pass through a 0.5 mm orifice into a differentially pumped region before being orthogonally accelerated into the 40 cm reflectron TOF mass spectrometer where they are separated according to their m/z. Typically, ion mobility drift times are on the order of microseconds (μs) to milliseconds (ms), while the flight times are on the order of μs. This time differential means that several hundred mass spectra are generated after each laser pulse. The mass spectra are stored individually with their associated ion mobility drift times. This cycle is repeated for several hundred laser shots until there is enough intensity to plot ion mobility as a function of m/z. A mobility resolution of 30 (FWHM) and a mass resolution of 3000 (FWHM) at 1000 m/z is obtained. Ions were detected using a microchannel plate and four-anode detector. Mass spectra are acquired after each laser shot, at intervals of every 30 to 150 μs, taking into account the mass range. A time-to-digital-converter in ion-counting mode was used to acquire the signal. Data are plotted as two-dimensional contour plots of signal as a function of mobility and m/z using IDL software (Research Systems, Boulder, CO).
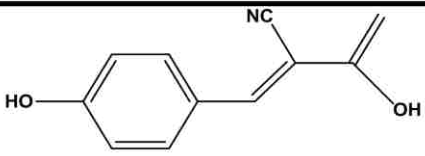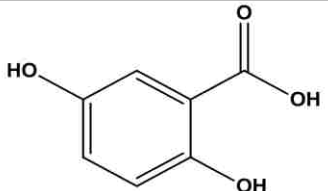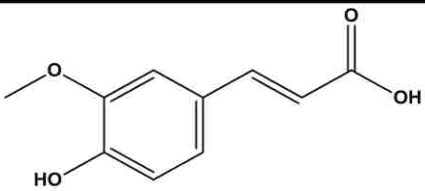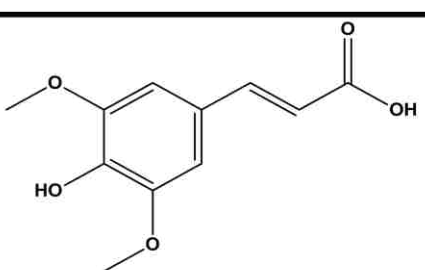
Vacuum ultraviolet (VUV) post-ionization was performed with a 157 nm fluorine excimer laser. The 349 nm desorption laser beam was focused onto the target and the VUV laser beam was parallel to the target several millimeters away. The repetition rate of the lasers was set to 200 Hz and the delay time between the two lasers was 500 μs. The VUV was focused to a spot size of 0.5 mm x 1 mm, using a custom-built nitrogen purged enclosure with adjustable controls. This configuration allows the VUV laser to ionize the neutrals in the laser desorbed plume. The ions were separated in the ion mobility cell and then by the TOF, as described above.

2.4 Ionization

Matrix Assisted Laser Desorption Ionization

MALDI is a soft ionization technique that can be used for the analysis of large biomolecules. Using this technique, molecular weight and structural information from intact biomolecules can be obtained. MALDI is similar to LDI, a process in which a UV or IR laser can be used; however, MALDI utilizes a matrix, which is typically a small organic acid. The choice of matrix depends on the wavelength of the laser being used and the analyte being investigated. Typically, the matrix to analyte molar ratio ranges from 1000:1 to 10000:1. [231, 232] A list of commonly used UV matrices is shown in Table 2-1.

Table 2-1 Commonly used UV MALDI matrices.

Matrix	Structure	$(M+H)^+$ mono	Laser λ	Sample types
a-cyano-4-hydroxycinnamic acid **CHCA**		190.0504	337 355	Nucleotides, peptides, lipids
2,5-dihydroxybenzoic acid (Gentisic acid) **DHB**		155.0344	337 355	Oligosaccharides, nucleotides, peptides
3-methoxy-4-hydroxycinnamic acid (Ferulic acid) **FA**		194.0579	266 337 355	Proteins
trans-3,5-dimethoxy-4-hydroxycinnamic acid (Sinapinic acid, Sinapic acid) **SA**		255.0763	266 337 355	Peptides, proteins, lipids

The analyte and matrix solution are mixed together and allowed to dry and co-crystallize. The co-crystallized mixture is then irradiated with a pulsed laser as shown in Figure 2.10. The matrix has three primary functions; the first is to absorb the energy of the laser and form ions, the second is to act as a solvent for the analyte to minimize aggregation, and lastly, to aid ionization by proton transfer to the analyte. The MALDI ablation plume contains ions and neutral species. In MALDI mass spectra, singly protonated ions are typically produced. MALDI is tolerant of impurities such as salts and buffers.
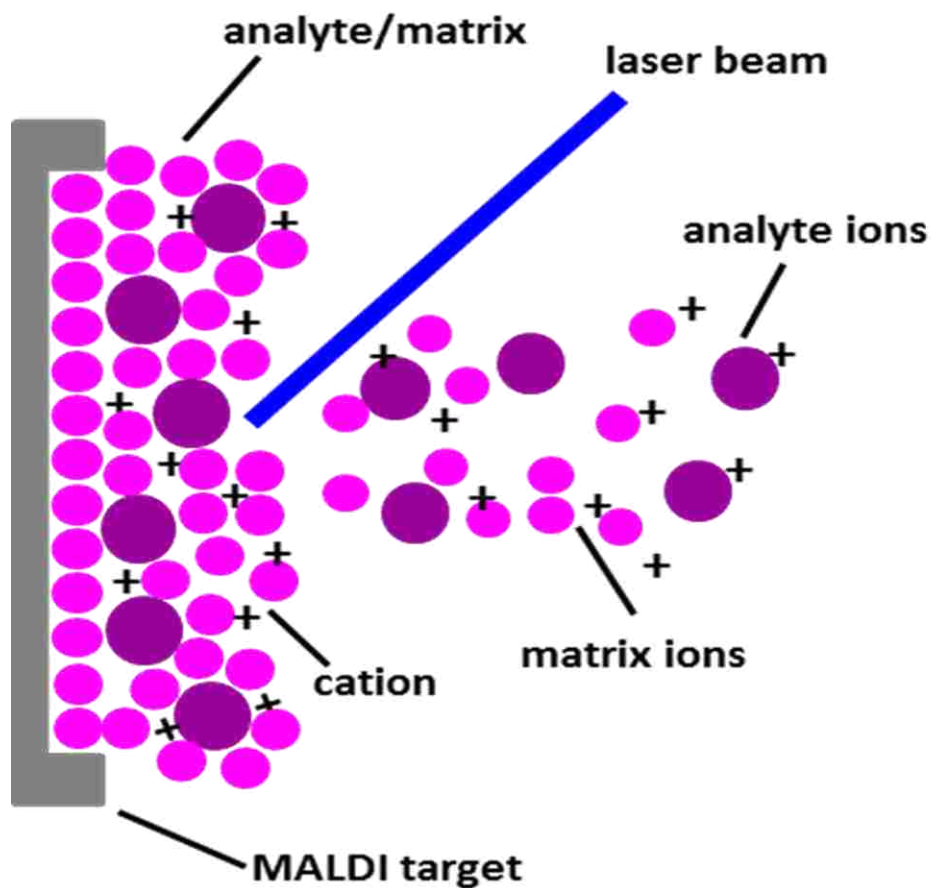
Figure 2.10. Illustration of analyte and matrix ions before and after laser irradiation of sample on MALDI target.

Nano-assisted Laser Desorption Ionization Mass Spectrometry

A number of methods have been investigated for matrix-free analysis MS using nano-structured targets to avoid low mass (less than 1000 Da) interference from matrix ions.[233, 234, 235, 236] Researchers have investigated a number of nano-structured surfaces, including porous silicon, silicon nanowires, carbon nanotubes, and porous alumina.[236] These matrix alternatives absorb the energy of the laser and aiding in ionization. Based on these architectures, 100 spot disposable nanostructure-assisted laser desorption ionization (NALDI) targets have been commercially developed for the analysis of low mass molecules.[209, 234, 236] The nanostructures are silicon nanowires grown from silane vapor with a diameter of 20 nm and range in length from 100 nm to 500 nm, with a density of 100 nanostructures/μm^2.[234, 235] The top layer of the of inorganic nanostructures is coated with a hydrophobic organic layer that allows sample droplets to adhere to the surface of the NALDI target.[234] Similar to the role of the MALDI matrix, the silicon nanowire structures are able to desorb the laser energy and aid ionization.[209]

Laser Desorption Vacuum Ultraviolet Post-ionization

The MALDI plume contains both ions and neutral species, although significantly more neutral species are formed. Only the ionized species are detected in the mass spectrometer. To ionize the desorbed neutral species, a second laser can be used for photoionization.[237] The second laser can be a UV laser or an IR laser.[238] Plume photoionization is similar to MALDI, with the addition of a second laser for ionization, however a matrix is typically not used.[239] The ionization of desorbed neutrals can increase the ionization efficiency. For this work, a VUV laser was used.

At VUV wavelengths molecules are ionized by a single photon if the ionization energy (IE) is less than the photon energy. VUV wavelengths are in the range of 105 nm to 165nm correspond to photon energies of 7.5 eV to 11.8 eV.[239] A commonly used VUV source in MS is the 157 nm fluorine (F_2) excimer laser.[237, 240] The F_2 excimer laser has a pulse width of 10 ns at 7.8 eV.[241] Although the

photon energy of some VUV sources, such as the F_2 laser, is lower than the IEs of most biomolecules, this can be advantageous for the detection of low IE analytes in a mixture with high IE analytes.[239] However, biomolecules with high IEs can be derivatized with low IE aromatic compounds that act as chromophores for post-ionization and detection.

2.5 Laser Ablation Sample Transfer

Laser ablation sample transfer (LAST) is a technique conducted under ambient conditions that uses a pulsed laser to ablate an analyte for collection into a solvent, which can then be analyzed using MS.[242] A UV or IR laser can be used, but IR lasers are more effective because they have a greater penetration depth and more material is removed from the sample surface.[243, 244] In this work, the IR source used is a wavelength tunable pulsed mid-infrared optical parametric oscillator (OPO) at 2.94 μm. The 2.94 μm wavelength is used because it is near the peak of the OH stretch absorption of water and other solvents.

The LAST sample preparation setup has a 3 mL syringe mounted on a manually controlled *xyz* stage (Model 461, Newport, Irvine, CA). A Petri dish containing freshly cultured bacterial colonies was placed directly beneath the mounted syringe and irradiated by the infrared laser as shown in Figure 2.11.[242] The syringe was connected to a Luer taper adapter union that contained a 360 μm OD and 50 μm ID coated fused silica capillary. The syringe was operated manually, which allowed different droplet sizes to be produced. A video camera and a macro lens was used to observe the droplet size.

The OPO source (OPOTEK, Carlsbad, CA) was used at 2.94 μm with a repetition rate of 2 Hz. The laser was directed at the target at a 45° angle and focused onto the target with a 250 mm focal length lens. The spot size of the laser beam at the capillary tip was approximately 200 μm x 300 μm as

determined with laser burn paper. The maximum laser energy was 1.75 mJ with no attenuation. The laser was attenuated using the laser software control.
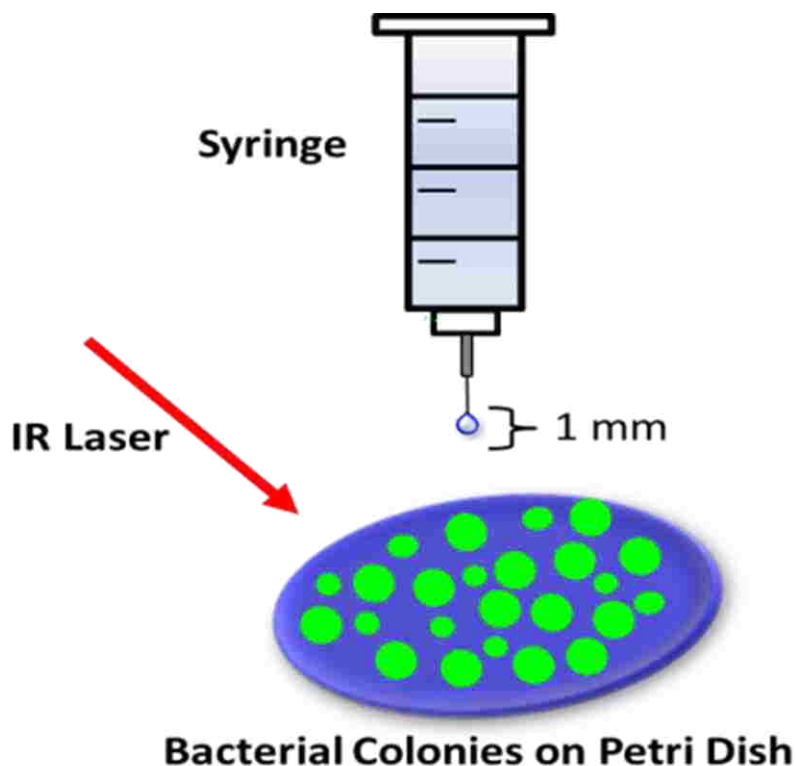
Figure 2.11. Laser ablation sample transfer (LAST) setup.

Petri dishes containing bacterial cultures for ablation were placed below the syringe, which contained a mixture of 70% acetonitrile and 30% of 0.1 % TFA. The distance between the colonies on the Petri dish and the bottom of the droplet was 1 mm and the droplet was 1 mm in diameter. The laser irradiated the bacterial colonies for 60 laser shots at 25 mJ. After ablation of the sample and its collection in the droplet, the syringe was removed from the *xyz* stage so that the droplet containing the material collected from the bacterial colonies was deposited on the NALDI target. NALDI mass spectra were obtained using the MALDI-TOF/TOF mass spectrometer.

2.6 Databases

Bioinformatics is the utilization of computation and analysis to interpret biological data.[245] High-throughput technological advances for bioanalysis have afforded researchers the ability to obtain and store large data sets. Bioinformatic tools, such as databases, are used to manage large data sets for bioanalysis for molecule identification as well as structure functions relationships. These databases contain biomolecule sequence information and spectra that is used to determine biomolecule and microorganism identification. When using a protein sequence database, experimental data such as *m/z* values from mass spectra can be compared with information in the database; while, in a matching or fingerprint database, mass spectra can be directly compared to the mass spectra database.

Rapid Microorganism Identification Database

The Rapid Microorganisms Identification Database (RMIDb) is a database for microorganism identification by mass spectrometry using the masses of proteins and peptides from whole cell intact microorganisms and trypsin or acid treated cells.[246] The RMIDb contains protein sequence data from the Ventor Institute's Comprehensive Microbial Resource (CMR), UniProt's Swiss-Prot and TrEMBL, Genbank's Protein, and RefSeq's Protein and Genome collection. The database uses a Glimmer algorithm[247, 248] to predict proteins of microorganisms that have limited sequence information compared to well-characterized proteins of microorganisms with completed genomes. These possible protein sequences are from a number of different protein database sources. Since its initial development, the code for Glimmer has been rewritten to include improvements in sensitivity and specificity.[248] The latest version of Glimmer is Glimmer3, which was used in this work.[249] If a Glimmer3 sequence is the only matching sequence for a specific *m/z*, this means there is no protein sequence in the database that corresponds to the given mass. There is a possibility that the protein

sequence does not exist or it could be a real protein that is simply missing from the protein sequence database(s).

In total, the RMIDb has 47,130,460 protein sequences (21,057,195 distinct protein sequences) from 86,145 organisms, representing 35,318 species available for searching as of January 2011. The RMIDb has protein sequences from protein annotations on 1140 sequenced genomes representing 800 species. For identification, the RMIdb can be used to perform searches for peptides and proteins from all sources. Information that can be specified in the database query for all searches include the charge of the *m/z* values as well as mass error. The list of possible proteins or peptides from the database that are a match to the proteins or peptides in the mass spectrum is determined by a p-value that ranges from 0 to 1.[15] The p-value is dependent upon the number of matches of the specific *m/z* value, the number of predicted fragment ions for MS/MS spectra and their masses, and the number of fragment ions generated.[15] Small p-values indicate a high probability of identification.

Bacteria Fingerprint Matching

MALDI Biotyper software has an integrated database and is designed for whole cell microorganism identification using MALDI MS.[118] This microbial database has a total of 3290 spectra corresponding to a number of microorganisms including yeasts, fungi, viruses, and bacteria. The reference spectra in the database are grouped according to microorganism taxonomy. All microorganisms have a protein fingerprint profile or signals attributed from biomarkers based upon its molecular composition. In this case, the software measures high abundance proteins and ribosomal proteins as identifiable biomarkers for identification. Ribosomal proteins are routinely found in MALDI spectra of whole cell bacteria. Microorganism cells from agar cultures, broth cultures, or

lyophilized cells can be transferred to a target or extracted and analyzed using MALDI, see Figure 2.12 for workflow schematic.
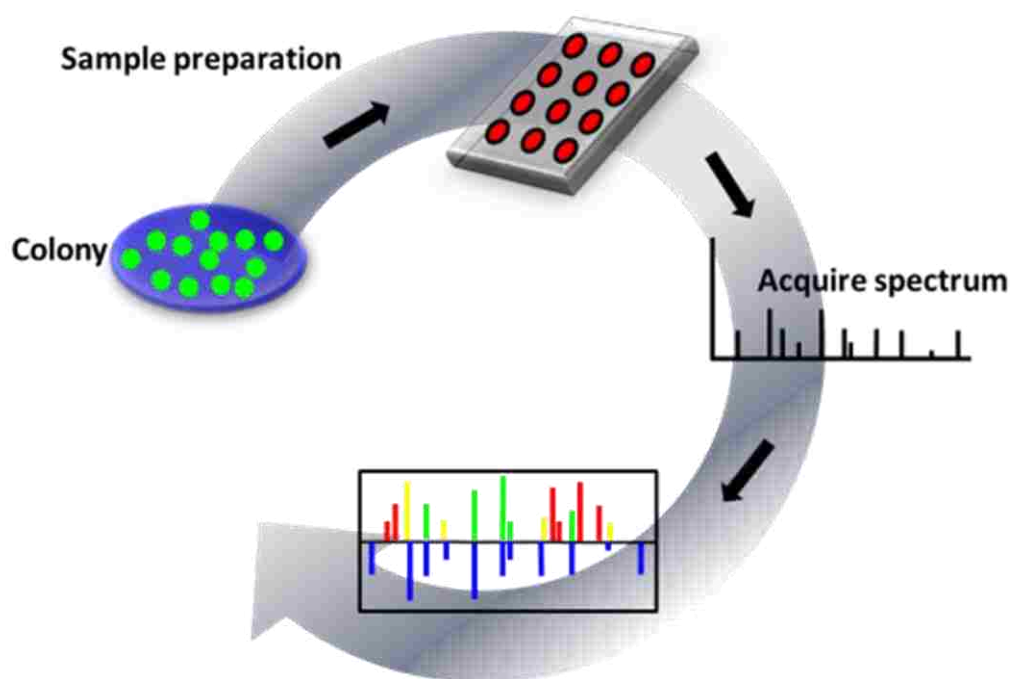
Figure 2.12. Workflow for using MALDI Biotyper software for microorganism identification.

The reference spectra libraries are called main spectral projection (MSP) libraries and contain lists of peaks and intensities of all microbial strains in the integrated microbial database. Each MSP is composed of an average of 20 independent peak lists which contains peak position, peak intensities, and peak frequency among the set of 20 spectra for the most prevalent peaks.[33,34] Once experimental mass spectra are imported into the MB and before searching for an identification, MB uses an alignment function to calibrate the unknown spectra against the reference spectra to reduce the number of mass deviations.[106] Then using an integrated pattern matching algorithm, which considers *m/z*

values, peak intensity, and how often each peak appears compared to reference spectra, the experimental spectra are compared to the reference spectra. After this process, a graphical identification window appears that shows the experimental spectrum that sits above an inverted spectrum from the reference library. This illustrates the similarities and differences between the experimental spectrum and the spectrum from the database that the experimental spectrum most closely matches as seen in Figure 2.13.
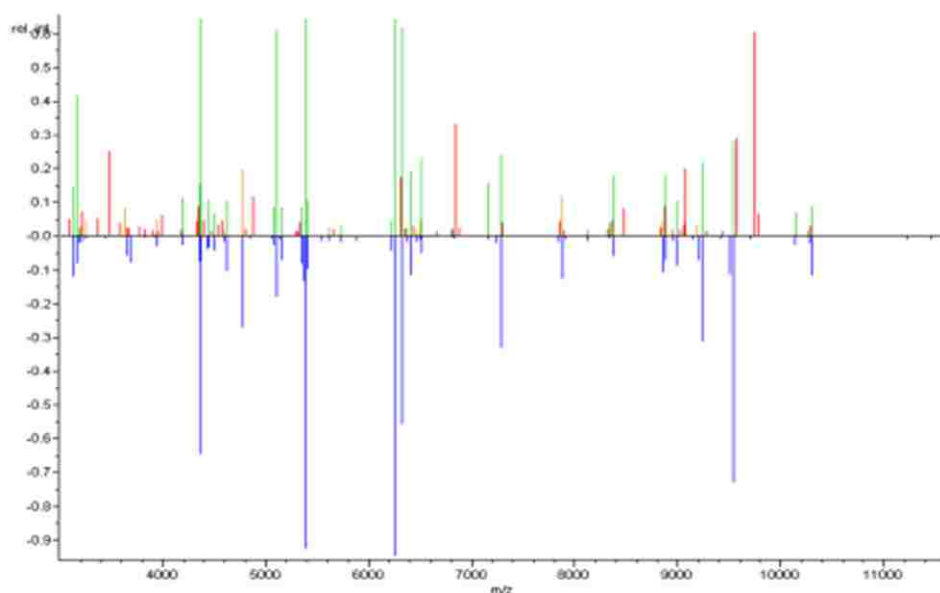
Figure 2.13. MALDI Biotyper graphical identification window. The top spectrum is the observed experimental spectrum and the inverted spectrum at the bottom is the spectrum from the database that is most closely related to the experimental spectrum.

A score table of ten possible matches is produced with score values in decreasing order. The score is calculated based on the correlation of peak position, peak intensities, and peak frequency of the experimental and reference spectra of the matched peaks.[14, 100, 106] From these comparisons, three resulting scores are calculated: (1) the relative score, which can have a maximum value of 1, reflects the number of peaks of the reference spectrum that are a match with peaks from the unknown

58

spectrum; (2) the relative p-number, which also can have a maximum value of 1, is the sum of the number of peaks matched within the error window and half the number of peaks that lie outside of the error window divided by the total number of peaks in the unknown spectrum; (3) the intensity correlation between the matched peaks. The product of the relative score, relative p-number, and the intensity correlation is multiplied by 1000 and converted to its common logarithm score of 0 to 3.[6,36,37] A score of 0 means there is no match and a score of 3 is a perfect match and is only achieved when spectra are matched with themselves.[6]

MALDI Biotyper (MB) was developed for and has primarily been used to identify microorganisms in clinical settings.[13,36,38,39] Based upon score values it can be determined whether an identification is correct at the species or genus level. This is shown in Table 2-2. A score >2.00 is displayed in green and is considered to a probable identification at the species level; a score in the range of 1.7-1.99 is displayed in yellow and is considered to be a probable identification at the genus level, and score <1.7 is displayed as red and is not reliable for genus identification.

Table 2-2. Explanation of possible identifications.

Range	Description	Symbols	Color
2.300.. 3.000	highly probable species identification	(+++)	green
2.000.. 2.299	secure genus identification, probable species identification	(++)	green
1.700.. 1.999	probable genus identification	(+)	yellow
0.000.. 1.699	no reliable identification	(-)	red

When the processing program is run on the same computer as the mass spectrometer acquisition program, it can be configured to automatically import the acquired spectra and search the database for identification. For analysis of closely related species or subtyping, the MB software also uses other bioinformatics tools such as dendrograms and principal component analysis (PCA). Both of these tools can identify patterns within the data and graphically show their differences and similarities. A dendrogram is a tree-like visual representation that illustrates the relationship of one species to another. The PCA method, a statistical method, is able to reduce a large data set that has a number of dependent variables (in this case different intensities and peak positions for defined masses) to a smaller data set that retains most of the information of the larger set of data. Additionally, MB allows users to create their own reference spectra and reference libraries.

2.7 Samples and Reagents

Analytes and Matrices

Lyophilized *Bacillus subtilis* ATCC 6633 and *Escherichia coli* strain W ATCC 9637 used in the MALDI-IM TOF MS studies were purchased from Sigma Aldrich (St. Louis, MO) and used without further purification. Other cultures used in this study including *Escherichia coli* 35218, *Escherichia coli* 21332, and *Enterobacter aerogenes* 13048, and were purchased from American Type Culture Collection (Manassas, VA) as ampules and cultured in the laboratory. Fumed silica, bentonite, and pollen (from *Juglans nigra*-black walnut) used in the bacterial interferent studies were purchased from Fisher Scientific (Pittsburgh, PA). Diesel particulate, which was also used in the bacterial interferent studies, was purchased from the National Institute of Standards and Technology (Gaithersburg, MD).

The matrix α-cyano-4-hydroxycinnamic acid (CHCA; Sigma-Aldrich) was stored at -20 °C and used without further purification. Saturated matrix solutions were prepared by dissolving 30 mg of CHCA matrix in 1 mL of 1:1 ACN/0.1% TFA. For the MALDI-IM TOF MS investigation, the saturated matrix was mixed with the suspension in a 1:2 ratio of bacterial suspension/matrix solution of which a 1 μL volume was deposited on the target and allowed to dry. Matrix solutions for the bacterial interferent studies were prepared by dissolving 20 mg of CHCA matrix in 1 mL of 1:1 50% ACN/2.5% TFA.

Culturing Methods

Bacteria were cultured by suspending bacterial pellet in 0.75 mL of nutrient broth. The suspended bacterial solution was then poured into a test tube containing approximately 6 mL of nutrient broth. Several drops of the suspension were used to inoculate a Petri dish containing nutrient agar. Next the test tube and plate were incubated at 30 °C for *B. subtilis* and 27 °C for *E. coli.* After 24 hours, 1 mL aliquots of the bacteria-nutrient broth solution was transferred into six 500 mL growing flasks containing 250 mL of nutrient broth. The suspensions were incubated for 24 hours at the proper temperature for each bacteria sample. The cloudy bacterial solutions were placed in micro-centrifuge tubes and centrifuged at 3200 RPM for 30 minutes. Next, the bacterial pellet was washed with nanopure water and centrifuged again for 30 minutes at 3200 RPM twice after pouring off the supernatant from the centrifuge tube was poured off. Any remaining supernatant was poured off and some samples were analyzed immediately and others were lyophilized and analyzed at later date.

Calibration Standards

Mass calibration for the mass spectrometer was achieved using Bruker Mass Calibration Standards. For the analysis of compounds in the range of 700 to 3500 Da, Bruker Peptide Calibration Standard II was used. This standard contains a mixture of nine standard peptides for calibration, as shown in Table 2-3. The masses for the peptide calibration mixture can be observed as protonated monoisotopic masses or average mass. Monoisotopic mass is the exact mass of an ion or molecule using the mass of the most abundant isotope of each element,[250] whereas, the average mass is the average of all of the natural isotopes. The peptide calibration standards were received as dry peptides in a micro centrifuge tube. A volume of 125 µL of 0.1 % TFA in nanopure water was added to dissolve the peptides or proteins and mixed well in the micro-centrifuge tube. A volume of 1 µL of the peptide or protein standard was mixed with 1 µL of CHCA in an organic-acidic solvent mixture of 1:1 (v/v) ACN:0.1% TFA in nanopure water and deposited respectively on a MALDI target and allowed to dry.

Table 2-3. List of Bruker Peptide Calibration II Standard peptide masses.

Peptide Calibration Standard	$[M + H]^+$ monoisotopic	$[M + H]^+$ average
Bradykinin	757.3995	757.86
Angiotensin II	1,046.5418	1,047.19
Angiotensin I	1,296.6848	1,297.49
Substance p	1,347.7354	1,348.64
Bombesin	1,619.8223	1,620.86
ACTH clip 1-7	2,465.1983	2,466.68
ACTH clip 18-39	3,1.47.4710	3,149.57

The remaining peptides or proteins were stored at 20 °C until further use. The peptide calibration masses can be observed as a protonated monoisotopic molecular ion peaks [M+H] + or average protonated molecular ion peaks. A MALDI mass spectrum of the peptide calibration mixture is shown in Figure 2.14.
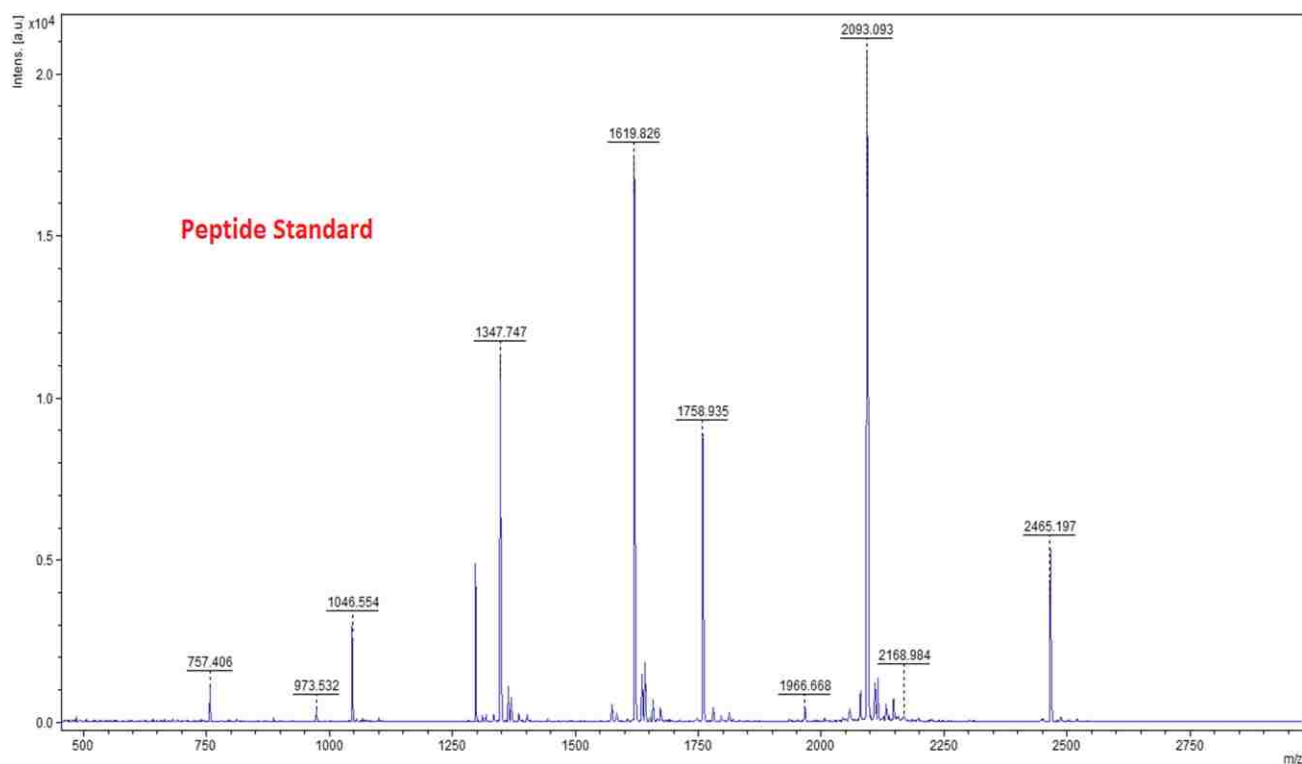
Figure 2.14. MALDI mass spectrum of the Bruker Peptide Calibration II Standard.

Bruker Protein Calibration I Standard was used to observed compounds in the 4,000 to 20,000 Da range. The protein standards contained a mixture of four proteins: cytochrome c, insulin, ubiquitin, and myoglobin. The observed protonated average masses of the proteins from protein mixture are listed in Table 2-4. The protein calibration standards were received as dry protein in a micro centrifuge tube and were prepared in the same manner as the peptide calibration mixture, with the exception of the choice of using 1 µL of SA matrix in an organic-acidic solvent mixture of 1:1 (v/v) CAN/0.1% TFA in

nanopure water, instead of CHCA. A MALDI mass spectrum of the protein calibration mixture with

CHCA matrix is shown in Figure 2.15.

Table 2-4. List of Bruker Protein Calibration I Standard protein masses.

Protein Calibration Standard I	$[M + H]^+$ average
Insulin $[M + H]^+$	5734.51
Ubiquitin I $[M + H]^+$	18565.76
Cytochrome C $[M + H]^+$	12360.76
Myoglobin $[M + H]^+$	16952.30
Cytochrome C $[M + 2H]^{2+}$	6180.99
Myoglobin $[M + 2H]^{2+}$	8476.65
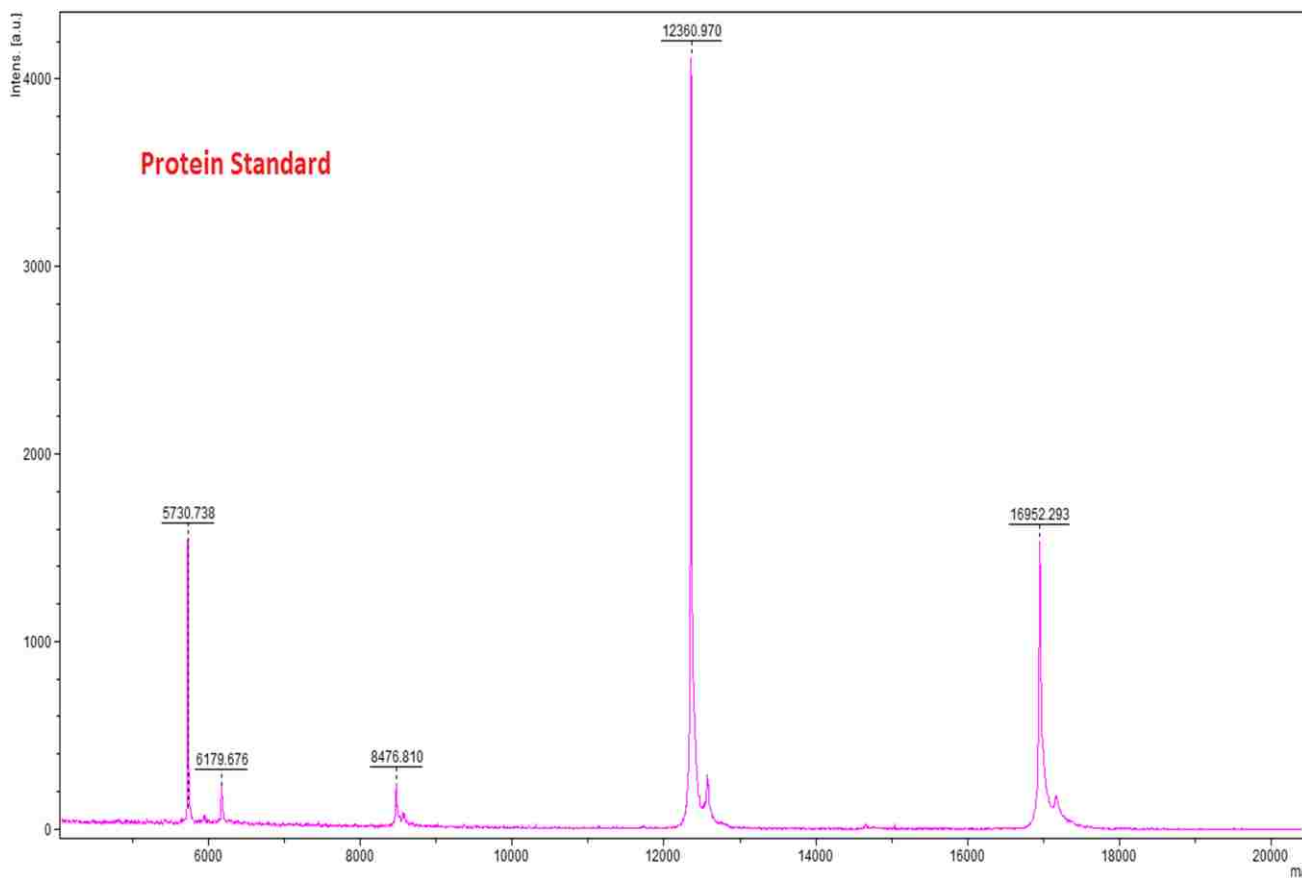
Figure 2.15. MALDI mass spectrum of Bruker Protein Calibration I Standard.

A Bruker Bacterial Test Standard (BTS) was used to calibrate the MALDI TOF MS for the study conducted in Chapter 4. The BTS is an extract that contains peptides and proteins from *E. coli* DH5alpha spiked with high mass proteins, ribonuclease (RNAse) and myoglobin, in the range of approximately 3600 to 16950. The average masses of the BTS are shown in Table 2-5. The RL29 protein is observed as a doubly charged protonated molecule ($[M + 2H]^{2+}$) , while other proteins from the BTS mixture is observed as singly charged protonated molecules. The acceptable mass tolerance is for each BTS compound is $\pm$ 300pm.

Table 2-5. List of Bruker Bacterial Test Standard (BTS) peptides and proteins.

Bacterial Test Standard	Avg Reference mass	$\pm$ 300 ppm range
RL29 $[M + 2H]^{2+}$	3637.8	3637.7 – 3638.8
RS32 $[M + H]^{+}$	5096.8	5095.3 – 5098.3
RS34 $[M + H]^{+}$	5381.4	5379.8 – 5383.0
RS33meth $[M + H]^{+}$	6255.4	6253.5 – 6257.3
RL29 $[M + H]^{+}$	7274.5	7272.3 – 7276.7
RS19 $[M + H]^{+}$	10300.1	10297.0 – 10303.2
RNAse A $[M + H]^{+}$	13683.2	13679.1 – 13687.3
Myoglobin $[M + H]^{+}$	16952.3	16947.2 – 16957

The BTS calibration mixture was received as a dry mixture in a mcirocentrifuge tube. The calibration mixture was prepared by dissolving in a 50 uL mixture of 50% pure acetonitrile, 47.5% nanopure water, and 2.5% trifluoroacetic acid and pipetting up and down a minimum of 20 times to ensure adequate mixing. The BTS was then allowed to incubate for five minutes at room temperature. After the five minute incubation period, the standard was pipetted up and down a minimum of 20 times and

stored at 20 °C until needed. The BTS was used by depositing 1 µL on the MALDI target and after drying it was overlaid with 1 µL of saturated CHCA matrix prepared in 1:1 (v/v) of 50% ACN and 2.5% TFA in nanopure water. A MALDI mass spectrum of the BTS calibration mixture is shown in Figure 2.16.
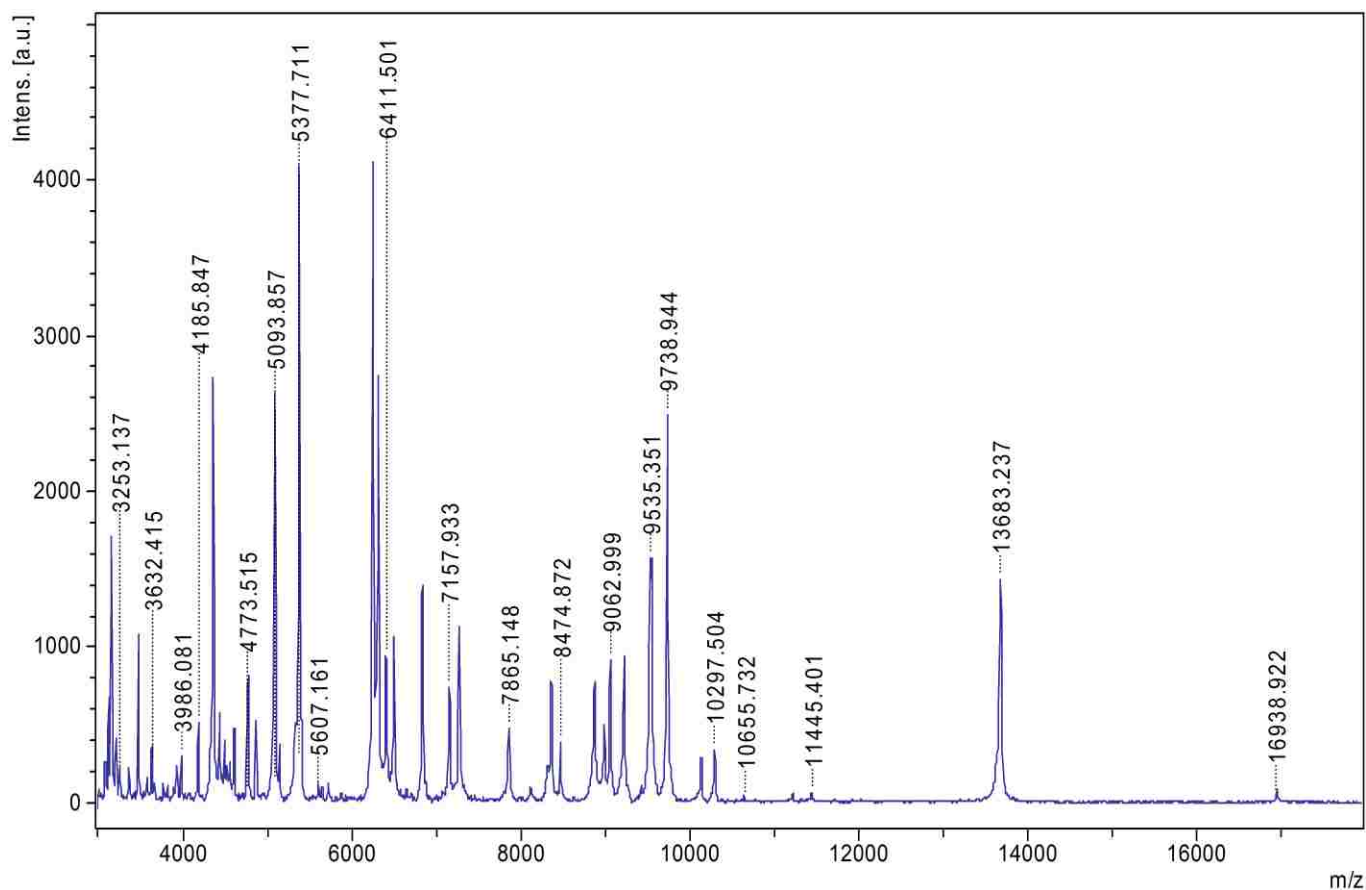
Figure 2.16. MALDI mass spectrum of the Bruker Bacterial Test Standard for calibration.

CHAPTER 3. MATRIX ASSISTED LASER DESORPTION IONIZATION ION MOBILITY TIME-OF-FLIGHT MASS SPECTROMETRY OF BACTERIA*

In this chapter, the detection and identification of *B. subtilis* 6633 and *E. coli* 9637 bacteria using MALDI-TOF-IM MS and MALDI-TOF MS is described. MALDI-TOF and MALDI-TOF-IM MS were conducted in parallel to assess the effectiveness of MALDI-IM-TOF MS for microorganism identification. Mass spectra from each experiment were compared and peaks greater than or equal to 4,000 *m/z* were submitted to the RMIdb database for identification. VUV post-ionization MALDI-IM-TOF MS experiments were also conducted for each species and additional peaks were observed for *B. subtilis*.

3.1 Introduction

Mass spectrometry was first used for bacteria fingerprinting in 1973.[78] Using pyrolysis with electron impact ionization MS, it was observed that different species and strains within a species have different spectral fingerprints. However, researchers did acknowledge the limitations of this technique due to the fragmentation caused by electron ionization. Since then, advances in soft-ionization techniques, particularly matrix-assisted laser desorption ionization (MALDI), have led to broader use of mass spectrometry for the study of bacteria.[251] MALDI typically produces singly charged ions, which can reduce spectral congestion. The characterization of bacteria using matrix-assisted laser

desorption ionization time-of-flight mass spectrometry (MALDI-TOF MS) has been demonstrated by a number of groups.[107, 111, 252, 253, 254, 255, 256] The MALDI approach to bacteria detection is attractive because of its low detection limit and tolerance for impurities. Identification is based upon characteristic peaks, termed biomarkers, that are attributed to molecules such as proteins, peptides, DNA, lipids, polysaccharides, and lipopolysaccharides.[257] Spectra can be used to generate a reference library in which pattern matching algorithms can be applied to compare spectra for identification. Most identifications are based on highly abundant and conserved ribosomal proteins which tend to dominate bacterial mass spectra.[9] Using these approaches, MALDI has demonstrated the ability to identify bacteria at the species and genus levels and strains within a species.[9, 10, 258]

It is standard practice to identify microorganisms using in-house databases or using public database searches.[111, 259] There are some molecules found in bacteria that are conserved among different species, which makes distinguishing one species from another difficult.[107, 260, 261] Analyzing bacteria mixtures can also be difficult due to spectral congestion and interferences due to isobaric lipids, peptides and other biomolecules. In addition, if bacteria are to be identified from collected material such as bioaerosols, significant background interferences may be encountered. To address these issues, there is a need for rapid analysis methods that have the ability to differentiate one bacterial species from one another based upon their characteristic profiles even if the biomarkers are obscured in mixtures of bacteria or background interferences.

Ion mobility spectrometry (IMS), as introduced in Chapter 1 and described in Chapter 2, is a fast gas phase separation technique that separates ions based upon their charge and collision cross section.[75] Molecules in the sample to be investigated are ionized and the ions enter the mobility drift tube. In the drift tube, ions drift in a weak electric field and a buffer gas at a pressure of a few Torr. Ions with greater collision cross sections collide more times with the buffer gas than the smaller ions,

thus smaller ions traverse the drift cell more quickly. This means that ions of the same mass but different size can be separated.

Ion mobility spectrometry combined with mass spectrometry (IMMS) can be used to investigate complex mixtures that are often encountered in bacterial biomarker identification, including both background and environmental interferences and complex mixtures of bacteria.[76] Both electrospray ionization (ESI) and MALDI have been used for analyte ionization for IMMS investigations. But for rapid bacteria identification, MALDI has the advantage of faster sample preparation, tolerance of impurities, and the propensity to produce singly charged ions, which can reduce spectral congestion. In IMMS, ions drift in the presence of a weak electric field through an intermediate pressure buffer gas (typically helium) and are separated according to the ratio of their size to charge. This separation occurs on a millisecond time scale and is characterized by the ion mobility drift time.[75] Different classes of molecules common in biological samples and complex mixtures such as peptides, lipids, carbohydrates, and nucleic acids are separated in the first dimension by size-to-charge and then in the second dimension by mass-to-charge.

The plot of ion mobility drift time as a function of m/z is a mass-mobility correlation represented in two-dimensional space for multiple components as groupings of peaks with different slopes that are called trend lines. Ions of a particular biomolecular class tend to lie on a single trend line. Each biomolecular class has different collision cross sections, for example oligonucleotides > carbohydrates > peptides > lipids.[214-262] When investigating a complex mixture, results show multiple trend lines,[213, 222] thus, allowing initial identification of molecular classes.[214] By using IMMS, identification of multiple biomolecular ions can be achieved at once, which decreases identification times.

IMS has been used as a tool for bacterial biomarker profiling.[180, 181, 263] Snyder and co-workers used IMS to indirectly detect *E. coli* (ATCC 11303) by monitoring the reaction of *in vivo E. coli* β-

galactosidase enzyme with (o-nitro-phenyl) β-D-galactopyranoside (ONPG), an enzyme assay used to detect water contaminated with *Enterobacteriaceae*.[180] Similarly, IMS with thermal desorption for sample introduction was used to generate fingerprints and differentiate between bacterial strains of whole cell bacteria directly from colonies on agar plates.[181] Using IMS in conjunction with MS, more than 200 metabolites from *E. coli* cultures were detected.[188]

In this chapter, we report the identification of microorganisms utilizing MALDI-IM-TOF MS and MALDI-TOF MS. Initial studies focused on testing IMMS for bacteria identification and then this technique was used to study common bacteria such as *E. coli* and *B. subtilis*, which are both well studied using mass spectrometry and have been investigated by a number of groups.[264, 265, 266, 267, 268]

3.2 Experimental

A total of 20 mg/ml of each lyophilized *Bacillus subtilis* ATCC 6633 and *Escherichia coli* strain W ATCC 9637 cells were suspended in 1:1 ACN/0.1% TFA and vortexed. Saturated matrix solution of α-cyano-4-hydroxycinnamic acid (CHCA) was prepared by dissolving 30 mg of CHCA matrix in 1 mL of 1:1 ACN/0.1% TFA. The matrix solution was mixed with the suspension in a 1:2 ratio of bacterial suspension to matrix solution. A 1μL volume was deposited on the target and allowed to dry. Samples were prepared in the same manner for the MALDI-TOF MS and MALDI-IM-TOF MS experiments. Details of both of the instruments used are described in detail in Chapter 2, Sections 2.1 and 2.2, respectively.

3.3 Results and Discussion

MALDI-TOF MS and MALDI-IM-TOF MS experiments were performed on dried-droplet intact whole cell *B. subtilis* and *E. coli*. The information obtained from the MALDI spectra is compared with spectra obtained from the MALDI-IM-TOF MS experiments. Peaks from the *E. coli* spectra were searched for possible identification using Rapid Microorganism Identification Database. Additionally, VUV post-ionization MALDI-IM-TOF MS experiments were performed to obtain more information from the intact bacteria.

MALDI-TOF & MALDI-TOF IM MS of *B. subtilis*

A MALDI-TOF mass spectrum of *B. subtilis* is shown in Figure 3.1. As seen in Figure 3.1(a), a number of peaks in the range of 1–4 kDa were observed. The first cluster of peaks near 1100 *m/z* in Figure 3.1(a) is attributed to two classes of lipopeptide isoforms known as surfactins and mycosubtilins (iturin family), which have been previously identified using MALDI MS.[264, 265, 269, 270, 271] Lipopetides are a class of non-ribosomally generated amphiphilic peptides that are categorized according to their structure and activity and can be found in a number of different species of *Bacillus*. Surfactins are composed of a β-hydroxy fatty acid (C_{13} to C_{16}) linked to a cyclic lipoheptapeptide with n = 9-11, where n is the number of CH_2 groups.[264] Mycosubtilins are similar to surfactins but contain a β-amino fatty acid sequence (C_{14} to C_{17}), n = 11-13. The broad distribution of peaks from 2000 *m/z* to near 3000 *m/z*, separated by 14 Da (CH_2 group), is from the ionization of molecules in the peptidoglycan layer of the bacterial cell wall.
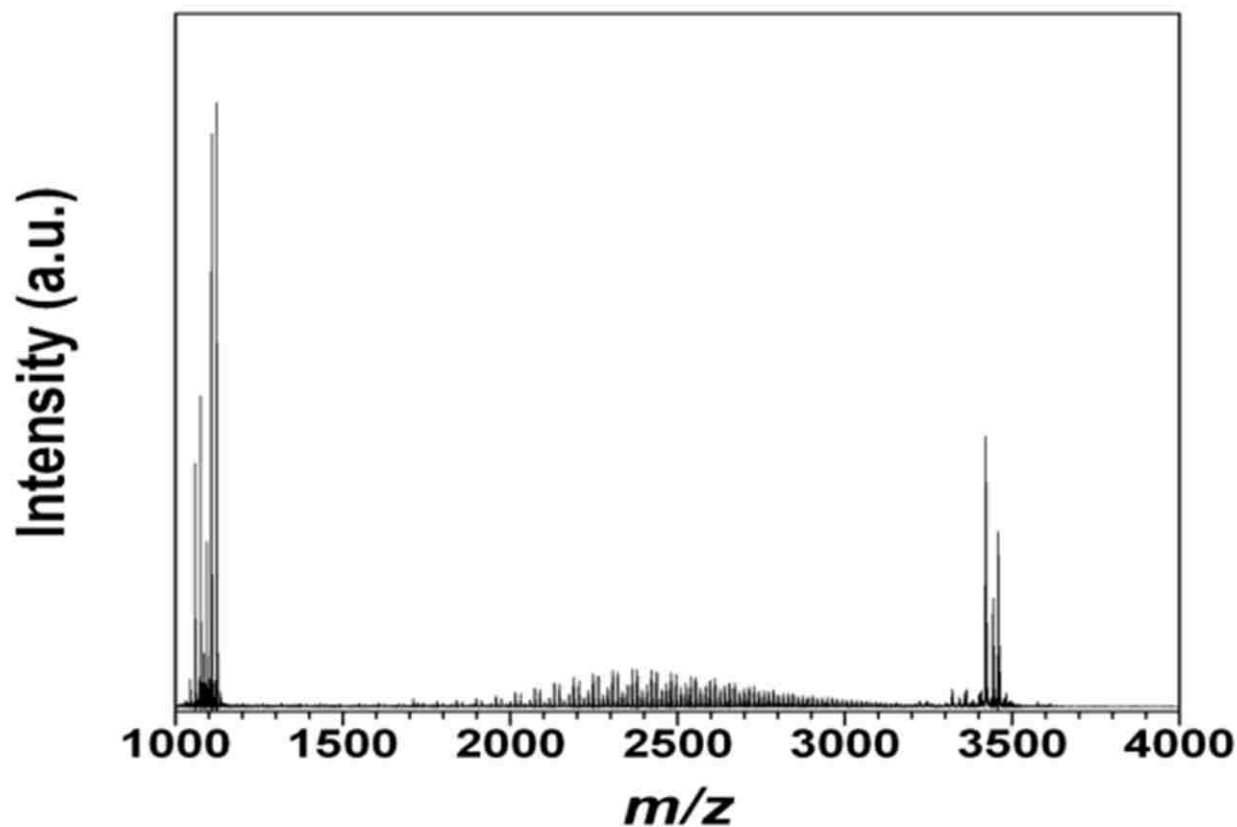
Figure 3.1(a). MALDI mass spectra of *B. subtilis* using α–cyano-4-hydroxycinnamic acid (CHCA) matrix.

The expanded spectrum of Figure 3.1(a) is shown in Figure 3.1(b). The peak detected at *m/z* 1044 corresponds to the surfactin b-C_{15} sodium adduct and the peaks at 1058 and 1074, correspond to surfactin a-C_{15} sodium and potassium adduct ions (Figure 3.1(b)). The peaks at 1085, 1107, and 1123 *m/z* (Figure 3.1(b)) correspond to H^+, Na^+, and K^+ adducts of mycosubtilin-C_{17}, respectively. The peak at 1093 corresponds to mycosubtilin-C_{16} sodium adduct (Figure 3.1(b))
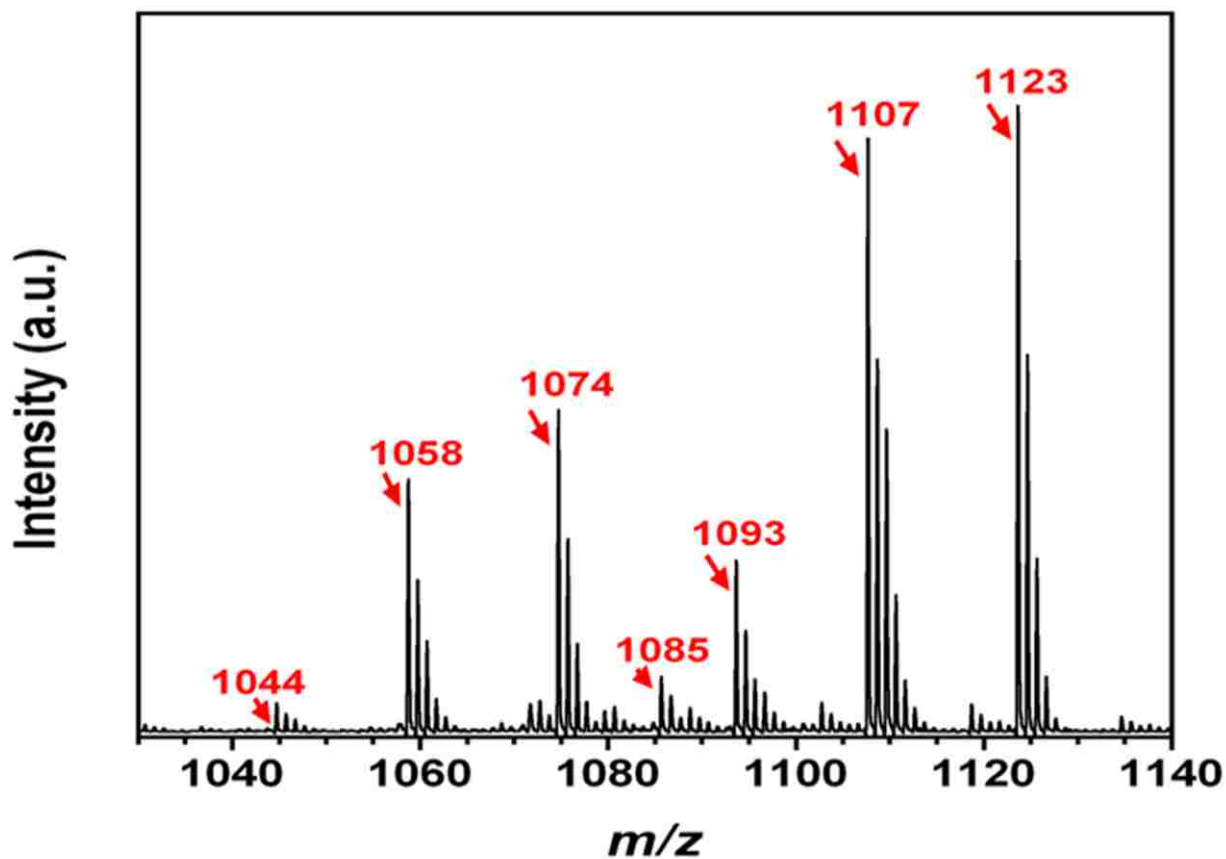
Figure 3.1(b). Expanded view of *B. subtilis* lipopeptide products.

The third cluster of peaks near 3500 *m/z* shown in Figure 3.1(c) correspond to a 32-amino-acid pentacyclic lantibiotic ribosomally synthesized as a prepeptide which undergoes posttranslational modification resulting in the mature protein subtilin, which is a lantibiotic that can be found in different strains of *B. subtilis*.[264, 265, 270] The peak at 3319 *m/z* corresponds to the protonated ribosomally synthesized lantibiotic subtilin and the intense peak at 3419 *m/z* is attributed to lantibiotic subtilin with a N-terminally succinylated subtilin. Sodium and potassium adducts of the succinylated subtilin gives rise to peaks that are observed at 3441 *m/z* and 3457 *m/z*, respectively.
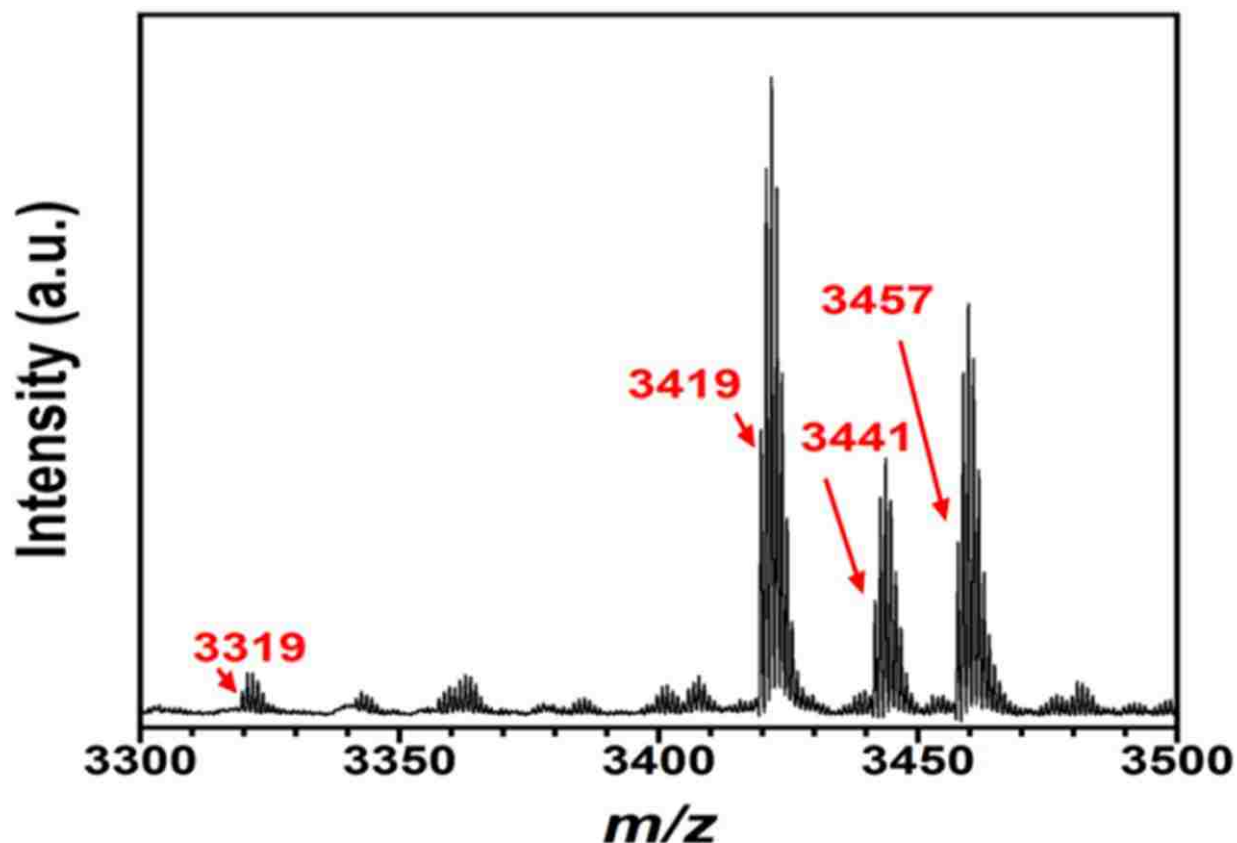
Figure 3.1(c). Expanded view of *B. subtilis* subtilin with adducts and a protecting group.

The two-dimensional MALDI ion mobility mass spectrometry contour plot from *B. subtilis* is shown in Figure 3.2. The mass spectrum was obtained using a 349 nm laser at a repetition rate of 200 Hz. The plot above the top x-axis is the mass spectrum obtained by integrating the signal over all mobility times and the plot on the right hand y-axis is the ion mobility trace obtained by integrating over the *m/z* values. The plot shows three groupings of peaks in the range between 1000 and 3500 *m/z* on two distinct trend lines. From previous work,[183, 214] it can be inferred that the upper trend line corresponds to lipids whereas the lower trend line corresponds to peptides. The strong signal on the lower trend line 1100 *m/z* results from lipopeptides. In the middle of the contour plot, the features on the upper trend line correspond to lipids. The island of signal at the upper right of the plot corresponds to subtilin.
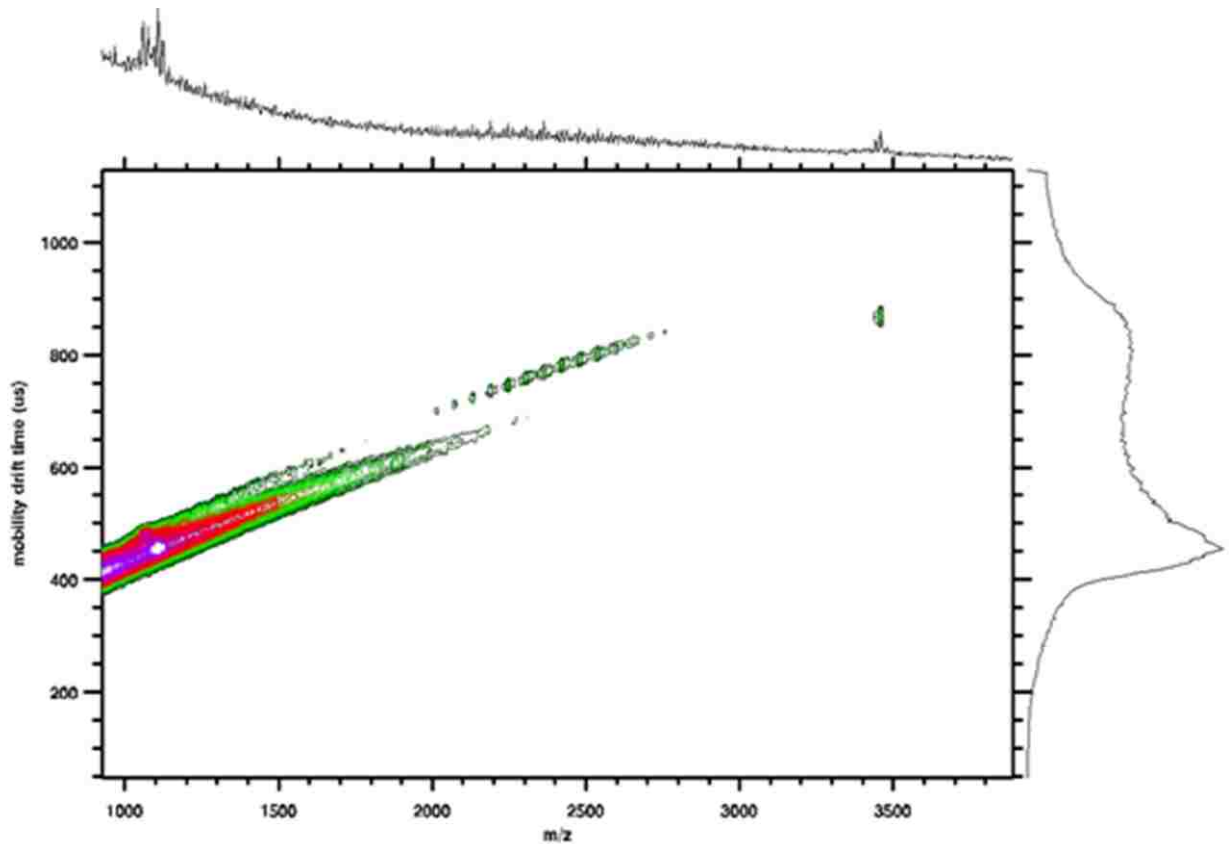
Figure 3.2. UV MALDI-IM-TOF MS 2D contour plot of whole cell *B. subtilis*.

The first cluster of peaks in the mass spectrum of the 2D contour plot of Figure 3.2 is shown below in an expanded view in Figure 3.3. The pattern of the first cluster of peaks in the mass spectrum of the 2D contour plot is typically found for lipopeptides, representative of surfactin and mycosubtilin of the iturin family.[264] One can see that the two most intense peaks at 1058 *m/z* and 1074 *m/z* with a mobility drift time of 470 μs in the first cluster are attributed to surfactin-C_{15} with sodium and potassium adducts just as in the MALDI-TOF MS spectrum in Figure 3.1(b). Isoforms mycosubtilin-C_{16} and mycosubtilin-C_{17} are observed at 1093 and 1107 *m/z*, respectively, both with Na$^+$ adducts and a

mobility drift time of 440 μs. The peak at 1123 *m/z* with a mobility drift time of 440 μs is assigned as

the potassium adduct of mycosubtilin-C_{17}, as observed in the MALDI MS spectrum of Figure 3.1(b).
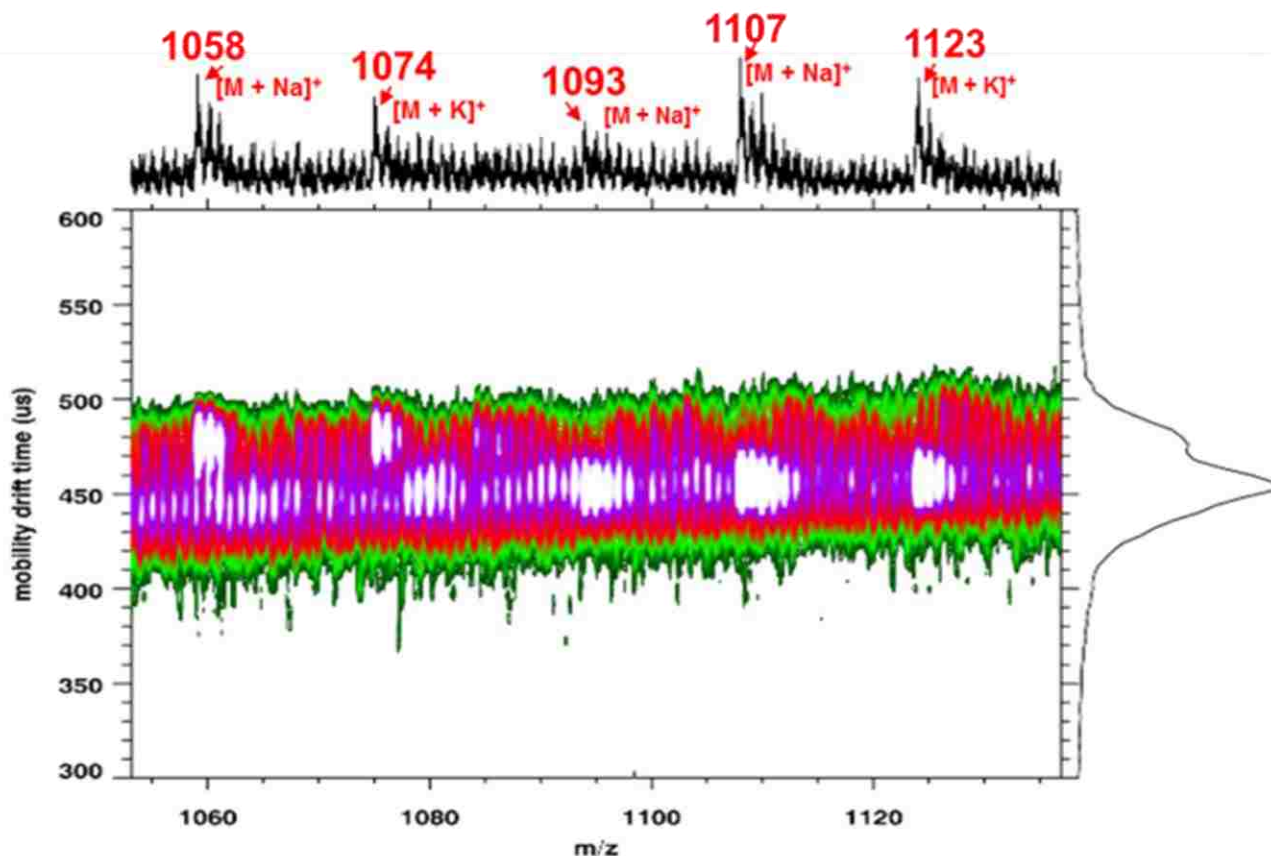
Figure 3.3. UV MALDI-IM-TOF MS 2D contour plot of lipopeptide products with Na^+ and K^+ adducts from whole cell *B. subtilis*.

The second cluster of peaks in the middle of the spectrum in Figure 3.2, from approximately

1900 *m/z* to near 3000 *m/z* with a mobility drift time range of 670 μs to 790 μs, is shown in an

expanded view below in Figure 3.4. These peaks are separated by the mass of CH_2, 14 Da, and are

attributed to the peptidoglycan layer of the bacterial cell wall.
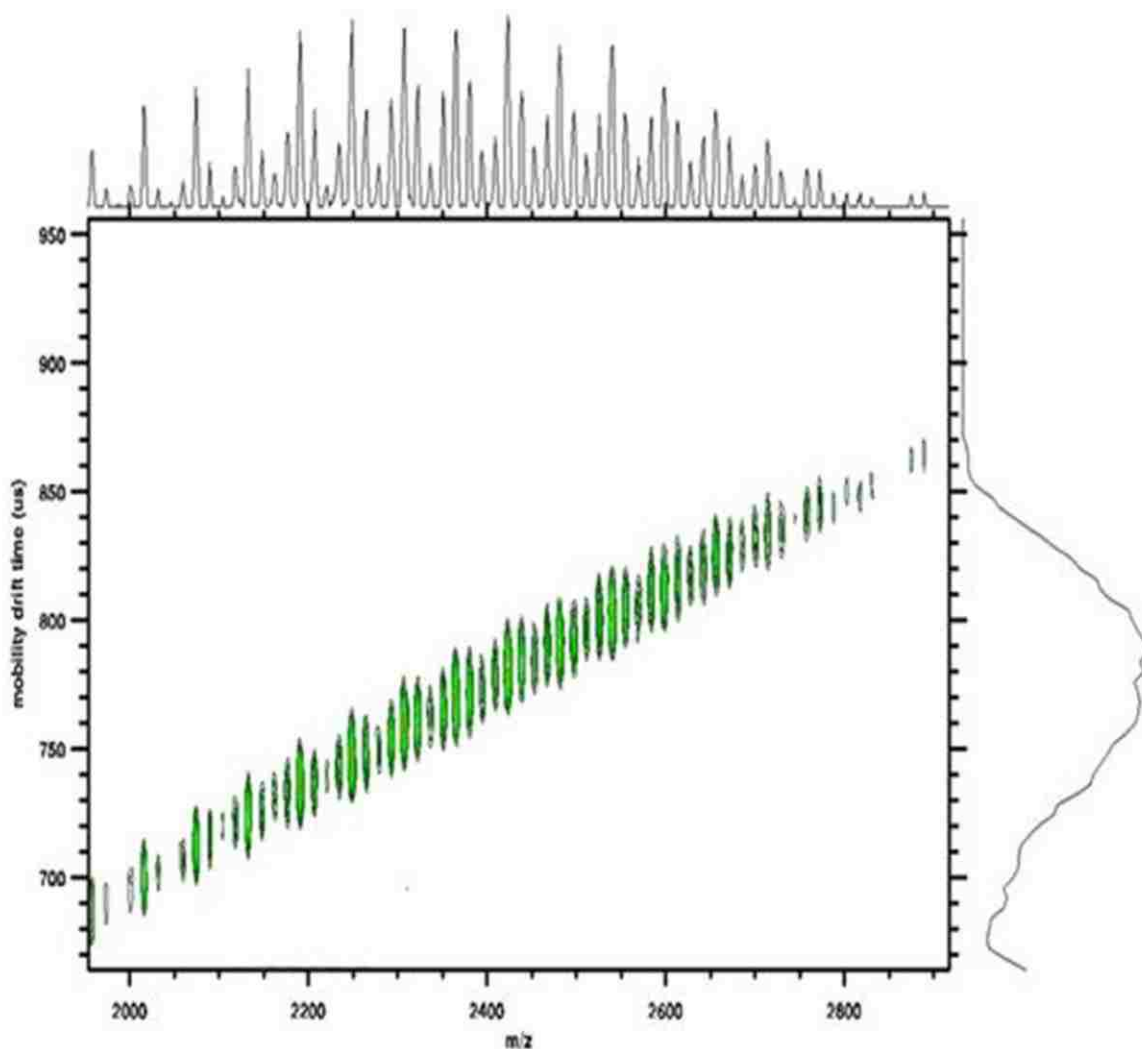
Figure 3.4. UV MALDI-IM-TOF MS 2D contour plot of fatty acids separated by 14 Da from whole cell *B. subtilis*.

In Figure 3.5, the expanded view of the third cluster near 3450 *m/z* with a mobility drift time of 870 μs from Figure 3.2 is shown. The peak seen at 3441 *m/z* is assigned to the $[M + Na]^+$ peak of succinated subtilin; the K^+ adduct appears at 3457 *m/z*. The subtilin or succinated subtilin protonated molecule peaks were not observed in the spectrum of Figure 3.1(c). The peaks attributed to subtilin as well as the lipopeptides are in agreement with spectra shown in current mass spectrometry literature.[264]
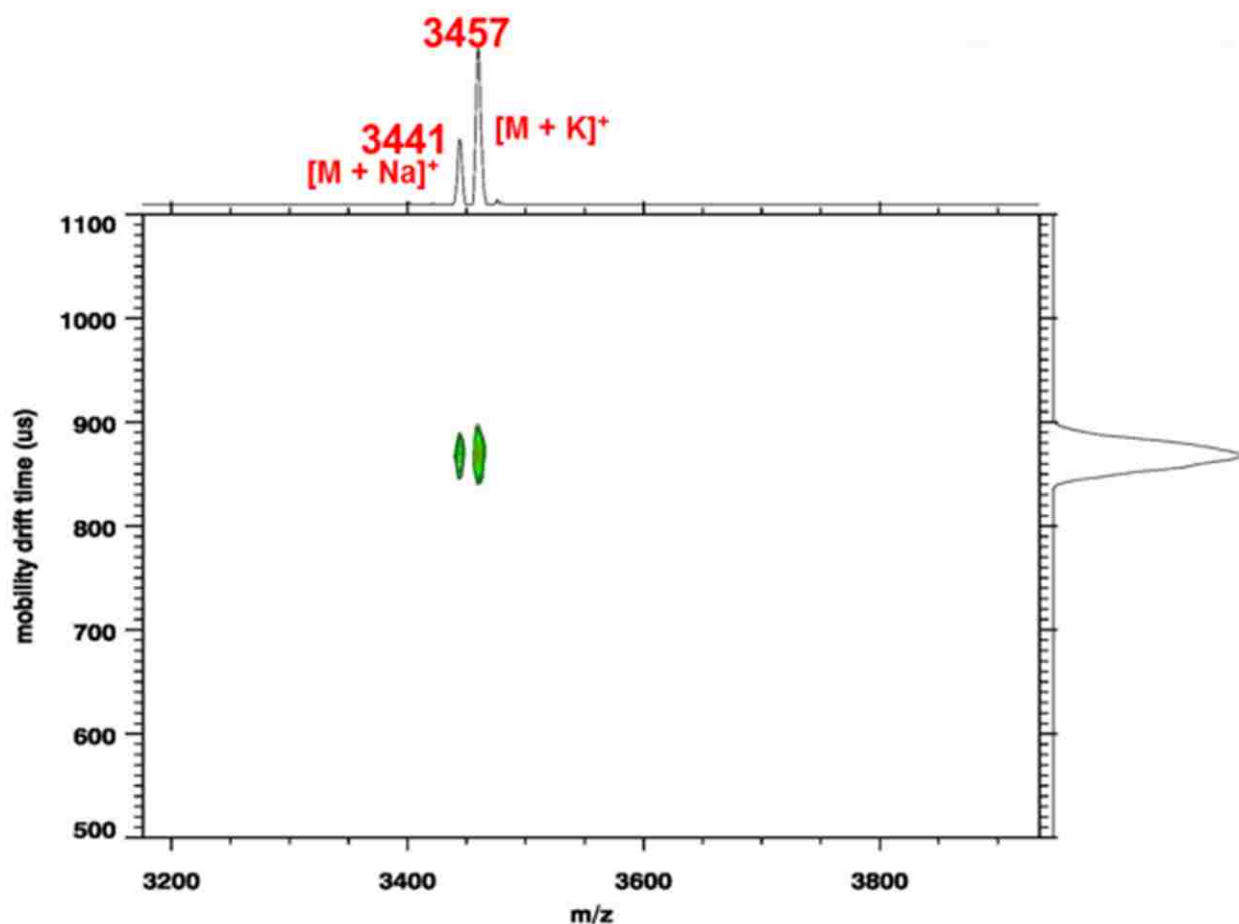
Figure 3.5. UV MALDI-IM-TOF MS 2D contour plot of whole cell *B. subtilis*. The peaks correspond to N-terminal succinylated subtilin with Na$^+$ and K$^+$ adducts.

To obtain additional information, VUV post-ionization MALDI-IM-TOF MS was used for the analysis of *B. subtilis*. As expected, the groupings of the isoforms of surfactins and mycosubtilins observed using UV MALDI-IM-TOF MS have the same mobility and lie on the same trend lines, although a few additional lipopeptides were observed (Figure 3.6). These additional lipopeptides are associated with peaks in the x-axis of the contour plot at 1079, 1090, and 1329 *m/z*. The peaks at 1079 and 1090 *m/z* lie on the same trend line with the aforementioned surfactins and mycosubtilins, suggesting they are isoforms of surfactin and mycosubtilin in the form of Na$^+$ and K$^+$ adducts,

respectively. Although, the ion peak at 1329 *m/z* peak lie on the same trend line as the mycosubtilin family, it is yet to be identified. In Figure 3.6, a peak corresponding to mycosubtilin-C_{17} with a K^+ adduct is observed at 1123 *m/z* in the VUV post-ionization MALDI-IM-TOF MS spectrum of *B. subtilis*.
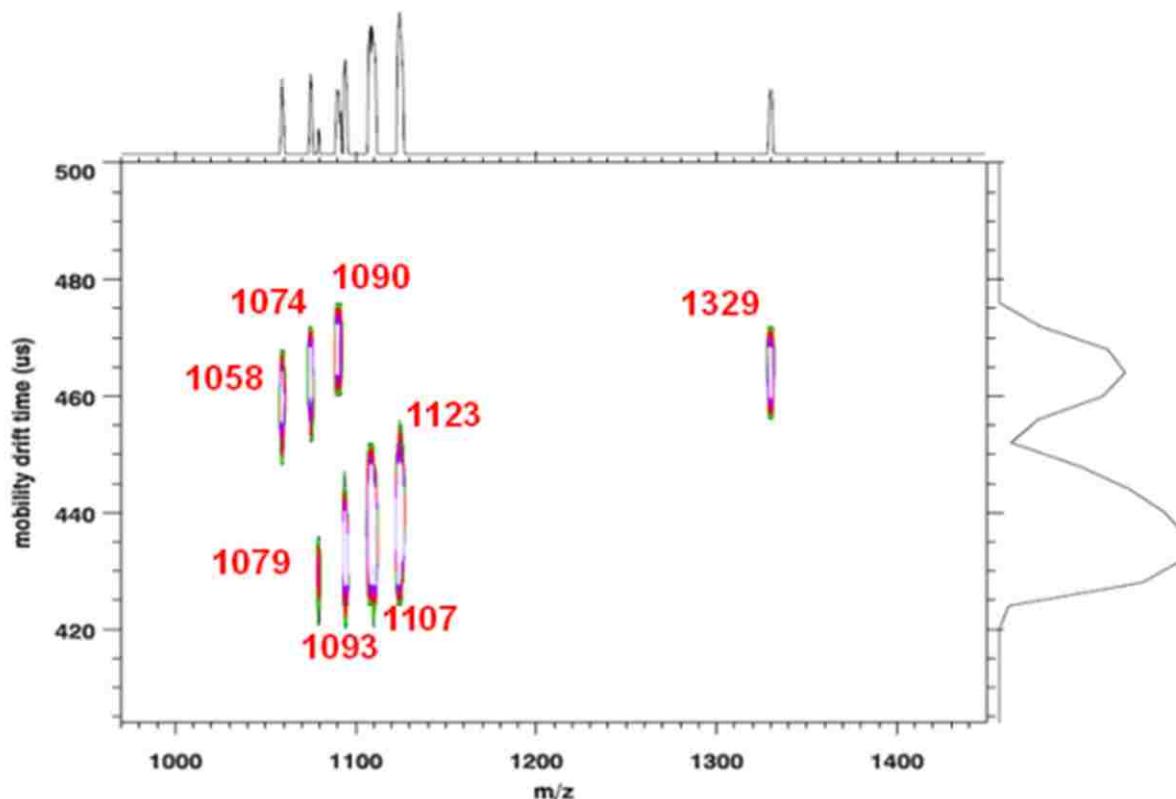
Figure 3.6. VUV post-ionization MALDI-IM-TOF MS 2D contour plot of whole cell *B. subtilis*. Additional peaks at 1079, 1090, and 1329 *m/z* were observed.

MALDI-TOF & MALDI-TOF IM MS of *E. coli*

In Figure 3.7, the MALDI spectrum from the analysis of *E. coli* is shown. This spectrum is similar to previous published spectra of *E. coli*.[104, 266, 267] The peak positions and assignments are listed in Table 3.1. All peaks with *m/z* values between 4000 and 15,000 *m/z* were searched against the Rapid Microorganism Identification Database (RMIDb).[246]
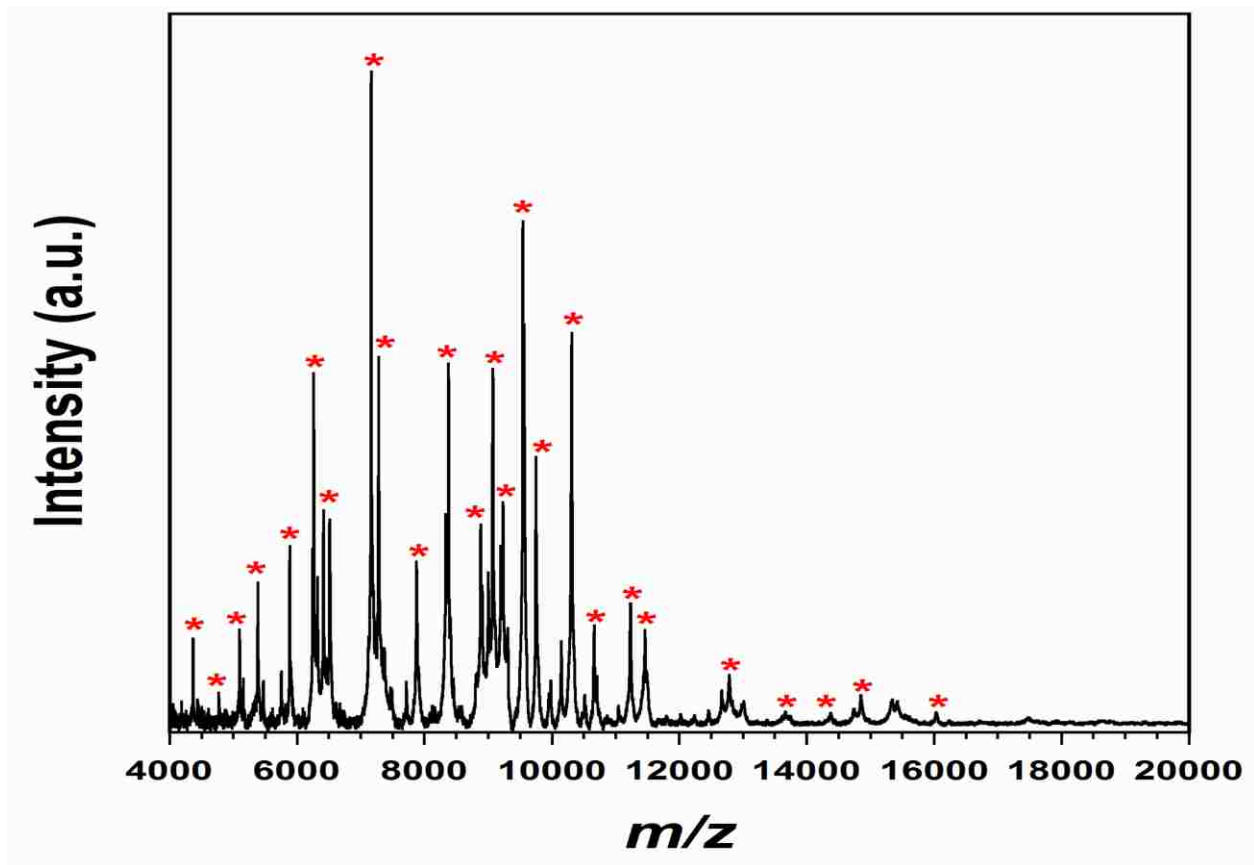
Figure 3.7. MALDI- TOF MS mass spectra of *E. coli* using CHCA matrix.

The model (type of proteins) used for this search was Bacterial Ribosomal Proteins from all sources, which included Genbank, TrEMBL, SwissProt, RefSeq, Ventor Institute's Comprehensive Microbial Resource (CMR), and Glimmer3. The search was conducted using *m/z* values corresponding to a + 1 charge (singly protonated). The mass error window selected for the search performed was $\pm$ 10. Of the observed peaks, most correspond to ribosomal subunit proteins, four (5097, 5384, 6416, and 7280 *m/z*) have been previously identified as singly charged ribosomal proteins,[272] while a few are Glimmer3 predictions. Glimmer3 is an algorithm that predicts protein sequences on bacterial genomes.[249] These possible protein sequences are obtained from a number of protein database sources.

80

Table 3-1. Ribosomal proteins detected from E. coli by MALDI-TOF MS

Observed Mass	Theoretical Mass	Proteins Description	Organism	Accession Number
4366	4365	50 S R protein L36	*E. coli* E24377A	A7ZSI8
5097	5096	30 S R protein S22	*E. coli* E2348168	Z15486706
5384	5381	50 S R protein L34	*E. coli* E2348168	A7ZTQ9
6416	6411	50 S R protein L30	*E. coli* E24377A	A7ZSJ1
7164	7158	50 S R protein L35	*E. coli* S88	B7MAS7
7280	7274	50 S R protein L29	*E. coli* E24377A	A7ZSK1
7877	7872	50 S R protein L31	*E. coli* E24377A	A7ZUF1
8376	8369	30 S R protein S21	*E. coli* UT189	215488396
8884	8876	50 S R protein L28	*E. coli* E24377A	A7ZT18
9544	9548	G3 prediction	*E. coli* 536	GL82531
4366	4365	30 S R protein S15	*E. coli* E2438169	215488483
5097	5096	30 S R protein S19	*E. coli* E2438169	215488616
5384	5381	G3 prediction	*E. coli* 536	GL8253
6416	6411	30 S R protein S14	*E. coli* E2438169	218555864
7164	7158	50 S R protein L18	*E. coli* E24377A	A7ZSJ3
7280	7274	50 S R protein L29	*E. coli* E24377A	A7ZSK1
7877	7872	50 S R protein L36	*E. coli* E24377A	A7ZSI8
8376	8369	30 S R protein S22	*E. coli* E2348168	Z15486706
8884	8876	50 S R protein L34	*E. coli* E2348168	A7ZTQ9
9544	9548	50 S R protein L30	*E. coli* E24377A	A7ZSJ1
10146	10138	50 S R protein L35	*E. coli* S88	B7MAS7
10309	10300	50 S R protein L29	*E. coli* E24377A	A7ZSK1
11233	11229	50 S R protein L31	*E. coli* E24377A	A7ZUF1
11460	11464	30 S R protein S21	*E. coli* UT189	215488396
12780	12770	50 S R protein L18	*E. coli* E24377A	A7ZSJ3
14372	14365	50 S protein L29	*E. coli* E24377A	A7ZSK1

If Glimmer3 is the only matching protein sequence, this means there is no protein sequence that matches the given mass. There is a possibility that the protein sequence does not exist or it could be a real protein that is simply missing from the protein sequence database.

A 2D contour plot resulting from the analysis of *E. coli* is shown in Figure 3.8. The plot shows two trend lines that correspond to a total of 18 peaks.
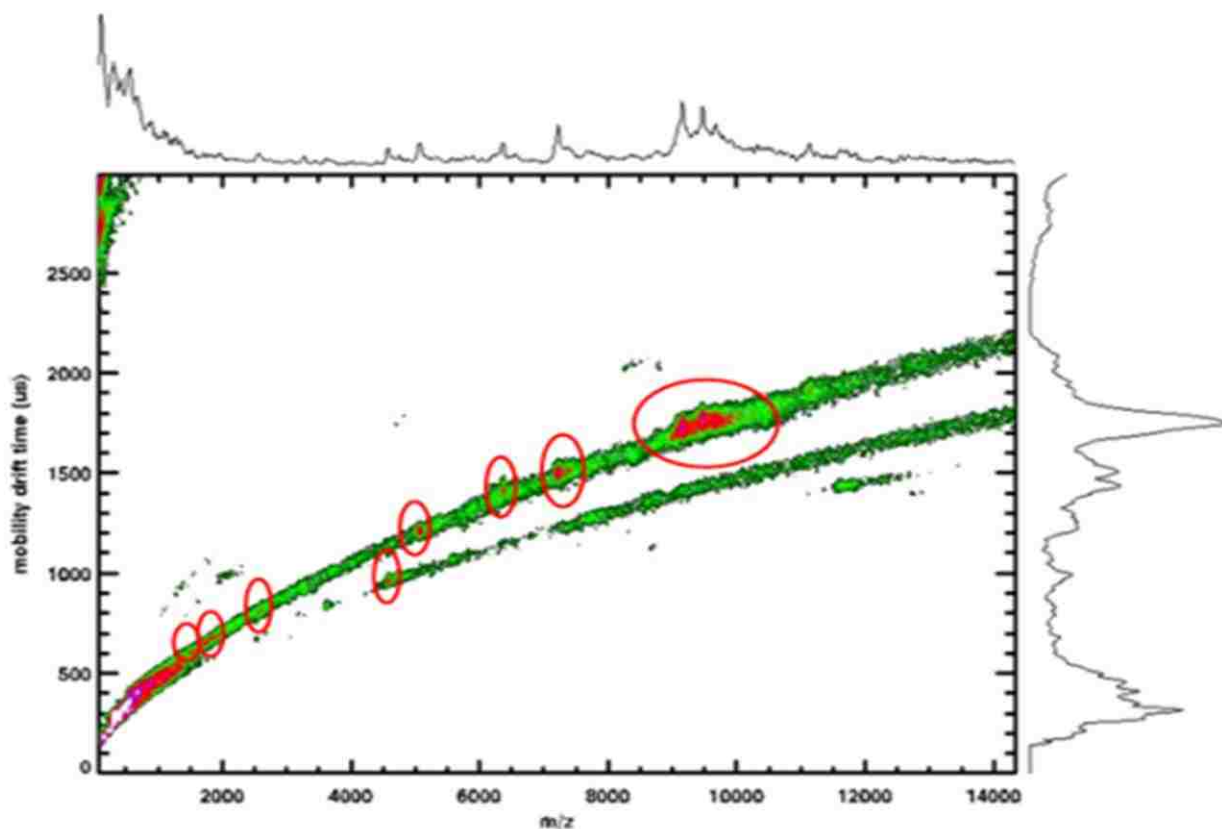
Figure 3.8. UV MALDI-IM-TOF MS 2D contour plot of whole cell *E. coli*.

The peaks were observed in the mass range of 1000 to 12,000 *m/z* with a mobility time of 670 to 1780 μs. For this analysis, masses of peaks of 4000 *m/z* or greater were searched against the Rapid Microorganism Identification Database using the model Bacterial Ribosomal Proteins from all sources.

The search was conducted using *m/z* values with a +1 charge (singly protonated). The error window for the search was ±10 Da. The RMIDb search from the MALDI-IM TOF MS data yielded one possible identification, which was a Glimmer3 prediction at 4742 *m/z* corresponding to a protein with accession number GL10468.1400. Most of the peaks from the MALDI-TOF MS data listed in Table 3.1 were identified as ribosomal proteins, while a few values were assigned as Glimmer 3 predicted sequences.

Using MALDI-IM-TOF MS, it was possible to separate in *B. subtilis* isoforms of a class of non-ribosomally generated lipopetides (surfactins, mycosubtilins), a ribosomally synthesized lantibiotic (subtilin), and a polymer-like pattern thought to be associated with the peptidoglycan layer of the cell wall. Furthermore, an additional surfactin isoform (1090 *m/z*) and an additional mycosubtilin isoform at (1079 *m/z*) were observed when using VUV post-ionization MALDI-IM-TOF MS, as well as a $[M + H]^+$ ion, at 1329 *m/z* that most likely corresponds to a lipopeptide of the mycosubtilin family, suggested by its position on the trend line with other mycosubtilins. The ion at 1329 *m/z* was only observed in the VUV post-ionization MALDI-IM TOF MS experiments. MALDI-IM-TOF MS was also effective in separating proteins from *E. coli*.

The strategy of MALDI-IM-TOF MS studies in parallel with the MALDI-TOF MS studies highlights the added advantage of the ion mobility dimension. In Figure 3.2, the two different trend lines observed in the two-dimensional fingerprint of the *B. subtilis* establishes the presence of different molecular classes of biomolecules, which in this case are peptides and lipids, before any database search. In Figure 3.3, the divergence of ions of the same biomolecular class from the trend line is the result of structural differences.[213] In this case, both lipopeptides, the surfactins and mycosubtilins, have similar drift times but the mycosubtilins lie slightly below the lipopeptide trend line due to a more compact structure. The surfactins are linked by a β-hydroxy fatty acid whereas mycosubtilins have a β−amino fatty acid linkage. The unidentified weak signals in the 1-D mass portion of the plot in the range 1050 to 1150 *m/z* are attributed to isoforms of surfactins and mycosubtilins, which have also

been noted in recent work.[264, 265] The difference in the mobility drift time of the surfactin and mycosubtilins can be seen more distinctly in the VUV MALDI-IM-TOF MS data of Figure 3.6. Figure 3.6 also shows that three additional peaks were observed when using VUV MALDI-IM-TOF. One of the additional peaks observed is at 1090 *m/z*. This lies on the same trend line as the previously identified 1058 and 1074 *m/z* peaks. The other two additional peaks observed at 1079 and 1329 *m/z* lie on the same trend line as the mycosubtilins. These additional peaks lie on the surfactin and mycosubtilin trend lines, suggesting they are isoforms of the surfactin and mycosubtilin families.

3.4 Summary

In this chapter, MALDI-IM-TOF MS was used for the detection and identification of *B. subtilis* ATCC 6633 and *E. coli* ATCC 9637. MALDI-TOF MS was conducted in parallel as confirmation. Isobaric lipids, peptides, and proteins were separated on IMMS trend lines, which allowed the type of biomolecule to be distinguished prior to *m/z* separation. A number of proteins detected from *E. coli* using MALDI-TOF MS could be identified; however, when using MALDI-IM-TOF MS, a Glimmer3 predicted sequence was obtained for only one of the number proteins detected in *E. coli*. Lipopeptides, surfactin and mycosubtilin, were identified from *B. subtilis* were observed on different trend lines because of their structural differences using both MALDI-IM-TOF MS and MALDI-TOF MS. Additional lipopeptides were identified using VUV post-ionization MALDI-IM-TOF MS. These observations show the promise of MALDI-IM-TOF MS as a microorganism biomarker identification tool.

CHAPTER 4. MALDI MICROORGANISM IDENTIFICATION IN THE PRESENCE OF INTERFERENTS

In the previous chapter, the use of MALDI and MALDI IM-TOF MS for detection and identification of lyophilized bacteria was described. However, as previously discussed, the identification of bacteria during field analysis can be complicated by the presence of environmental interferents and weaponizing agents. To address this challenge, bacterial species were prepared with possible interferents at various mass ratios and analyzed using MALDI TOF MS. The effect of interferents on the identification of bacteria was evaluated using a bacteria fingerprinting software (MALDI Biotyper). We were able to determine that bacterial identification was possible in the presence interferents and the amount of interferent present before a correct species or genus identification was no longer possible.

4.1 Introduction

Detecting microbial pathogens in an ambient environment is not straightforward. A number of interferences may be encountered: humic-like substances (HULIS), secondary organic aerosols (SOA), minerals/mineral dust, benign bacteria, mold spores, and polycyclic aromatic hydrocarbons (PAH).[20] In addition, there are other background particulate sources: pollen, dust, smog and man-made particulate that include industrial pollutants and vehicle exhaust.[17, 18, 273] The problem of background particulate in field analysis can be two-fold: a highly concentrated environmental background concentration can mask the presence of biological agents and there is the possibility of background particulate generating false positives.[16, 17]

MALDI of collected particles containing biological molecules have been aerosolized in the laboratory for proof-of-concept collection, detection, and identification.[274] Lyophilized whole cells of

E. coli were nebulized and collected on a target pre-coated with matrix or a target to which matrix is added to the collected material and analyzed using MALDI MS. The MALDI mass spectra of the collected *E. coli* cells were comparable to the MALDI mass spectra of dried-droplet *E. coli*, although the mass spectra of the collected material had fewer peaks above 10,000 *m/z*. In a subsequent study, collected whole cells of *E. coli* were enzymatically-digested on target and analyzed using MALDI MS. The mass spectrum of the digested *E. coli* cells showed a number of peptide fragments that were searched in a protein database for identification.[275] Although, the *E. coli* species in both sampling studies could be identified, the studies do not fully address the issue of detection in a real-world setting.

Approaches to bioaerosol sampling can be challenging and often has to be modified, depending on the properties of the target bioaerosols. Traditionally, capture and culture methods have been used.[139] Sampling is further compounded when interferents are present. Some detection strategies have used separation techniques to isolate components of the collected bioaerosols, while other strategies undertake analysis in the presence of interferences. To date, there are no standard methods used for bioaerosol sampling or characterization.[18] Sampling analysis methods employ a number of collection devices such as impact samplers, filtration systems, and cyclones for off-line and on-line analysis.

An automated pathogen detection system (APDS) has been developed for bioaerosol collection and detection of *B. anthracis, B. thurigiensis, and Y. pestis*.[276] The APDS has a collector, which is an impactor that collects particles from 1 to 10 μm in size; a microfluidics module that disperses the sample and reagents; a collection of 7 immunoassays (3 for bioagents and 4 assay controls) that was developed for use with a flow cytometer. The immunoassays use polystyrene microbeads, which have immobilized antibodies and are embedded with fluorescent dyes that are activated when the antigen

binds to the microbeads. The activated microbeads are read by the flow cytometer. The APDS was tested by using a Collison nebulizer to generate individual *B. anthracis* and *Y. pestis* respirable-size particles and a mixture of the two species, over a range of concentrations. Signals for each species were only observed when that particular species was released. When *B. anthracis* and *Y. pestis* were released as a mixture, both species were detected. For both studies, no false positives were reported and there was no indication of inhibition, non-specific binding, or cross-reactivity for any of the species.

Fergenson *et al.* used a dual polarity ATOF MS in real-time to differentiate aerosolized *B. thuringiensis* and *B. atrophaeus*.[163] Experiments were also conducted to detect these species in the presence of other aerosolized biological material that could potentially be present in the environment, such as, background aerosols (diesel, smoke, dust) and "white powders" that could be present in a bioterrorism hoax situation. The ATOF MS spectra of *B. thuringiensis* and *B. atrophaeus* were identical with the exception of the differences in intensity of sodium and potassium adduct peaks in the spectra. In the presence of background aerosols and aerosolized biological and non-biological materials, *Bacillus* spores were detected.

Both of the examples of aerosol analysis methods listed above are ideal sampling and collection methods; however, in the first example, possible interferents were not considered. The use of the dual polarity ATOF system in the second example does account for interferences but identifications are at the genus level. Using MALDI for collected bioaerosols is advantageous because little sample preparation is needed, it is able to tolerate impurities, and a large set of possible biomarkers can be screened for identification because of its extended mass range.

The presence of background aerosols and interferents can also present challenges in a battlefield environment. As previously discussed in Chapter 1, in addition to background aerosols and

interferents, weaponizing agents such as fumed silica or bentonite may also be encountered in a battlefield environment or in the event of a bioterrorist attack in a civilian setting.[40, 277] These particulates together create a complex background that can change depending on the weather and other conditions. In such an event, the goal is to collect the sample, perform minimal sample pre-treatment, and obtain an accurate identification in the presence of these interferents.

In the work described in this chapter, the goal was to determine how contaminants found in collected bioaerosols may affect bacteria detection and identification using MALDI TOF MS and MB. Microorganism identification in the presence of naturally occurring and man-made background interferents and weaponizing agents was evaluated. The MALDI mass spectra of bacteria in the presence of these interferents were searched against reference mass spectra in the MB database for identification.

4.2 Experimental

Lyophilized *Enterobacter aerogenes* 13048 and *E. coli* 35218 were purchased from *American Type Culture Collection (*ATCC) in Manassas, VA and diesel particulate was purchased from the National Institute of Standards and Technology (Gaithersburg, MD). Fumed silica, bentonite, pollen from *Juglans nigra* (black walnut), and α-cyano-4-hydroxycinnamic acid (CHCA), were purchased from Sigma Aldrich (St. Louis, MO) and used without further purification. HPLC grade acetonitrile (ACN 99.9%), formic acid (99.9%) and trifluoroacetic acid (TFA; 99%) were purchased from Fisher Scientific (Pittsburgh, PA). A total of 5 mg/ml of the cells were suspended in 1:1 ACN/0.1% TFA. Saturated matrix solutions were prepared by dissolving 20 mg of CHCA matrix in 1 mL of a 1:1 (v/v) mixture of 50% acetonitrile (ACN) and 2.5% trifluoroacetic acid (TFA) in nanopure water.

All interferent solutions were prepared by adding 1 μL of ethanol to 5 mg of each interferent. A 5 mg quantity of the bacteria was centrifuged in a mixture of 300 μL water and 900 μL ethanol for 2 min at 5000 rpm. The supernatant was removed and 50 μL of 70% formic acid and 50 μL of acetonitrile were added followed by centrifugation at 5000 rpm for 2 min. A 1 μL mixture of the supernatant and interferent was deposited onto a MALDI target (MTP BigAnchorChip 384) and air dried at room temperature followed by a 2 μL volume of saturated CHCA matrix that was also allowed to dry at room temperature.

Spectra were generated from ten individually prepared mixtures of *E. aerogenes* and *E. coli* with each interferent at different mass ratios. Initially, ten microcentrifuge tubes containing mixtures of individual interferents and bacterial species were prepared at equal mass (1x) and overlaid with CHCA matrix after air drying at room temperature. Once samples were analyzed, the spectra were imported into MALDI Biotyper for identification based on score values. The score values of the 10 spectra were averaged to obtain a value representative of each bacterium and interferent at each ratio. If a correct species and genus identification was obtained (score value 2.0) for a 1x bacterial species and interferent mixture, the bacterial species was further analyzed with five times as much interferent (5x) and ten times as much interferent (10x) or until identification was no longer possible (score value <1.7). For bacterial species that could not be identified at the species level (score $\geq$ 2.0) in a bacterial and interferent mixture at 1x, the amount of bacteria was doubled to obtain half as much interferent as bacteria (0.5x) or until a correct genus level identification could be achieved ($\geq$ 1.7) .

The Bruker UltrafleXtreme MALDI TOF/TOF instrument used for analysis in this chapter was discussed in detail in Chapter 2, Section 2.3. In this study, 65% of the laser energy was initially used to acquire each mass spectrum and was increased to a maximum of 85% if significant signal could not be

obtained. The MB mass fingerprint software used for identification was described in detail in Chapter 2, Section 2.6.

4.3 Results and Discussion

To show the effect of interferents on *E. aerogenes* and *E. coli,* both species and each interferent were analyzed individually, followed by the analysis of *E. aerogenes* and *E. coli* with each interferent. The individual mass spectra of *E. coli* and *E. aerogenes* and mass spectra of interferents are shown below. Mass spectra of *E. coli* and *E. aerogenes* with each interferent at various ratios are also presented.

MALDI-TOF MS analysis for *E. aerogenes* and *E. coli* was conducted and searched against the MALDI Biotyper database to establish species identification without any interferents. A total of 21 peaks from the *E. coli* species were observed in the MALDI mass spectrum in the range from 4 to 14 kDa, shown in Figure 4.1(a). The spectrum was compared to spectra in the reference library for a possible match. The search against the reference spectra resulted in a correct species identification with an average score of 2.3. In the mass spectrum of *E. aerogenes*, 24 peaks were observed and compared to the reference library and a score of 2.4 was obtained, as indicated in Figure 4.1(b).

MALDI MS spectra of each interferent was also recorded is the *m/z* range of 0 to 14,000 at 50% laser energy. There were no peaks observed apart from the CHCA matrix peaks and its fragments in the region below *m/z* 1,000 shown in Figure 4.2. A monomer and a dimer of the CHCA matrix was observed in the mass spectra of pollen, fumed silica, diesel particulate, and bentonite, while, a trimmer, in addition to a monomer and dimer, was also observed for both bentonite and diesel particulate. The intensity of the CHCA matrix peaks varied with each interferent.
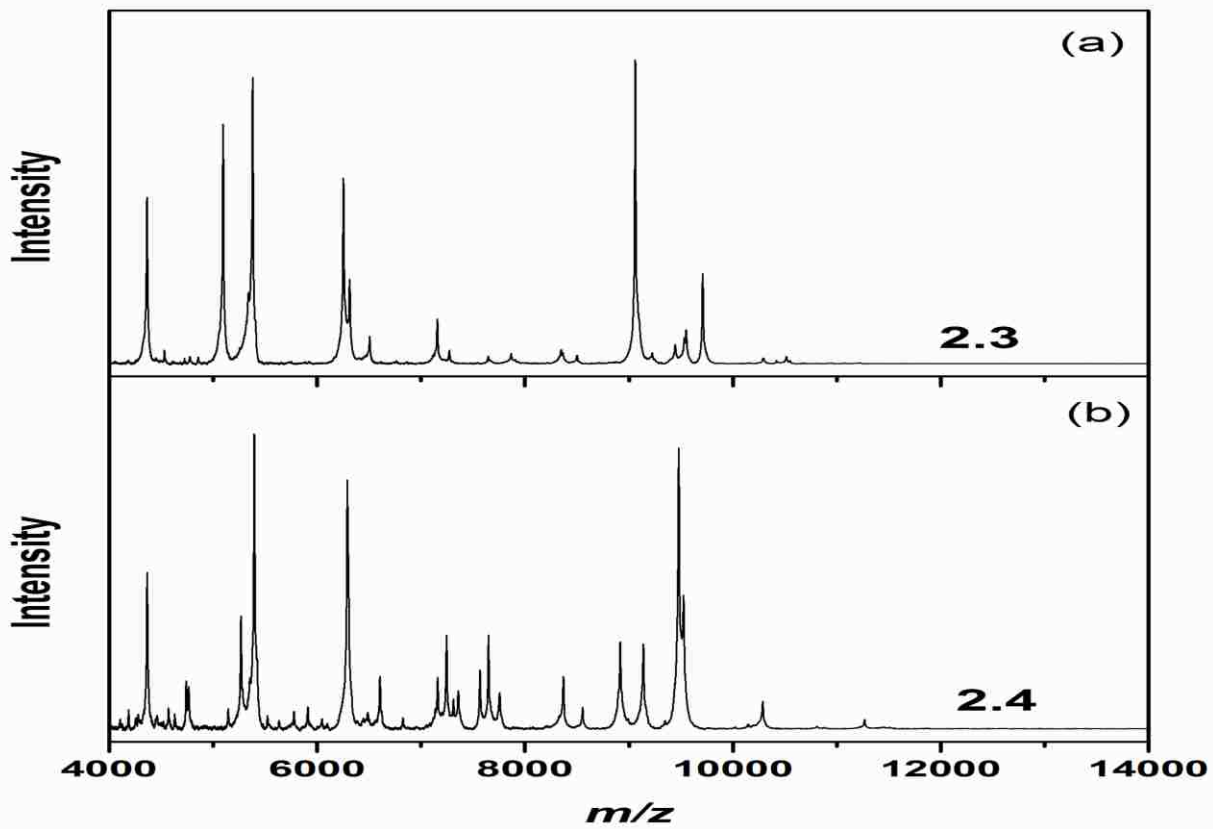
Figure 4.1. MALDI mass spectra of (a) *E. coli* and (b) *E. aerogenes* with no interferents.
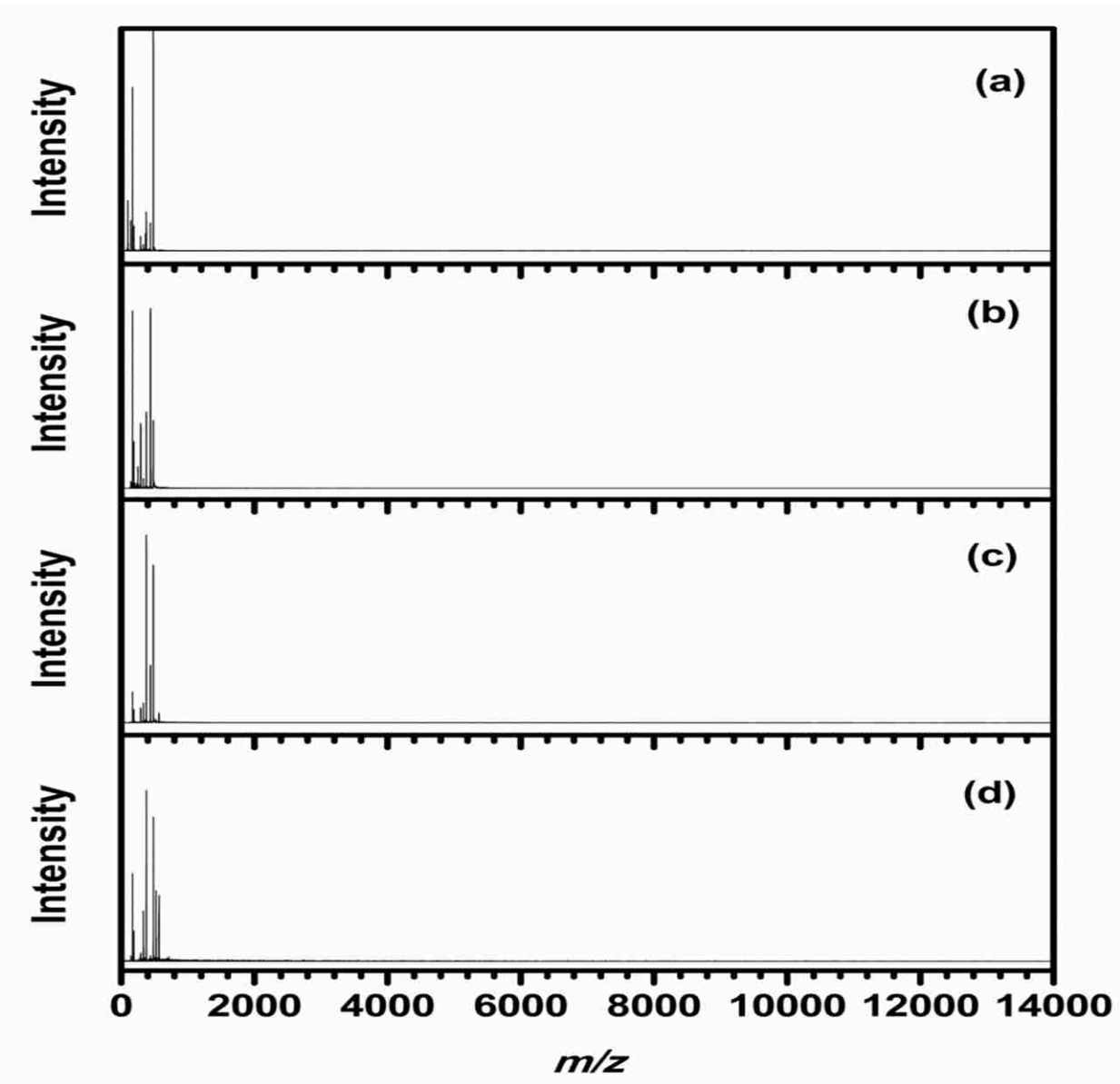
Figure 4.2. MALDI mass spectra of interferents: (a) pollen, (b) fumed silica, (c) diesel particulate, and (d) bentonite.

A summary of the results of the ten replicates analyzed for both *E. coli* and *E. aerogenes* species with each interferent to give an average score value and standard deviation for each combination is shown in Table I.

Table 4-1 Score values of microbial species analyzed with interferents.

Species	Interferent	Ratio	Avg Score Value	Std
E. coli	Fumed silica	1x	2.1	0.13
		5x	1.9	0.09
		10x	1.6	0.11
E. aerogenes	Fumed silica	1x	2.3	0.09
		5x	2.1	0.13
		10x	2.0	0.30
		20x	1.5	0.09
E. coli	Bentonite	1x	2.2	0.07
		5x	1.6	0.03
E. aerogenes	Bentonite	1x	1.7	0.07
		0.5x	2.2	0.16
E. coli	*Juglans nigra*	1x	2.2	0.09
		0.5	1.7	0.08
E. aerogenes	*Juglans nigra*	1x	2.1	0.18
		5x	2.1	0.17
		10x	1.7	0.34
E. coli	Diesel particulate	1x	1.5	0.08
		0.5x	2.0	0.06
E. aerogenes	Diesel particulate	1x	1.7	0.14
		0.5x	2.2	0.10

Fumed silica

  E. coli and fumed silica were mixed in equal amounts (1x). *E. coli* was correctly identified at the species level with a score of 2.1 $\pm$ 0.13, in the presence of fumed silica. An increase in fumed silica to 5x resulted in a correct genus identification of *E. col.,* whereas, at 10x, identification could not be determined. Mass spectra of *E. coli* in the presence of fumed silica at different ratios are shown in Figure 4.3.
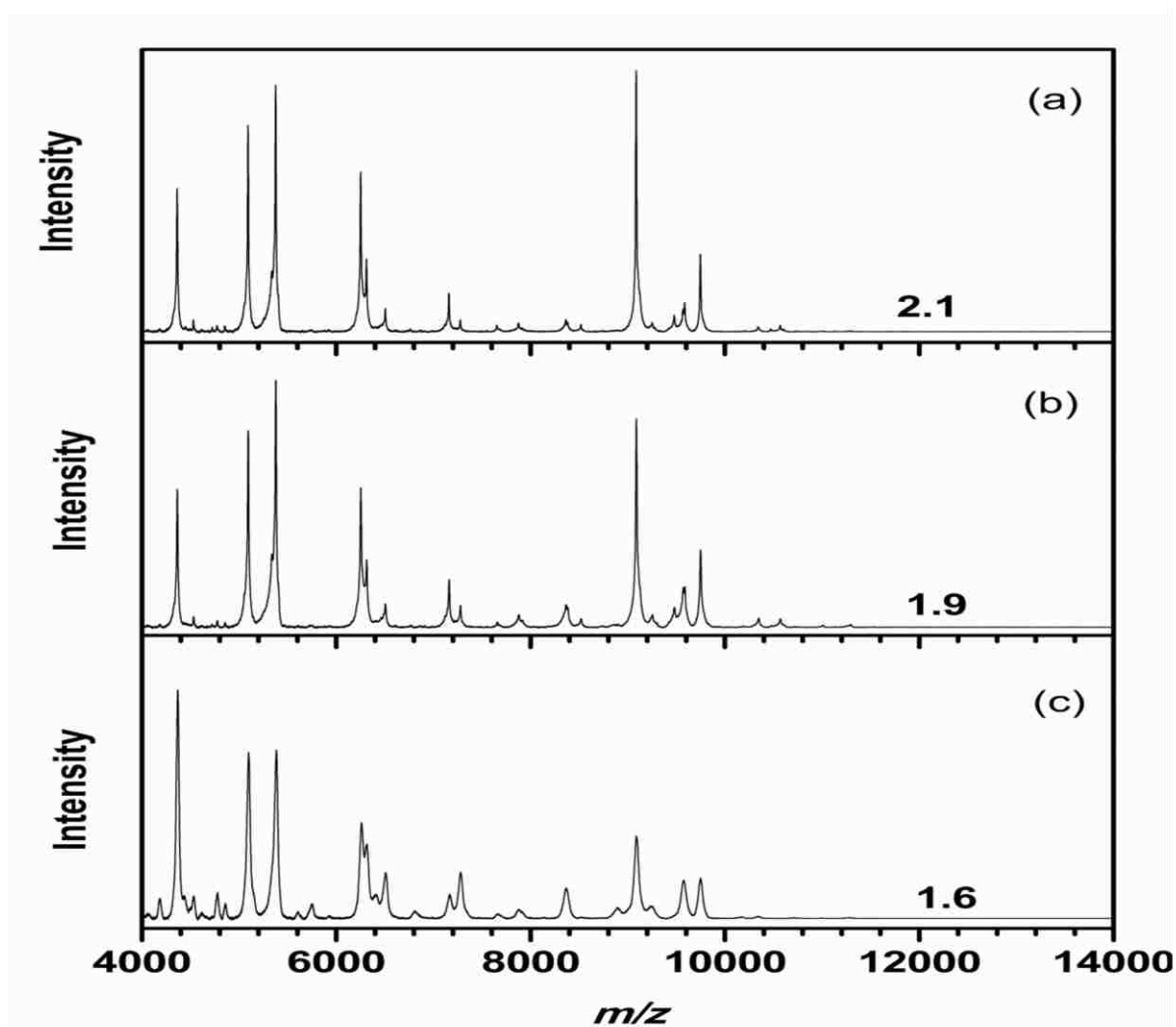
Figure 4.3. *E. coli* and fumed silica at (a) 1x interferent, (b) a 5x interferent, and (c) 10x interferent. Species identification could be determined at 1x, while genus identification was achieved at 5x, and at 10x a reliable identification was not possible.

A correct genus and species identification was determined for *E. aerogenes* when mixed with fumed silica mixture at 1x interferent to bacteria. Identification at the species level was obtained at 5x and 10x. A reliable identification score for 20x could not be achieved. Mass spectra of the *E. aerogenes* and fumed silica mixtures at ratios from 1x to 20x are shown below in Figure 4.4.
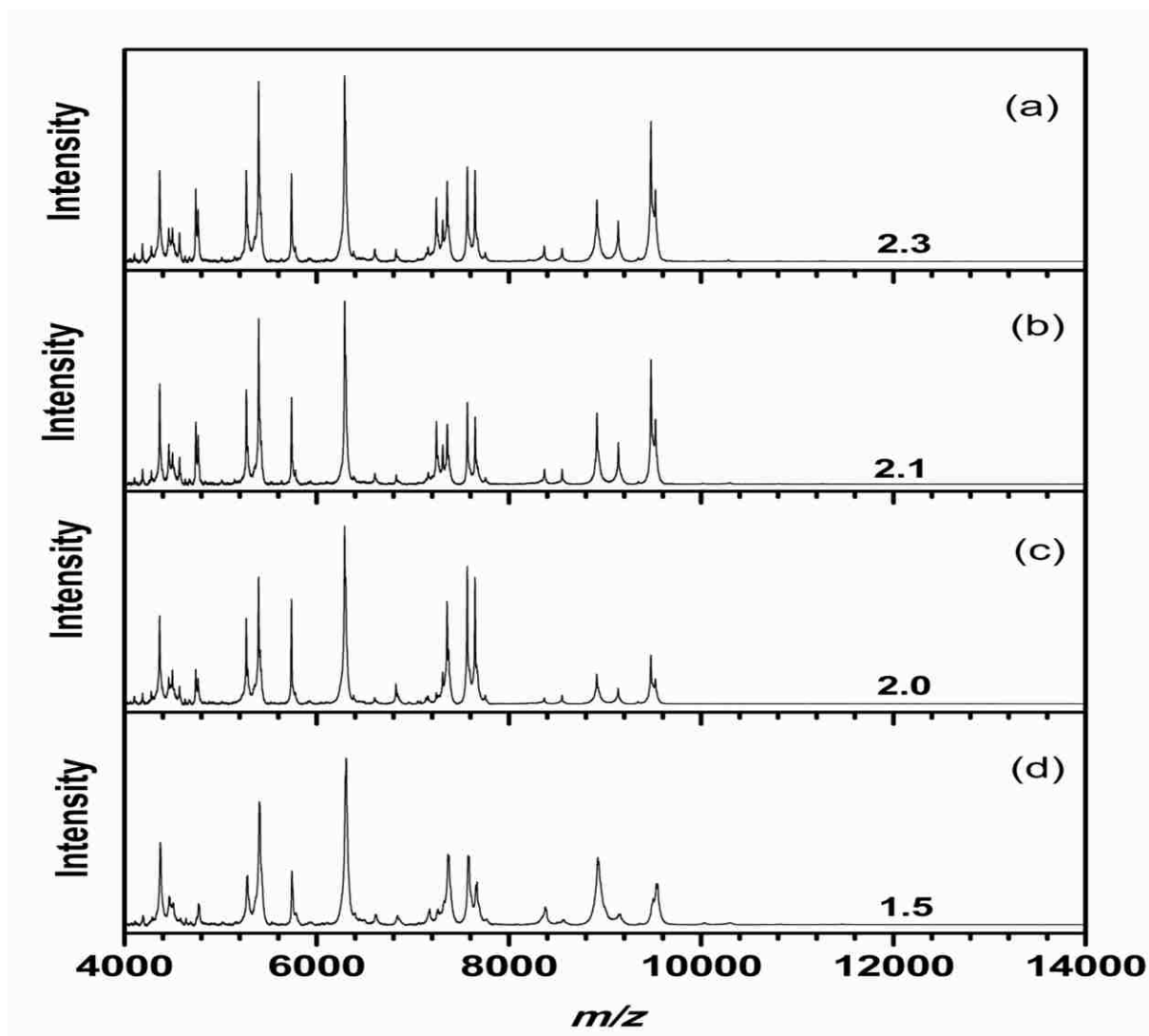
Figure 4.4. *E. aerogenes* with fumed silica at (a) 1x interferent, (b) 5x interferent, and (c) 10x interferent, and (d) 20x interferent. Identification for *E. aerogenes* could be determined at the genus and species level at 1x, genus level at 5x and 10x, but could not be identified at 20x.

When compared to the control, the number of peaks present in the mass spectra of the *E. aerogenes* and fumed silica mixture do not significantly change at the various ratios; however, the number of well resolved peaks decreased as the amount of fumed silica was increased.

Bentonite

E. coli was identified at the species level after being mixed with 1x bentonite. A positive identification could not be made when bentonite was increased to 5x. The resolution was lower and the number of well resolved peaks decreased. The mass spectra of the *E. coli* and bentonite mixtures at 1x and 5x are shown in Figure 4.5 (a) and Figure 4.5 (b), respectively.
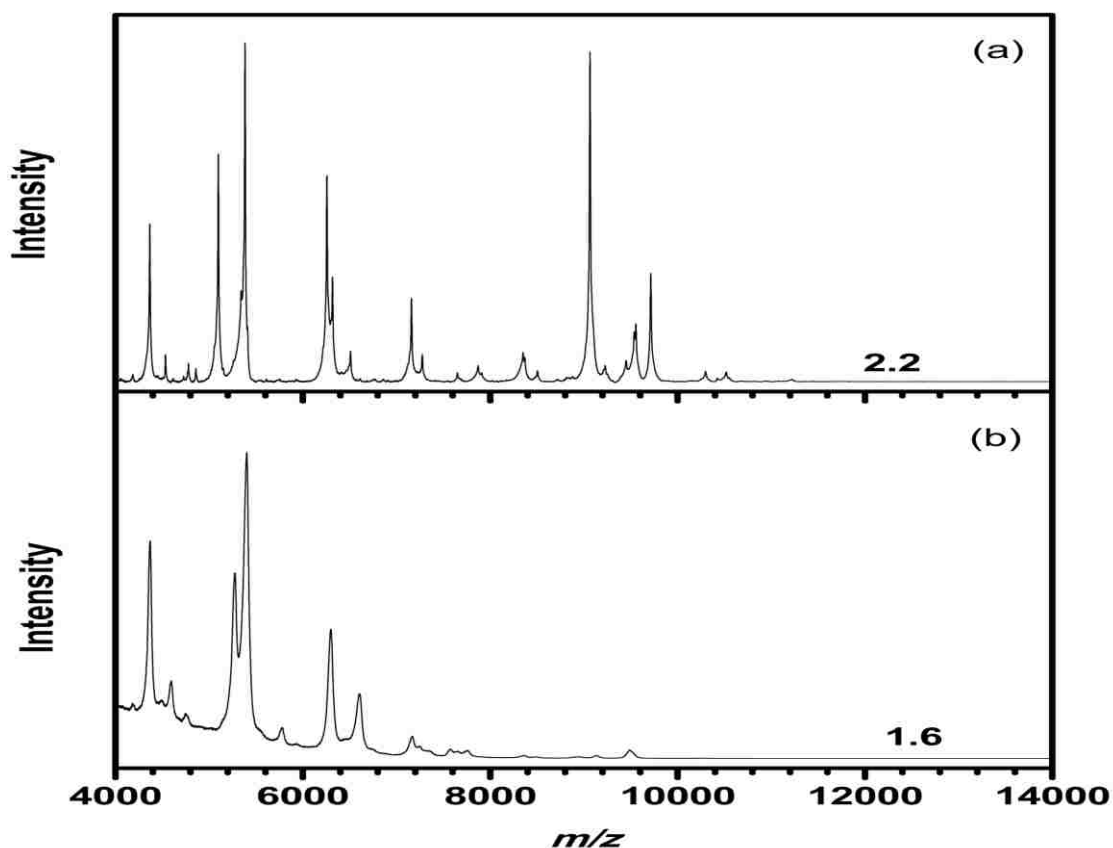
Figure 4.5. *E. coli* and bentonite at (a) 1x interferent by mass and (b) 5x interferent. A reliable species identification could be determined at 1x; however, at a 5x a genus identification could not be determined.

The *E. aerogenes* and bentonite mixture at 1x resulted in a probable genus identification. At 0.5x, species identification was possible. The increase in the amount of *E. aerogenes* improved the identification level to correct species identification.
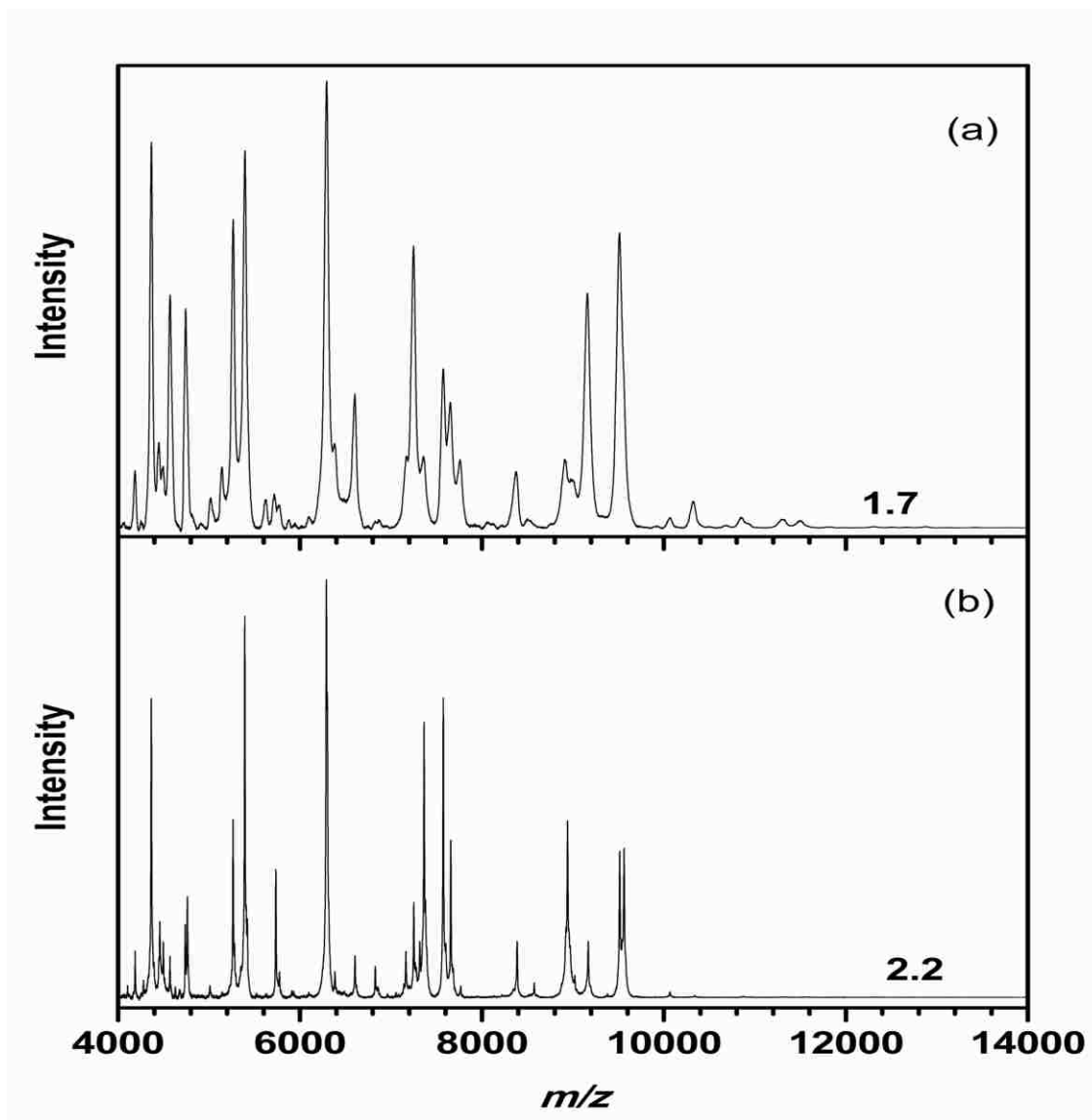
Figure 4.6. *E. aerogenes* and bentonite at (a) 0.5x interferent and (b) 1x interferent. A correct genus identification could be not determined at 1x but a correct species identification could be determined at 0.5x, as indicated by the score value of 1.7.

Juglans nigra

Probable genus identification was achieved for *E. coli* for the analysis of a mixture of *E. coli* and *Juglans nigra* at 1x. In the presence of 0.5x *Juglans nigra*, *E. coli* was identified at the species level.
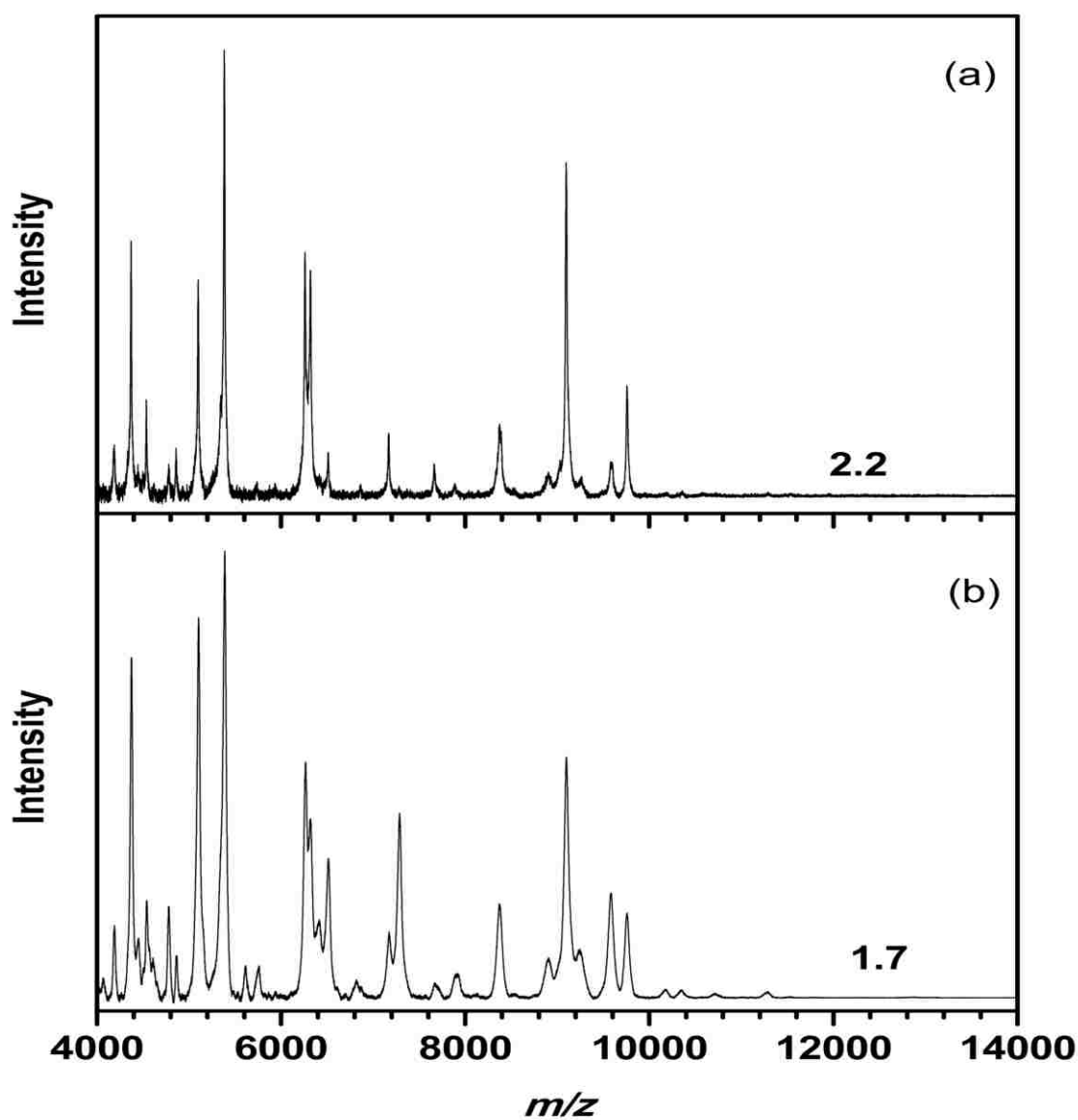
Figure 4.7. *E. coli* and *Juglans nigra* at (a) 0.5x interferent and (b) 1x interferent. A reliable species identification could not be determined for the *E. coli* and *Juglans nigra* at 1x; however, at 0.5x, as indicated by the score value, genus identification could be determined.

Species level identification was achieved for *E. aerogenes* in the presence of *Juglans nigra* at 1x interferent. Correct species identification was also observed at 5x interferent. Although the mass spectra with 1x and 5x *Juglans nigra* appear significantly different, there is no significant change in the score value. At 10x *Juglans nigra,* the number of peaks remains approximately the same but the resolution of the spectrum is significantly decreased, resulting in a probable genus identification.
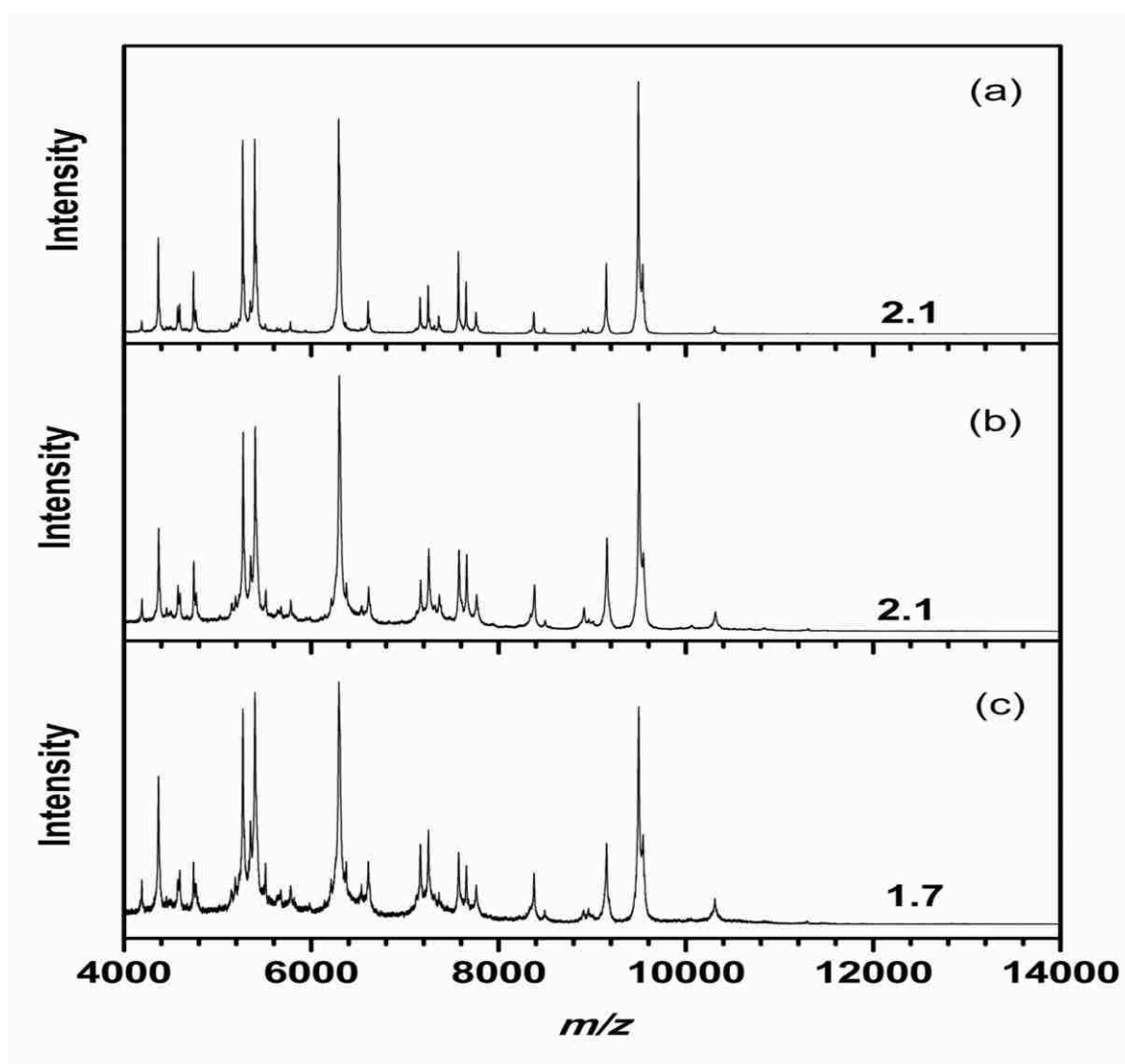
Figure 4.8. *E. aerogenes* and *Juglans nigra* at (a) 1x interferent, (b) 5x interferent, and (c) 10x interferent. A correct identification could be determined at the species level at 1x and 5x and no reliable identification could be determined at 10x.

Diesel Particulate

E. coli and *E. aerogenes* could not be identified with diesel particulate at 1x. At 0.5x, both *E. coli* and *E. aerogenes* were identified at the genus level. The mixtures of *E. coli* and diesel particulate and *E. aerogenes* and diesel particulate are shown in Figure 4.9 and Figure 4.10, respectively.
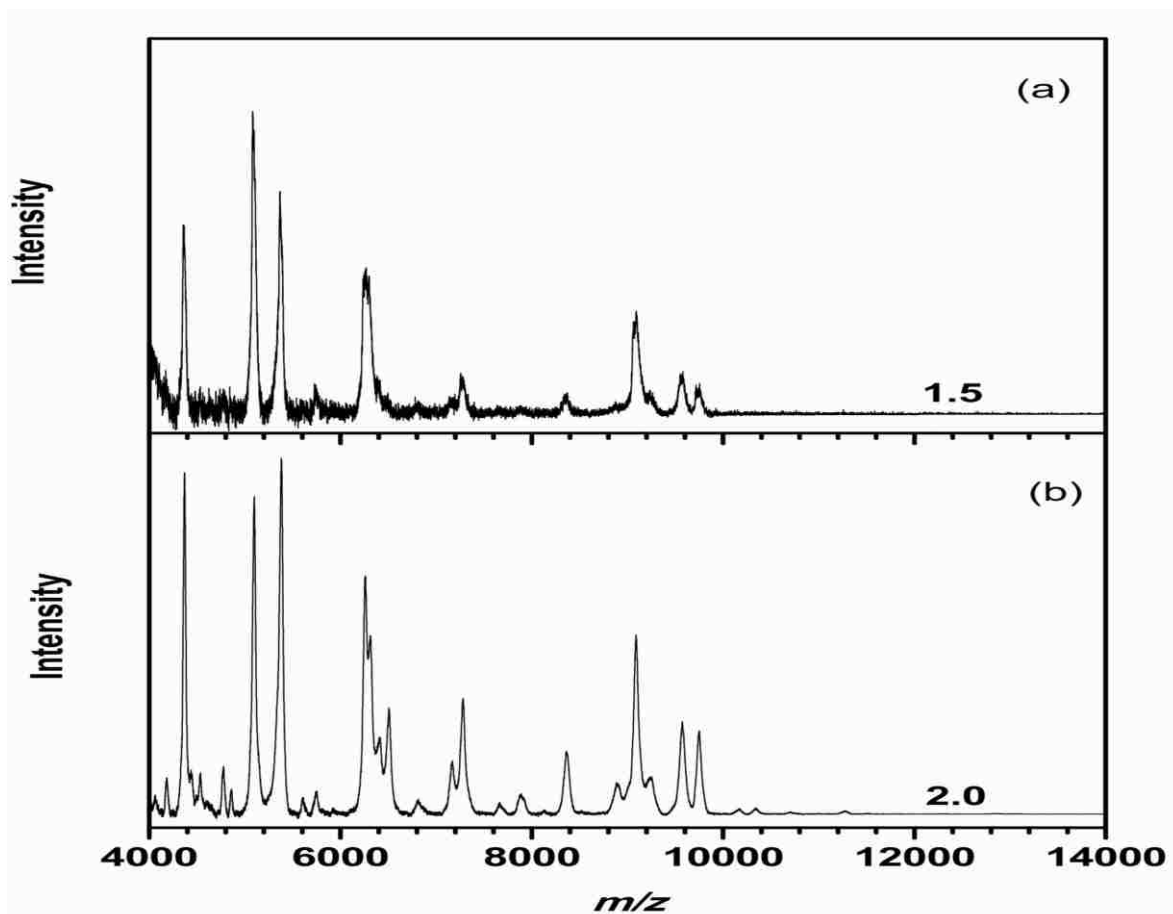
Figure 4.9. *E. coli* and diesel particulate at (a) 1x interferent (b) and 0.5x interferent. A reliable identification could not be determined for the *E. coli* and diesel particulate mixture at 1x, but a reliable genus and probable species identification could be determined at 0.5x as indicated by their score values.

4.4 Summary

In this study, we evaluated MALDI fingerprint identification of bacteria (species or genus level), in the presence of interferents.[17, 18, 20] Our results show that the identification level of each
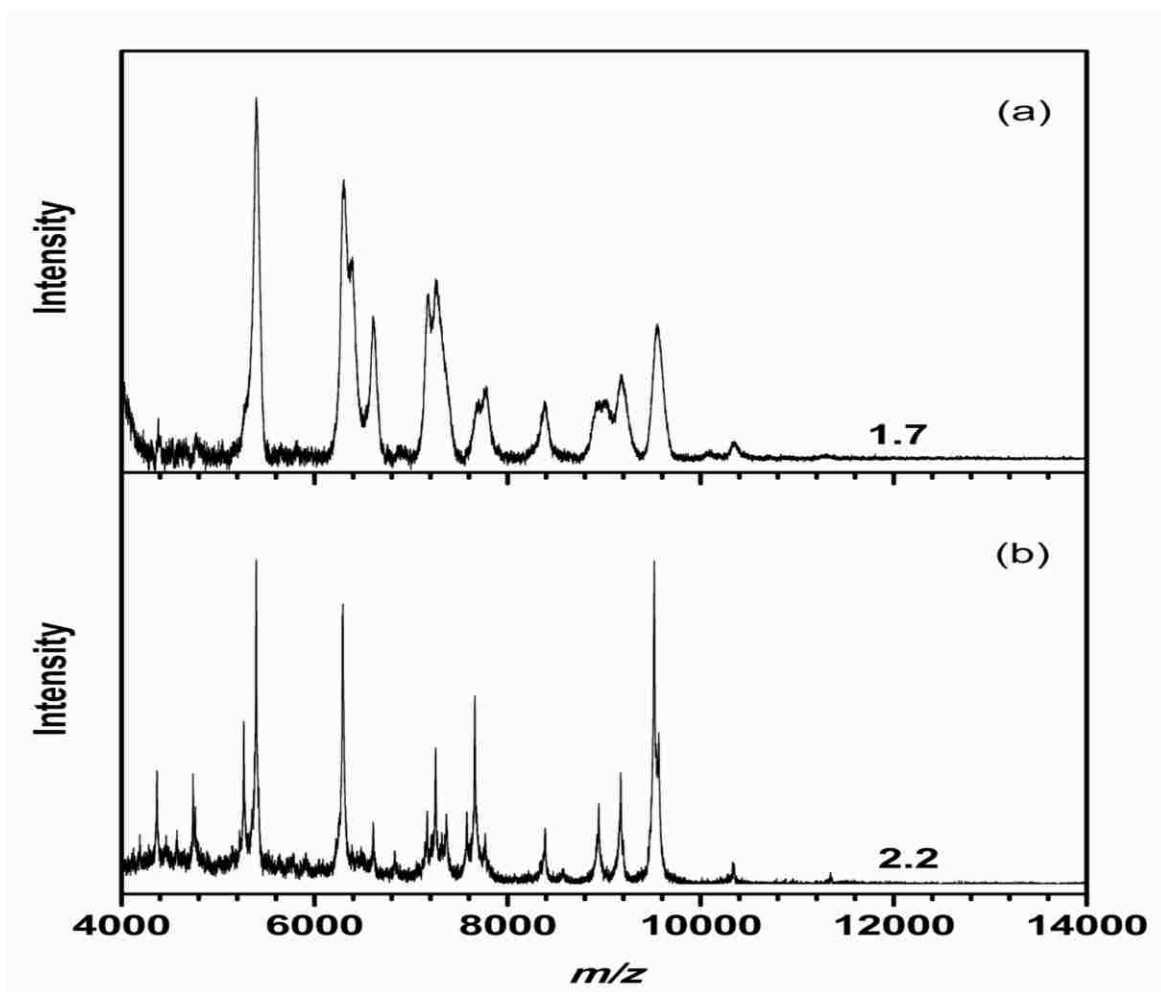
Figure 4.10. *E. aerogenes* and diesel particulate at (a) 1x interferent and (b) 0.5x interferent. A reliable identification could not be made at 1x but a probable species identification could be made at 0.5x.

species mixed with each interferent at different ratios depends on the interferent and species. The presence of interferents with bacterial species reduced the overall quality of the mass spectra. As the amount of interferent increased, peaks were not as well resolved. The presence of interferents can cause signal intensities to change, in some cases, the peak intensities were increased while, in some samples the peak intensities were decreased. Also, for some samples, as the amount of interferent increased, it was observed that some peaks were no longer present, possibly as a result of ionization

suppression caused by the presence of the interferent. The presence of the interferents affects the three reporting factors (peak position, peak frequency, and intensity) that Biotyper uses to determine identification.

The effect of interferents on *E. aerogenes* was not identical. *E. coli* could be identified at the species level at 1x interferents: fumed silica, bentonite, and pollen. As the amount of interferent increased, the overall quality of the mass fingerprint decreased. For 10x fumed silica, 5x bentonite, 1x pollen, and 1x diesel particulate, *E. coli* could not be identified. At 0.5x pollen and 0.5x diesel particulate, *E. coli* species identification was achieved. *E. aerogenes* could be identified at the species level in the presence of fumed silica and pollen at 1x, 5x, and 10x, respectively. However, the identification of *E. aerogenes* was no longer possible in the presence of 20x fumed silica. For the *E. aerogenes* and pollen mixture, 10x the amount of pollen was present before identification was no longer possible; this increase caused a decrease in signal intensity; however, the number of peaks remained the same. At 1x, identification could not be determined for *E. aerogenes* in the presence of bentonite and diesel particulate, but correct species identification could be obtained at 0.5x.

In a real-world scenario for the analysis of collected bioaerosols in an ambient environment, the presence of interferents affects the ability to detect signals from microorganisms because of their presence at low concentrations. Analysis methods, such as MALDI, that can detect samples in the presence of interferents should be employed.

CHAPTER 5. INFRARED LASER ABLATION SAMPLE TRANSFER WITH NANOSTRUCTURE-ASSISTED LASER DESORPTION IONIZATION ANALYSIS OF MICROORGANISMS

The goal of the research described in this chapter was to use ambient sampling for the analysis of microorganisms by laser desorption ionization mass spectrometry. An ambient sampling method using a tunable IR laser ablation source was used to sample cultures of *E. coli* and *B. cereus* from colonies in a Petri dish. After collection in a solvent droplet, the material was deposited on a nanostructured target for matrix-free LDI MS. A number of phospholipids were observed that can be used as identifiable biomarkers for both *E. coli* and *B. cereus* species.

5.1 Introduction

Typically, MALDI mass spectra peaks from whole cell bacteria are attributed to highly abundant proteins and ribosomal proteins.[111] However, lipid profiles can also be used to identify bacteria. Phosphatidylethanolamine (PE) and phosphatidylglycerol (PG) are phospholipids that are two of the major lipid classes found in microorganisms including both gram-negative and gram-positive bacteria.[278] When lipid profiles are of interest, extraction methods such as the Bligh-Dyer or the Folch method are often used.[279, 280] These methods use a combination of chloroform and methanol solvents for an overnight extraction or suspend whole bacterial cells in similar solvent combinations, for a shorter period of time, to simulate the Bligh-Dyer or Folch extraction method.[91, 92, 98, 137, 281]

A number of ionization methods have been used for bacterial lipid analysis. Pyrolysis MS was used to generate fatty acid methyl esters (FAMES), which are phospholipids that have been derivatized for analysis, from hydrolized and methylated suspensions of whole cell bacteria, for the identification of lipid profiles of bacteria.[78] Gidden *et al.* investigated lipid extractions of *E. coli* and *B. subtilis* as a function of growth phases using MALDI TOF/TOF.[281] PE and PG series were observed for both *E.*

coli and *B. subtilis* species. In *B. subtilis*, it was noted that the composition of phospholipids remained that same throughout the exponential growth phase. However, expression of PE was increased during the stationary growth phase, while, PG decreased during the stationary growth phase. During the exponential growth phase of *E. coli,* an increase in a specific C_{17} fatty acid was observed, and an increase in saturated fatty acids was observed in the stationary growth phase.

Ambient ionization methods have been used for the analysis of bacteria. Cooks and co-workers employed desorption electrospray ionization (DESI) MS to analyze different species of both gram-negative *E. coli* and *Salmonella typhimurium* whole cells by directly spraying a mixture of methanol and water onto the sample for droplet pick-up.[136] PE phospholipids were identified from the DESI MS spectra and it was concluded that *in situ* and strain differentiation microbial analysis could be performed using principal component analysis (PCA). Direct analysis in real-time (DART) MS was used to generate FAMES. Using this method, phospholipids observed from each of the *E. coli*, *Coxiella burnetii*, and *Streptococcus pyogenes* species can be used as biomarkers for identification.

Biomolecules such as phospholipids that are observed in the mass range less than *m/z* 1000 are often suppressed by the ionization of matrix ions that are also observed in the same mass range, which makes the use of MALDI MS for the analysis of small molecules challenging.[282, 283] To overcome this challenge, matrix-free LDI MS have been used for the analysis of low mass biomolecules. Fenselau and co-workers used a Fourier transform mass spectrometer with a 1.06 μm IR laser for LDI of bacterial cells suspended in a methanol and chloroform mixture to compare to MALDI analysis of bacterial cells using cobalt or graphite particles in a glycerol matrix.[284] From LDI analysis, a series of peaks attributed to PE with potassium adducts was observed, while peaks attributed to PE, PG, and dihexosyldiglycerides (DHDG) phospholipids were observed for MALDI analysis.

A technique known as desorption ionization on silicon (DIOS) uses inert porous silicon wafers as substrates for the analysis of small molecules, such as peptides and peptide mixtures. DIOS has also been used for a number of other applications including the analysis of fatty acids, peptides, and proteins.[236, 285, 286, 287] Porous silicon targets are prepared by electrochemical etching,[288, 289] a process that affects the pore size and shape of the silicon wafers, which can influence the efficiency of LDI.[289] Efforts to improve spectral quality and the effective mass range for small molecules have led to the search for other inert substrates materials. Inert surfaces with nanostructures such as silicon nanowires, carbon nanotubes, and porous alumina have been synthesized and used for LDI MS.[236] LDI with nanostructured targets has also been used for molecules less than 1000 Da.[209, 234, 235, 286, 287] Based on these nanomaterials, 100 spot disposable nanostructure targets have been commercialized as nano-assisted laser desorption ionization (NALDI) targets for the analysis of small molecules less than 1000 Da[209, 234, 236] and have been used for the analysis of polar and nonpolar compounds.[235, 290]

In this chapter, we describe the ablation of *E. coli* and *B. cereus* bacteria colonies with collection in a solvent droplet, using a mid-infrared laser ablation sample transfer (LAST), and analyzed using for matrix-free LDI, as discussed in Chapter 2. Ambient sampling allows material to be directly analyzed with little to no sample pretreatment. In this case, the solvent-captured bacteria were deposited on a nano-assisted laser desorption ionization (NALDI) target for matrix-free LDI TOF-MS.

5.2 Experimental

E. coli and B. cereus bacterial cells were cultured in individual Petri dishes using nutrient LB broth at the respective temperatures of 37 °C and 30 °C, for 24 hours. After the growth period, the Petri dishes were placed underneath the syringe of the LAST setup described in Chapter 2, Section 2.5. The solvent mixture of 70% acetonitrile and 30% of 0.1 % TFA contained in the syringe was then made to

form a 1 mm solvent droplet. The height of the syringe was manually adjusted using a xyz stage so that the distance between the bottom of the droplet and the cultured bacteria in the Petri dish was 1 mm. The bacterial colonies were irradiated for 60 laser shots with a maximum laser energy of 1.75 mJ and no attenuation, ablating the material into the solvent droplet. The syringe was removed from the xyz stage so that the droplet could be deposited onto the NALDI target. NALDI mass spectra were obtained using the MALDI-TOF/TOF mass spectrometer described in Chapter 2, Section 2.2. A loop of bacterial colonies from both *E. coli and B. cereus* was also taken from a Petri dish, smeared onto a MALDI target, and overlaid with CHCA matrix and analyzed using MALDI MS.

5.3 Results and Discussion

A NALDI mass spectrum of the NALDI target is shown in Figure 5.1. The peaks are well below *m/z* 1000. Background peaks from the silicon nanowire structures of the NALDI target are observed at *m/z* 81, 87, 103, 130, 174, 317, which can be seen in the inset of Figure 5.1. These background peaks can vary and become more abundant if compounds are difficult to ionize, their concentrations are near the limit of detection of the NALDI target, or from the analysis of empty spots on the NALDI target.
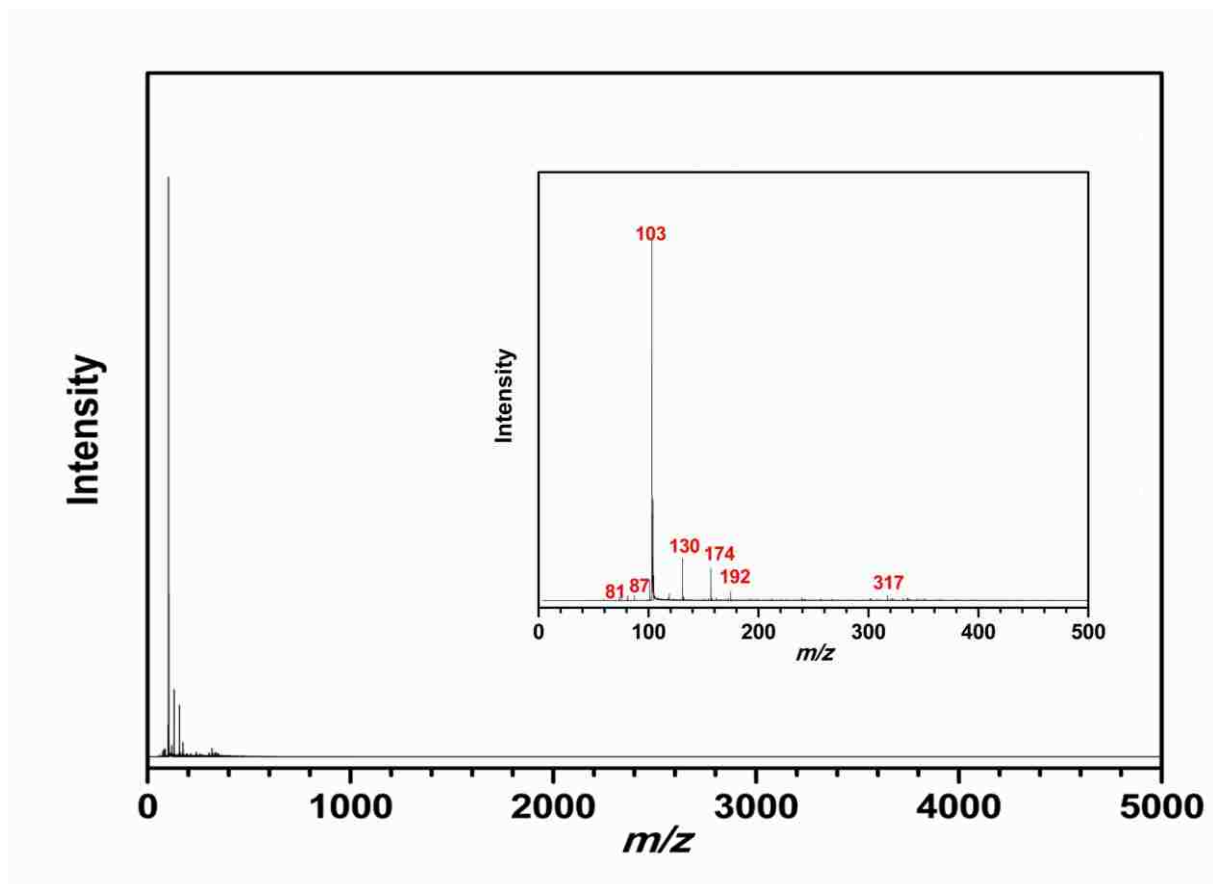
Figure 5.1. Laser desorption TOF mass spectrum of blank NALDI target.

An IR LAST NALDI spectrum of *E. coli* is shown in Figure 5.2(a). Both phosphatidylethanolamine (PE) and phosphatidylglycerol (PG) phospholipids were observed from *m/z* 600 to *m/z* 800. The peak observed at *m/z* 618 is the result of the loss of a PE head group $(CH_2CH_2NH_2)$.
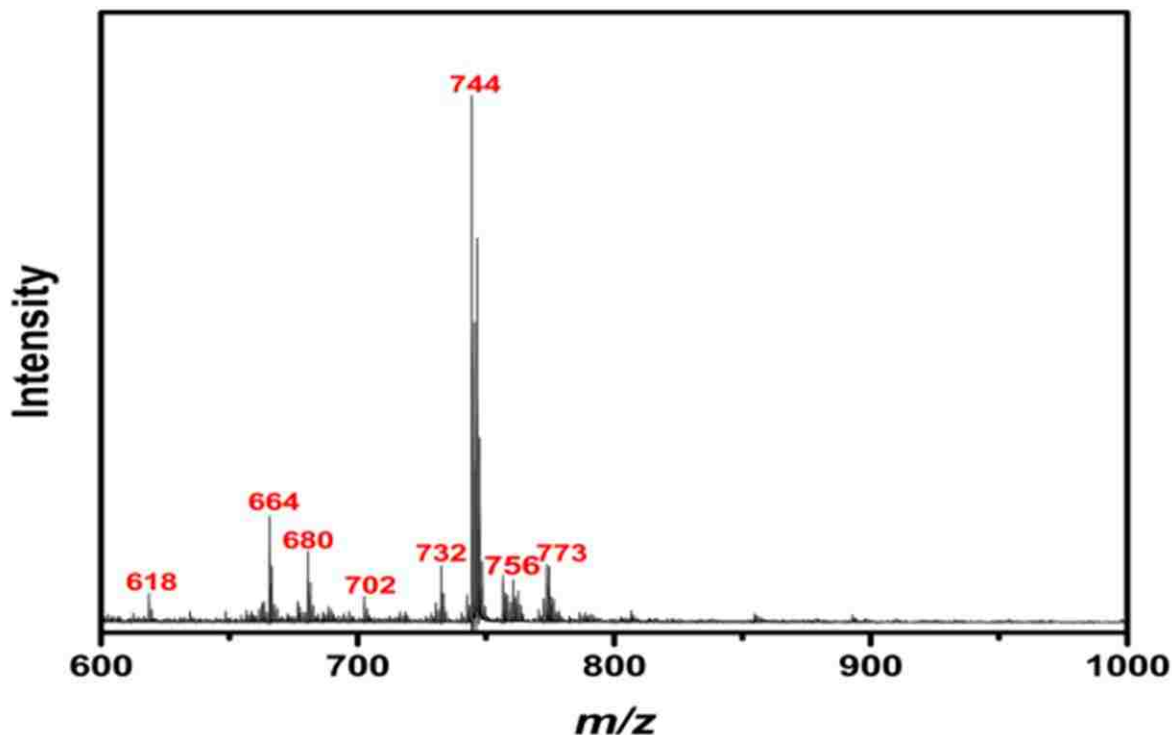
Figure 5.2 (a). NALDI mass spectrum of LAST bacterial colonies of *E. coli*. Various PE and PG phospholipids are observed in the mass range of 650-800 *m/z*.

In Figure 5.2 (b) an expanded view of the PE and PG series is shown. The peaks at *m/z* 664, 702, 732, and 744, and 756 are protonated PE phospholipids with fatty acid compositions C30:0, C33:1, C35:1, C36:2, and C34:1, respectively. Peaks at *m/z* 680 and *m/z* 773 are assigned as PG (C29:0) and PG (C36:2). The fatty acid moiety PE (C35:1) observed at 732 *m/z* has one double bond and the PG (C36:2) observed at 773 *m/z* has two double bonds. Whereas, the fatty acids of other PE and PG phospholipids observed in this series have no double bonds.
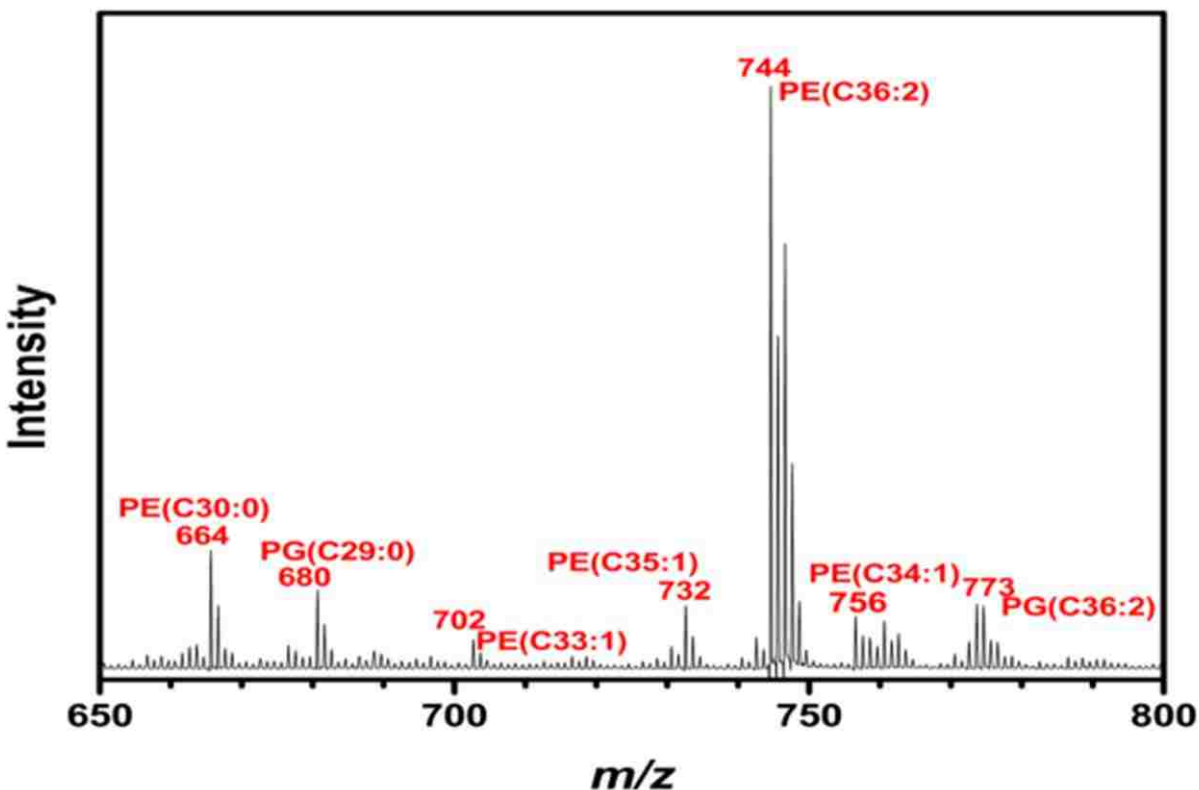
Figure 5.2 (b). Expanded view of a NALDI mass spectrum of LAST bacterial colonies of *E. coli*. The fatty acid composition of the PE and PG phospholipids observed in the series are indicated by the total numbers of carbons and the number of unsaturations (double bonds). For example, PE C33:1 has 33 carbon atoms and 1 double bond.

High mass peaks are observed in the MALDI spectrum of *E. coli* in the mass range up to *m/z* 14,000, shown in Figure 5.3. The high mass peaks observed in the spectrum are typically attributed to ribosomal proteins and highly abundant proteins. The peaks observed at lower masses, below *m/z* 500, are attributed to the CHCA matrix (see Figure 5.4). Ionization of matrix molecules can sometimes cause ion suppression of analyte molecules, which is attributed to the absence of peaks, low intensity peaks of some molecules, and poor signal-to-noise in the lower mass region of the spectrum. Often, during MALDI analysis, parameters are adjusted so that matrix ion peaks are suppressed during analysis.

109
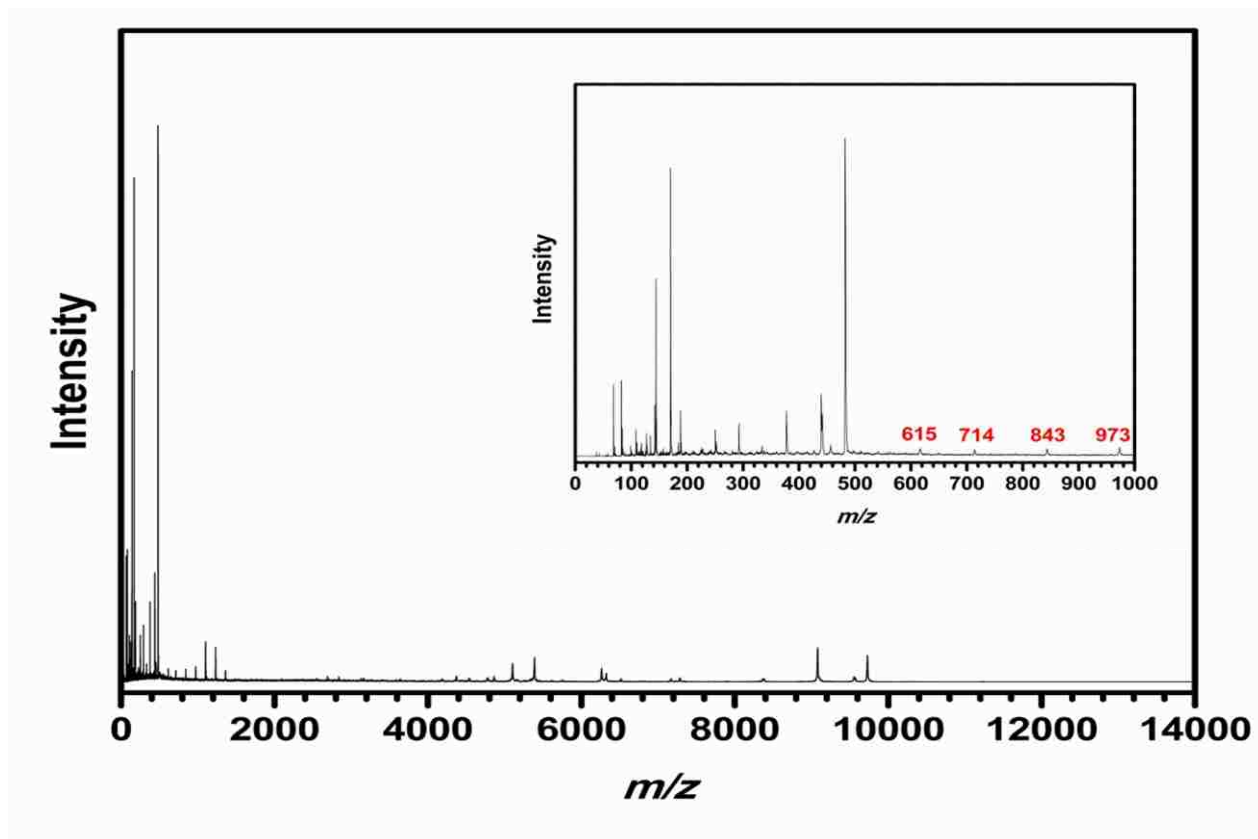
Figure 5.3. MALDI mass spectrum of *E. coli* bacterial colonies with CHCA matrix.

The MALDI spectrum of *E. coli* is shown to compare the type of biomarkers observed for LAST NALDI and MALDI MS. High intensity matrix ion peaks can be seen in the lower mass region below *m/z* 1,000 as well as four additional peaks at *m/z* 615, 714, 843, and 973. The peaks at *m/z* 615, 843, and 973 have been tentatively assigned as a PE, LPG, and DGDG phospholipids. The peak at *m/z* 714 has been identified as a PE phospholipid with a fatty acid composition of C34:2.

The MALDI spectrum of the CHCA matrix is shown in Figure 5.4. The matrix ions are observed in the low mass region, which often interferes with the analysis of small molecules. The observed peaks are attributed from matrix ions, clusters of matrix ions, and their fragments.
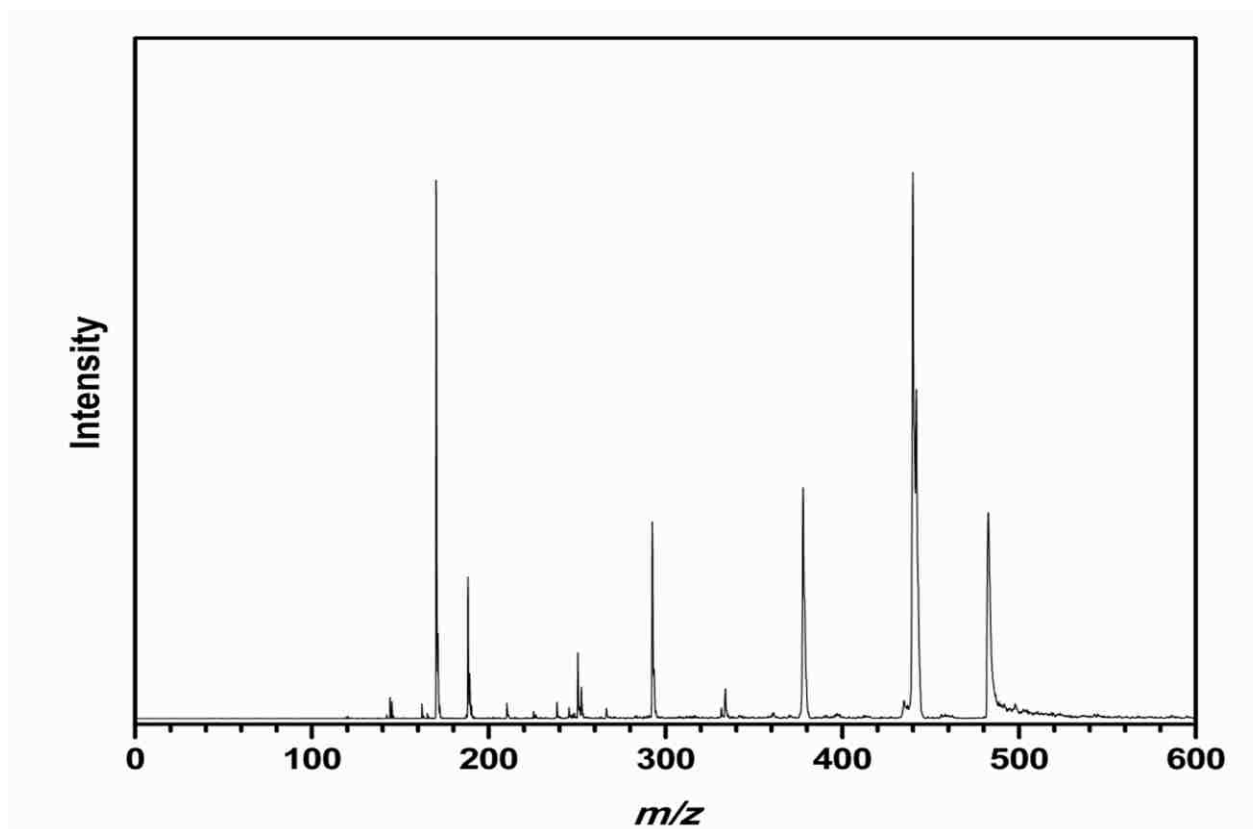
Figure 5.4. MALDI mass spectrum of CHCA matrix.

The NALDI spectrum of *B. cereus* is shown in Figure 5.5 (a). Several peaks are observed in mass range between *m/z* 600 and *m/z* 1150, which are assigned as PE, PG, DGDG, and TAG phospholipids and a lipopeptide. The peak at *m/z* 664 is a protonated PE and has a fatty acid composition of C30:0. Peaks at *m/z* 719 and *m/z* 736 are assigned as PG phospholipids with fatty acid composition C32:1 and C33:0, respectively. Fatty acid C32:1 is also observed with a potassium adduct at *m/z* 758 [C(32:1) + K$^+$]. A diglycosyldiglyceride (DGDG) phospholipid C31:0 is observed at *m/z* 878. The peak at *m/z* 854 is a triacylglycerol (TAG) with a fatty acid composition of C50:3. The peak at *m/z* 1123 is assigned as a mycosubtilin-C$_{17}$ lipopeptide with potassium adduct. Lipopeptides are amphiphilic peptides that are found in a number of different species of *Bacillus*.

111
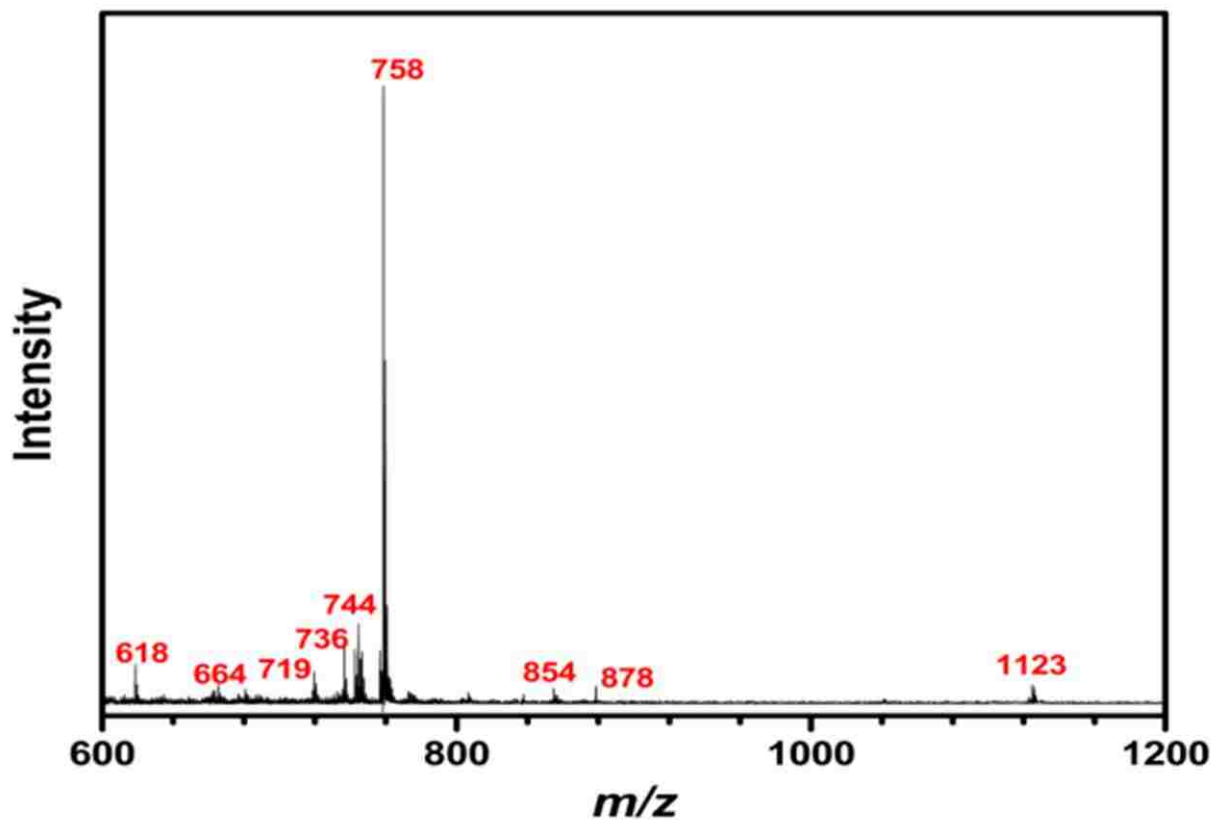
Figure 5.5 (a). NALDI mass spectrum of LAST bacterial colonies of *B. cereus*. Various PE, PG, TAG, and DGDG phospholipids and a lipopeptide are observed in the mass range of 650-1150 *m/z*.

An expanded view of the PE and PG phospholipid series observed from the NALDI spectrum of *B. cereus* is shown in Figure 5.5 (b).
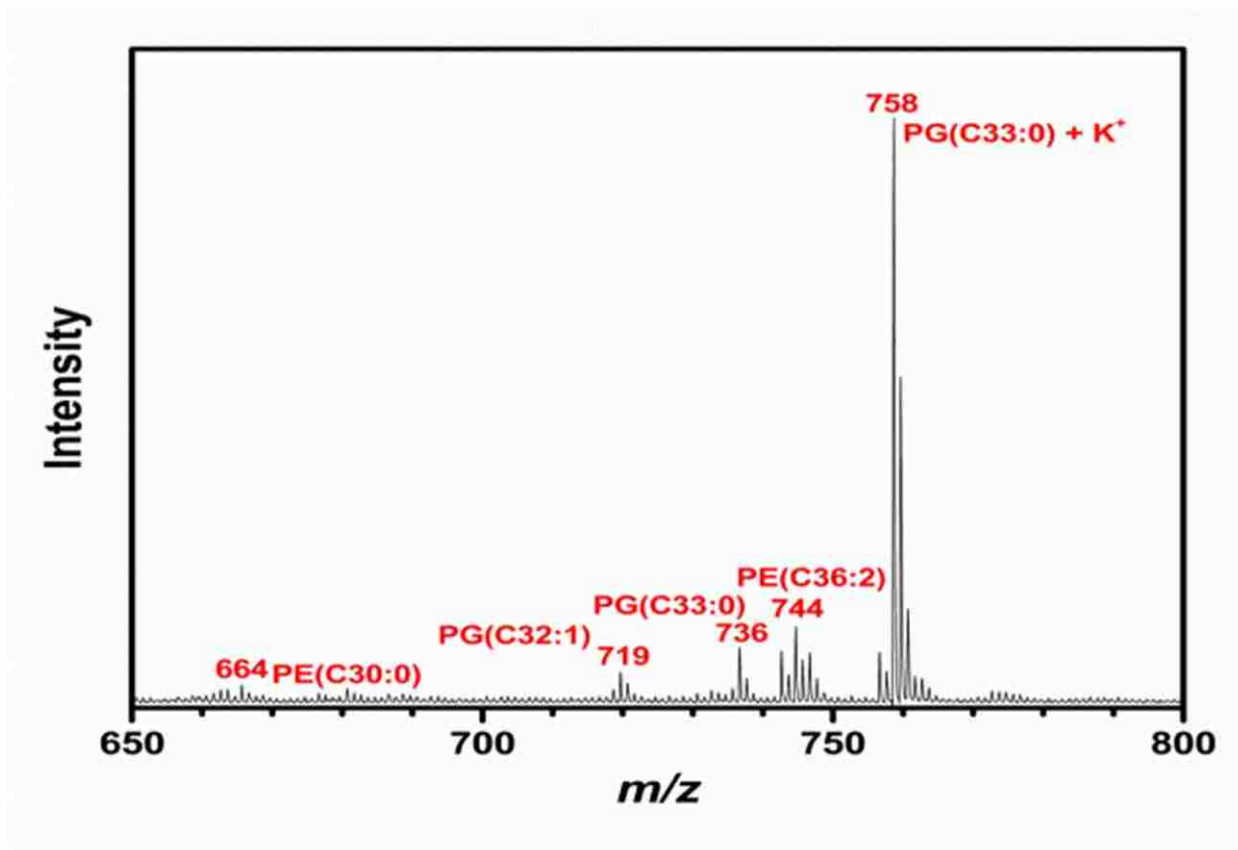
Figure 5.5. (b). Expanded view of NALDI mass spectrum of LAST bacterial colonies of *B. cereus*, showing the most dominating phospholipids of the series.

The NALDI spectra of both species contain PE and PG phospholipids observed at *m/z* 664 (C30:0) and 744 (C36:2) and PE *m/z* 618 with the loss of a head group. PE phospholipids are observed at *m/z* 618, 664 (C30:0), and 744 (C36:2). The PE series dominates the spectrum of the *E. coli* species and the PG series dominates the spectrum of the *B. cereus*.[291, 292] This observation is not surprising given that gram-negative bacteria have a higher percentage of PE phospholipids, whereas, gram-positive bacteria have a higher percentage of PG phospholipids.[291, 292] Nevertheless, there is also a difference in the class of phospholipids observed in the mass range greater than *m/z* 800 in the NALDI

spectrum of *B. cereus*. The peaks are attributed to a DGDG phospholipid at *m/z* 878 (C31:0) and a lipopeptide at *m/z* 1123, which are routinely observed in gram-positive bacteria, but rarely in gram-negative bacteria. A TAG phospholipid was also observed at *m/z* 854 (C50:3) in the *B. cereus* spectrum. Phospholipids observed in this work are in agreement with previously reported bacterial phospholipid data.[91, 92, 98, 136, 137, 284]

A MALDI spectrum of *B. cereus* is shown in Figure 5.6. Matrix ion peaks are observed in the lower mass region of the spectrum, below *m/z* 1000, and two additional peaks are observed at *m/z* 714 and *m/z* 843, shown in the inset of Figure 5.6. Both of these masses were also observed in the MALDI spectrum of *E. coli* in Figure 5.3. The peak at *m/z* 714 is assigned as a PE phospholipid (C34:2), while the peaks at *m/z* 843 is assigned as a LPG phospholipid.
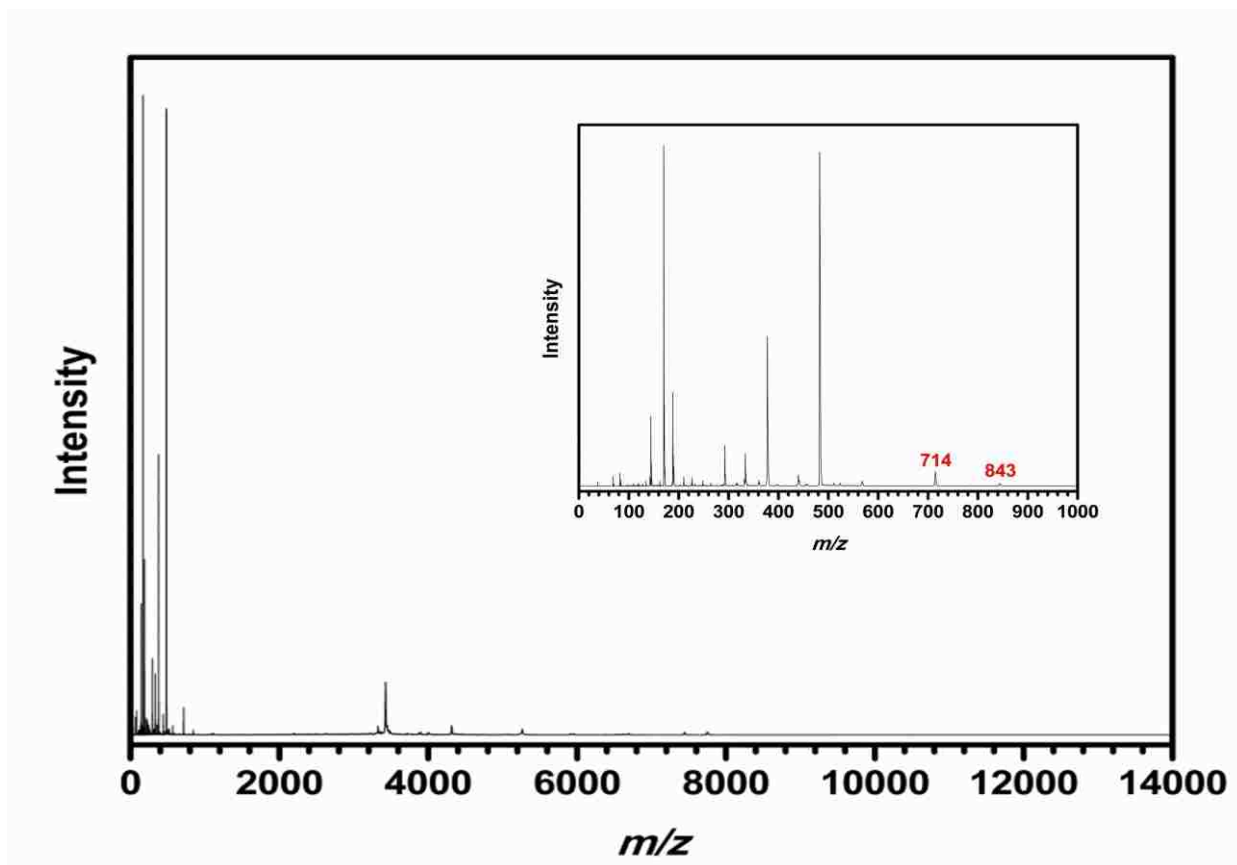
Figure 5.6. MALDI mass spectrum of *B. cereus* bacterial colonies with a CHCA matrix.

An expanded view of the higher mass peaks observed from the MALDI spectrum of *B. cereus* bacterial colonies in the range of *m/z* 3500 to 8000 is shown in Figure 5.7. These peaks can be attributed to highly abundant proteins and ribosomal proteins.
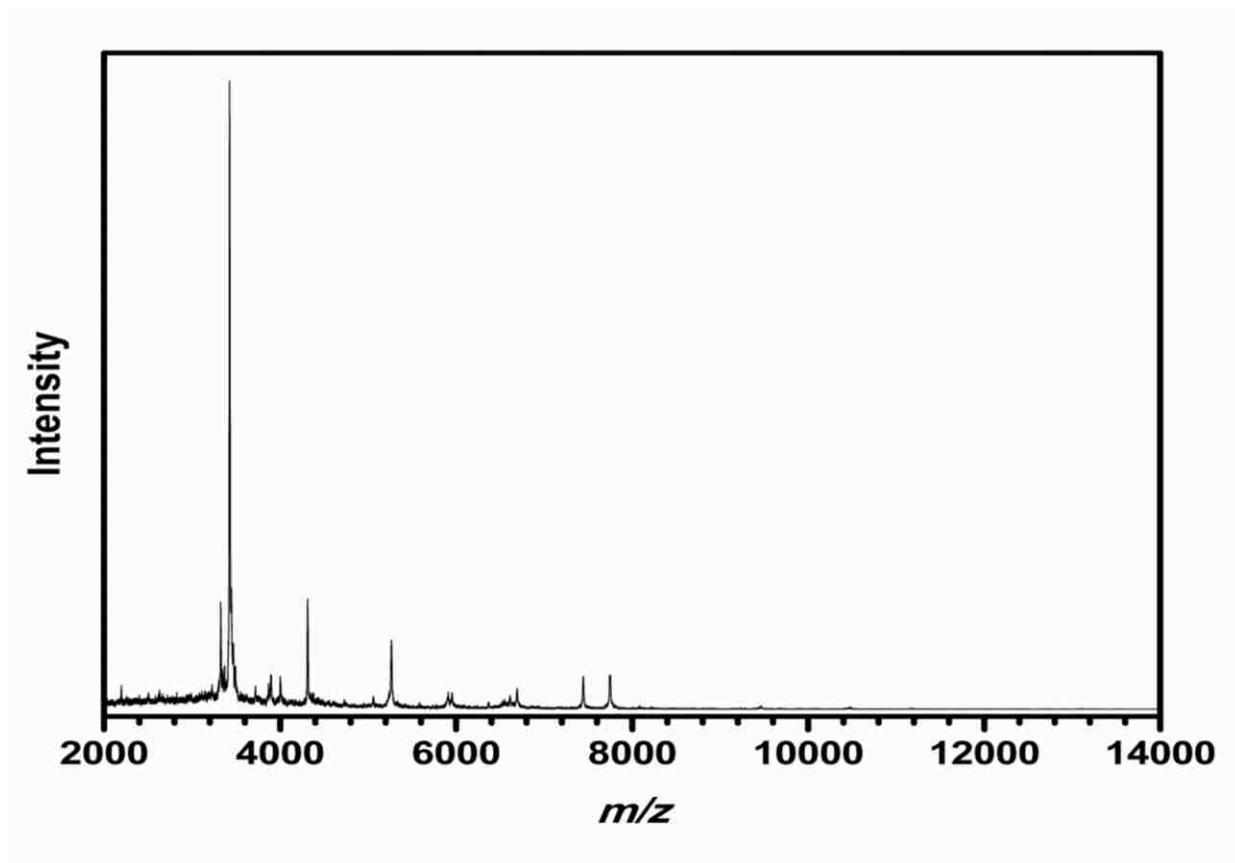
Figure 5.7. Expanded view of high mass peaks observed from the MALDI mass spectrum of *B. cereus* bacterial colonies.

5.4 Summary

In this study, bacterial colonies of gram-positive *B. cereus* and gram-negative *E. coli* were sampled directly from a Petri dish using a wavelength tunable IR laser source under ambient conditions. Without sample pretreatment, material from bacteria colonies was ablated into a solvent droplet and transferred to a NALDI target for matrix-free LDI analysis using a MALDI mass

spectrometer. The results showed that phospholipids could be identified from freshly cultured bacteria using LAST and a NALDI target for matrix-free LDI. PE and PG phospholipids were present in both the *B. cereus* and *E. coli* species; however, the series of phospholipids were not identical, but did contain PE and PG phospholipids that were common to both *B. cereus* and *E. coli*. PE was the dominant phospholipid species present in *E. coli*. In addition to the dominant PG phospholipid class observed for *B. cereus,* other classes of phospholipids and a lipopeptide that are only present in gram-positive bacteria were also observed. Although, identifiable high mass protein biomarkers are not observed using LAST NALDI, as they are in MALDI, phospholipids can also be used as identifiable biomarkers. The major advantage of LAST NALDI is its minimal sample preparation. Furthermore, LAST could easily translate to a field analysis technique because of its ability to capture material, which can be collected and analyzed at a later time, if necessary.

CHAPTER 6. CONCLUSIONS AND FUTURE DIRECTIONS

This dissertation describes the analysis of microorganisms using MALDI and IM TOF MS. Whole cell microorganisms were detected using both MALDI TOF MS and MALDI-IM-TOF MS. MALDI Biotyper, a mass spectrometry fingerprinting software database, was used in conjunction with MALDI TOF MS to identify whole cell microorganisms in the presence of interferents that may be present during sample collection in an ambient environment. Using laser ablation sample transfer under ambient conditions, an IR laser was used to ablate bacterial colonies into a solvent droplet, which was then deposited onto a NALDI target and analyzed using matrix-free LDI TOF MS. This works shows that MALDI and IMMS can be used for the detection and identification of whole cell microorganisms as well as whole cell microorganisms, in the presence of naturally occurring and man-made background particulate and weaponizing additives, with the use of a robust mass fingerprinting database, and LAST NALDI which has the potential of analysis using ambient techniques for field analysis.

The detection of whole cell microorganisms, *B. subtilis* and *E. coli* ATCC, using MALDI and MALDI-IM-TOF MS was presented in Chapter 3. MALDI and MALDI-IM-TOF MS were conducted in parallel to assess the effectiveness of MALDI-IM-TOF MS for whole cell microorganism identification. This study demonstrated that the bacteria *B. subtilis* and *E. coli* can be detected from lyophilized bacterial cells using MALDI-IM-TOF MS. An attractive feature of IMMS data is the separation of biomolecules such as isobaric lipids, peptides, and proteins on different trend lines, which allows the biomolecular class to be determined prior to *m/z* separation. In *B. subtilis*, these biomolecular structural differences were observed in the surfactin and mycosubtilin lipopeptides. Although, surfactin and mycosubtilin are closely related, they could be differentiated because of the deviation of the mycosubtilin lipopeptide below the surfactin trend line. It was also possible to observe additional peaks using VUV MALDI-IM-TOF MS that were assigned as surfactin and mycosubtilin

isoforms because of their presence on the surfactin and mycosubtilin trend lines. Proteins detected from *E. coli* lie on the same trend line; however, it was not possible to identify them. The *m/z* values of the peaks observed were searched in the RMIDb. A predicted sequence was obtained for one of the *m/z* values.

When collecting microorganisms from bioaerosols in ambient and battlefield environments other biological material may be present, in addition to naturally occurring and man-made aerosols and weaponizing agents. Detecting microorganisms in such a complex background is more difficult than the analysis of pure materials in the laboratory. Ideally, one would like to be able to detect and identify microorganisms in the presence of a complex background without having to conduct time consuming separation techniques. In Chapter 4, the detection and identification of microorganisms in the presence of possible interferents using MALDI TOF MS was described. *E. aerogenes* and *E. coli* bacteria were analyzed in the presence of interferents fumed silica, bentonite, and pollen. The effect of the interferents on the identification of bacteria at the genus and species level was assessed using bacteria mass fingerprinting software. Correct species identification for *E. coli* could be confirmed for *E. coli* and interferents fumed silica, bentonite, and pollen were present at 1:1 ratio in each *E. coli* and interferent mixture. However, at the same mass ratio, with diesel particulate, a genus identification level was determined for *E. coli*. Species identification for *E. aerogenes* with fumed silica and pollen at an equal mass ratio was achieved. Genus identification was determined for *E. aerogenes* with bentonite and diesel particulate. As the mass ratio of the interferent increased, the likelihood of species identification decreased with the exception of *E. aerogenes*.

In Chapter 5, under ambient conditions, microbial colonies were sampled directly from a Petri dish using a mid-infrared laser source at 2.94 μm. Gram-negative *E. coli* and gram-positive *B. cereus* bacterial colony particulate was ablated from a Petri dish and collected into a solvent droplet

suspended above a Petri dish. The solvent-captured material was then transferred to a NALDI target for analysis using a MALDI TOF mass spectrometer. PE and PG phospholipids were observed in the NALDI spectrum of both *E. coli* and *B. cereus*. However, not all of the PE and PG phospholipids were identical, an observation that can be used to differentiate gram-negative *E. coli* and gram-positive *B. cereus*. The spectrum of *E. coli* was dominated by PE, while PG was the dominant phospholipid in the *B. cereus* spectrum. Another distinguishing feature in the NALDI spectrum of *B. cereus* was the presence of a DGDG phospholipid and a lipopeptide, which are biomolecules typically found in gram-positive bacteria, in addition to a TAG phospholipid. In this work, we were able to demonstrate the use of LAST under ambient conditions, followed by NALDI MS for the analysis of whole cell bacteria captured in a solvent droplet. Furthermore, our results show that IR laser sources can easily ionize phospholipids, without sample pretreatment or the use of solvents that are typically employed for extraction for lipid analysis.

In the future, the detection and identification of bacteria should focus on collected and aerosolized material, which can also be applied to collected bioaerosols in the presence of naturally occurring and background aerosols and weaponizing agents. The bacterial species can be collected from particulate generated using a Collision nebulizer or LAST and analyzed using MALDI-IM-TOF MS and as well as matrix-free LDI-IM TOF MS. This two-dimensional has the potential to separate complex backgrounds that can hinder microorganism detection. To further demonstrate MALDI-IM-TOF MS as an ideal tool to investigate the complexities of bioaerosol sampling, an aerosol inlet should be designed that can be interfaced with a MALDI-IM-TOF MS system for online analysis. This would allow bioaerosols to be sampled directly by the MALDI-IM-TOF MS system for analysis, without any sample pre-treatment.

Mass spectra fingerprinting can also be used for the identification of bacteria in collected bioaerosols in the presence of interferents. A fingerprint library of collected bioaerosol mass spectra from numerous species can be created using MB. This library of bioaerosol mass spectra can be constructed by analyzing several samples of each strain of bacteria in the collected bioaerosols. It has been suggested that 20 spectra should be used to achieve an ideal average for a reference spectrum. The 20 spectra to be used for the reference spectrum are imported into the fingerprint library and the software is able to a generate peak list from replicate spectra for each strain. A single reference spectrum is created the average of the replicate spectra of each species. In the same manner, a database of collected bioaerosols in the presence of interferents can also be created.

The IR LAST technique should also be explored in the presence of interferents. IR lasers have shown selectivity towards particular biomarkers,[284] which could eliminate a number of possible biomolecule classes for biomarker identification. This innate selectivity of an IR laser source could also be used as an approach to indirectly remove or minimize the amount of interferents present in bioaerosols that could potentially interfere with detection.

REFERENCES

1. Eubanks, L. M.; Dickerson, T. J.; Janda, K. D., Technological Advancements for the Detection of and Protection against Biological and Chemical Warfare Agents. *Chem. Soc. Rev.* **2007,** *36* (3), 458-470.

2. Douwes, J.; Thorne, P.; Pearce, N.; Heederik, D., Bioaerosol Health Effects and Exposure Assessment: Progress and Prospects. *Ann. Occup. Hyg.* **2003,** *47* (3), 187-200.

3. Oren, M., Biological Agents and Terror Medicine Essentials of Terror Medicine. Shapira, S. C.; Hammond, J. S.; Cole, L. A., Eds. Springer New York: 2009; pp 195-221.

4. Neville, T., The Anthrax Letters: A Medical Detective Story. *Libr. J.* **2003,** *128* (18), 114-114.

5. Reefhuis, J.; Valiante, D.; Schill, D.; Pierce, M.; Bresnitz, E., Letters from Trenton: The Anthrax Investigation at the Source, New Jersey, 2001. *Am. J. Epidemiol.* **2002,** *155* (11), 324.

6. Bochner, B., Global Phenotypic Characterization of Bacteria. *FEMS Microbiol. Rev.* **2009,** *33*, 191-205.

7. Janda, J.; Abbot, S., Bacerial Identification for Publication: When Is Enough Enough? *J. Clin. Microbiol.* **2002,** *40* (6), 1887-1897.

8. Bich, C.; Zenobi, R., Mass Spectrometry of Large Complexes. *Curr. Opin. Struc. Biol.* **2009,** *19* (5), 632-639.

9. Demirev, P. A.; Fenselau, C., Mass Spectrometry for Rapid Characterization of Microorganisms. *Annu. Rev. Anal. Chem.* **2008,** *1* (1), 71-93.

10. Sauer, S.; Kliem, M., Mass Spectrometry Tools for the Classification and Identification of Bacteria. *Nat. Rev. Microbiol.* **2010,** *8* (1), 74-82.

11. Fenselau, C.; Demirev, P. A., Characterization of Intact Microorganisms by MALDI Mass Spectrometry. *Mass Spectrom. Rev.* **2001,** *20*, 157-171.

12. Petersen, C. E.; Valentine, N. B.; Wahl, K. L., Characterization of Microorganisms by MALDI Mass Spectrometry. In *Meth. Mol. Biol.* , Clifton, N.J., 2009; Vol. 492, pp 367-79.

13. La Scola, B.; Raoult, D., Direct Identification of Bacteria in Positive Blood Culture Bottles by Matrix-Assisted Laser Desorption Ionisation Time-of-Flight Mass Spectrometry. *Plos One* **2009,** *4* (11), e8401.

14. Elssner, T.; Kostrzewa, M.; Maier, T.; Kruppa, G., Microorganism Identification Based on MALDI-TOF-MS Fingerprints. In *Detection of Biological Agents for the Prevention of Bioterrorism*, Banoub, J., Ed. Springer Netherlands: 2011; pp 99-113.

15. Demirev, P. A.; Feldman, A. B.; Kowalski, P.; Lin, J. S., Top-Down Proteomics for Rapid Identification of Intact Microorganisms. *Anal. Chem.* **2005,** *77* (22), 7455-7461.

16.   Jensen, J. G. *Effect of Atmospheric Background Aerosols on Biological Agent Detectors*; Science Applications International Corporation: Alexandria, VA, 2007; pp 1-31.

17.   Battelle, *Chemical, Biological, Radiological, and Nuclear Defense (Cbrnd) Functional Needs Analysis/Functional Solution Analysis*; Battelle Crystal City Operations: Arlington, Virginia, 2005.

18.   Després, V. R.; Huffman, J. A.; Burrows, S. M.; Hoose, C.; Safatov, A. S.; Buryak, G.; Fröhlich-Nowoisky, J.; Elbert, W.; Andreae, M. O.; Pöschl, U.; Jaenicke, R., Primary Biological Aerosol Particles in the Atmosphere: A Review. *Tellus B* **2012,** *64*, 15598.

19.   Pohanka, M.; Kuča, K., Biological Warfare Agents. In *Molecular, Clinical and Environmental Toxicology*, Luch, A., Ed. Birkhäuser Basel: 2010; Vol. 100, pp 559-578.

20.   Poehlker, C.; Huffman, J. A.; Poeschl, U., Autofluorescence of Atmospheric Bioaerosols - Fluorescent Biomolecules and Potential Interferences. *Atmos. Meas. Tech.* **2012,** *5* (1), 37-71.

21.   Willey, J.; Sherwood, L.; Woolverton, C., *Prescott's Microbiology*. 8th ed.; McGraw-Hill: New York 2011.

22.   Harris, W. A.; Reilly, P. T. A.; Whitten, W. B., MALDI of Individual Biomolecule-Containing Airborne Particles in an Ion Trap Mass Spectrometer. *Anal. Chem.* **2005,** *77* (13), 4042-4050.

23.   Madiga, M. T.; Martinko, J. M.; Parker, J., *Brock Biology of Microorganisms*. 10th ed. ed.; Pearson Education, Inc.: Upper Saddle River, NJ, 2002.

24.   Driks, A., Overview: Development in Bacteria: Spore Formation in Bacillus Subtilis. *Cell. Mol. Life Sci.* **2002,** *59* (3), 389-391.

25.   Noah, D. L.; Huebner, K. D.; Darling, R. G.; Waeckerle, J. F., The History and Threat of Biological Warfare and Terrorism. *Emerg. Med. Clin. N. Am.* **2002,** *20* (2), 255-271.

26.   Szinicz, L., History of Chemical and Biological Warfare Agents. *Toxicology* **2005,** *214* (3), 167-181.

27.   Christopher, L. G. W.; Cieslak, L. T. J.; Pavlin, J. A.; Eitzen, E. M., Biological Warfare. *J Amer. Med. Assoc.* **1997,** *278* (5), 412-417.

28.   Meselson, M.; Guillemin, J.; Hugh-Jones, M.; Langmuir, A.; Popova, I.; Shelokov, A.; Yampolskaya, O., The Sverdlovsk Anthrax Outbreak of 1979. *Science* **1994,** *266* (5188), 1202-1208.

29.   Cox, C. S., Wathes, C.M., *Bioaerosols Handbook*. Lewis Publishers: Boca Raton, 1995.

30.   Hinds, W. C., *Aerosol Tecnology: Properties, Behavior, and Measurement of Airborne Particles*. 1999.

31.   Center, D. T. I., The Militarily Critical Technologies List Part Ii:Weapons of Mass Destruction Technologies. Defense, D. o., Ed. Washington, D. C., 1998.

32. Eitzen, E. M., Use of Biological Weapons. In *Textbook of Military Medicine*, U.S. Army Medical Research Institute of Infectious Diseases: Fort Detrick, Frederick, Maryland 21702-5011, 1997; pp 437-450.

33. Venkatesh, S.; Memish, Z. A., Bioterrorism--a New Challenge for Public Health. *Int. J. Antimicrob. Agents* **2003,** *21* (2), 200-206.

34. Jackson, S. N.; Murray, K. K., Matrix Addition by Condensation for Matrix-Assisted Laser Desorption/Ionization of Collected Aerosol Particles. *Anal. Chem.* **2002,** *74* (18), 4841-4844.

35. Koch, R., *Investigations into Bacteria: V. The Etiology of Anthrax, Based on the Ontogenesis of Bacillus Anthracis*. J. U. Kerns Verlag (Max Muller): Breslau, 1876; Vol. 2, p 277-310.

36. Friedlander, A. M., Anthrax: Clinical Features, Pathogenesis, and Potential Biological Warfare Threat. *Curr. Clin. Top. Infect. Dis.* **2000,** *20*, 335-349.

37. Baillie, L.; Read, T. D., Bacillus Anthracis, a Bug with Attitude! *Curr. Opin. Microbiol.* **2001,** *4* (1), 78-81.

38. Mock, M.; Fouet, A., Anthrax. *Annu. Rev. Microbiol.* **2001,** *55* (1), 647.

39. Primmerman, C. A., Detection of Biological Agents. *Linc.Lab. J.* **2000,** *12* (1), 1-30.

40. Matsumoto, G., Bioterrorism: Anthrax Powder: State of the Art? *Science* **2003,** *302* (5650), 1492-1497.

41. U. S. Army; U. S. Air Force; U. S. Navy; Marine, U. S. *Multiservice Tactics, Techniques, and Procedures for Biological Surveillance*; 2004; pp 1-248.

42. Walt, D. R.; Franz, D. R., Peer Reviewed: Biological Warfare Detection. *Anal. Chem.* **2000,** *72* (23), 738 A-746 A.

43. Lt. Colonel Wunderle, W. D., *U.S. Army Weapons Systems 2010-2011* Skyhorse Publishing Inc.: New York, 2010; p 360.

44. López-Campos, G.; Martínez-Suárez, J. V.; Aguado-Urda, M.; López-Alonso, V., Detection, Identification, and Analysis of Foodborne Pathogens Microarray Detection and Characterization of Bacterial Foodborne Pathogens. Springer US: 2012; pp 13-32.

45. Rasooly, A.; Herold, K. E., Food Microbial Pathogen Detection and Analysis Using DNA Microarray Technologies. *Foodborne Pathog. Dis.* **2008,** *5* (4), 531-550.

46. Stadtländer, C. T., Scanning Electron Microscopy and Transmission Electron Microscopy of Mollicutes: Challenges and Opportunities. In *Modern Research and Educational Topics in Microscopy*, Méndez-Vilas, A.; Díaz, J., Eds. 2007; Vol. 1, pp 122-131.

47. Grin, I.; Schwarz, H.; Linke, D., Electron Microscopy Techniques to Study Bacterial Adhesion. In *Bacterial Adhesion, Advances in Experimental Medician and Biology*, Linke, D.; Goldman, A., Eds. Springer Science: 2011; pp 257-269.

48. Chiarini García, H.; Gambogi Parreira, G.; Jiménez-Millán, J.; Melo, R. C. N.; Nieto, F., Electron Microscopy: Sem/Tem. CRC Press: 2010.

49. Barer, M. R., Viable but Non-Culturable and Dormant Bacteria: Time to Resolve an Oxymoron and a Misnomer? *J. Med. Microbiol.* **1997,** *46* (8), 629-631.

50. Bogosian, G.; Bourneuf, E. V., A Matter of Bacterial Life and Death. *Embo Rep.* **2001,** *2* (9), 770-774.

51. Oliver, J. D., Recent Findings on the Viable but Nonculturable State in Pathogenic Bacteria. *FEMS Microbiol. Rev.* **2010,** *34* (4), 415-425.

52. Sardessai, Y. N., Viable but Non-Culturable Bacteria: Their Impact on Public Health. *Curr. Sci. India* **2005,** *89* (10), 1650-1650.

53. Heidelberg, J.; Shahamat, M.; Levin, M.; Rahman, I.; Stelma, G.; Grim, C.; Colwell, R., Effect of Aerosolization on Culturability and Viability of Gram- Negative Bacteria. *Appl. Environ. Microbiol.* **1997,** *63* (9), 3585-3588.

54. Tracy, B. P.; Gaida, S. M.; Papoutsakis, E. T., Flow Cytometry for Bacteria: Enabling Metabolic Engineering, Synthetic Biology and the Elucidation of Complex Phenotypes. *Curr. Opin. Biotech.* **2010,** *21* (1), 85-99.

55. Cronin, U. P.; Wilkinson, M. G., The Potential of Flow Cytometry in the Study of Bacillus Cereus. *J. Appl. Microbiol* **2010,** *108* (1), 1-16.

56. Forster, S.; Snape, J. R.; Lappin-Scott, H. M.; Porter, J., Simultaneous Fluorescent Gram Staining and Activity Assessment of Activated Sludge Bacteria. *Appl. Environ. Microbiol.* **2002,** *68* (10), 4772-4779.

57. Greenfield, R. A.; Drevets, D. A.; Machado, L. J.; Voskuhl, G. W.; Bronze, M. S., Bacterial Pathogens as Biological Weapons and Agents of Bioterrorism. *Am. J. Med. Sci.* **2002,** *323* (6), 299-315.

58. Khan, M.; Pyle, B. H.; Camper, A. K., Specific and Rapid Enumeration of Viable but Nonculturable and Viable-Culturable Gram-Negative Bacteria by Using Flow Cytometry. *Appl. Environ. Microbiol.* **2010,** *76* (15), 5088-5096.

59. Banada, P. P.; Bhunia, A. K., Antibodies and Immunoassays for Detection of Bacterial Pathogens. In *Principles of Bacterial Detection: Biosensors, Recognition Receptors and Microsystems*, Zourob, M.; Elwary, S.; Turner, A., Eds. Springer New York: 2008; pp 567-602.

60. Wood, W. G., Immunoassays & Co.: Past, Present, Future? A Review and Outlook from Personal Experience and Involvement over the Past 35 Years. *Clin. Lab.* **2008,** *54* (11-12), 423-438.

61. Strachan, N. J. C.; Ogden, I. D., A Sensitive Microsphere Coagulation Elisa for Escherichia Coli O157:H7 Using Russell's Viper Venom. *FEMS Microbiol. Lett.* **2000,** *186* (1), 79-84.

62.   Lambiri, M.; Mavridou, A.; Richardson, S. C.; Papadakis, J. A., Comparison of the Tecra Salmonella Immunoassay with the Conventional Culture Method. *Lett. Appl. Microbiol.* **1990,** *11* (4), 182-184.

63.   Perelle, S.; Dilasser, F.; Malorny, B.; Grout, J.; Hoorfar, J.; Fach, P., Comparison of Pcr-Elisa and Light Cycler Real-Time Pcr Assays for Detecting Salmonella Spp. In Milk and Meat Samples. *Mol. Cell. Probe.* **2004,** *18* (6), 409-420.

64.   Charvat, A.; Abel, B., How to Make Big Molecules Fly out of Liquid Water: Applications, Features and Physics of Laser Assisted Liquid Phase Dispersion Mass Spectrometry. *Phys. Chem. Chem. Phys.* **2007,** *9* (26), 3335-3360.

65.   Moldenhauer, J., Overview of Rapid Microbiological Methods. In *Principles of Bacterial Detection: Biosensors, Recognition Receptors and Microsystems*, Zourob, M.; Elwary, S.; Turner, A., Eds. Springer New York: 2008; pp 49-79.

66.   Toze, S., Pcr and the Detection of Microbial Pathogens in Water and Wastewater. *Water Res.* **1999,** *33* (17), 3545-3556.

67.   Putzig, C. L.; Leugers, M. A.; McKelvy, M. L.; Mitchell, G. E.; Nyquist, R. A.; Papenfuss, R. R.; Yurga, L., Infrared Spectroscopy. *Anal. Chem.* **1994,** *66* (12), 26R-66R.

68.   Al-Holy, M. A.; Lin, M.; Cavinato, A. G.; Rasco, B. A., The Use of Fourier Transform Infrared Spectroscopy to Differentiate Escherichia Coli O157:H7 from Other Bacteria Inoculated into Apple Juice. *Food Microbiol.* **2006,** *23* (2), 162-168.

69.   Naumann, D., *Infrared Spectroscopy in Microbiology*. John Wiley & Sons, Ltd: 2006.

70.   Davis, R.; Mauer, L. J., Fourier Transform Infrared (Ft-Ir) Spectroscopy: A Rapid Tool for Detection and Analysis of Foodborne Pathogenic Bacteria. In *Current Research, Technology and Education Topics in Applied Microbiology and Microbial Biotechnology*, 2010; Vol. 2, pp 1582-1594.

71.   Schrader, B., *General Survey of Vibrational Spectroscopy*. Wiley-VCH Verlag GmbH: 2007; p 7-61.

72.   Maquelin, K.; Kirschner, C.; Choo-Smith, L. P.; van den Braak, N.; Endtz, H. P.; Naumann, D.; Puppels, G. J., Identification of Medically Relevant Microorganisms by Vibrational Spectroscopy. *J. Microbiol. Meth.* **2002,** *51* (3), 255-271.

73.   Efremov, E. V.; Ariese, F.; Gooijer, C., Achievements in Resonance Raman Spectroscopy: Review of a Technique with a Distinct Analytical Chemistry Potential. *Anal. Chim. Acta* **2008,** *606* (2), 119-134.

74.   Yang, H.; Irudayaraj, J., Rapid Detection of Foodborne Microorganisms on Food Surface Using Fourier Transform Raman Spectroscopy. *J. Mol. Struct.* **2003,** *646* (1-3), 35-43.

75.   Kanu, A. B.; Dwivedi, P.; Tam, M.; Matz, L.; Hill, H. H., Ion Mobility-Mass Spectrometry. *J. Mass Spectrom.* **2008,** *43* (1), 1-22.

76. Bohrer, B. C.; Merenbloom, S. I.; Koeniger, S. L.; Hilderbrand, A. E.; Clemmer, D. E., Biomolecule Analysis by Ion Mobility Spectrometry. *Annu. Rev. Anal. Chem.* **2008,** *1* (1), 293-327.

77. El-Aneed, A.; Cohen, A.; Banoub, J., Mass Spectrometry, Review of the Basics: Electrospray, MALDI, and Commonly Used Mass Analyzers. *Appl. Spectrosc. Rev.* **2009,** *44* (3), 210-230.

78. Meuzelaar, H. L. C.; Kistemaker, P. G., Technique for Fast and Reproducible Fingerprinting of Bacteria by Pyrolysis Mass-Spectrometry. *Anal. Chem.* **1973,** *45* (3), 587-590.

79. Twyman, R. M., Mass Spectrometry | Pyrolysis. In *Encyclopedia of Analytical Science*, 2nd ed.; Worsfold, P.; Townshend, A.; Poole, C., Eds. Elsevier: Oxford, 2005; pp 445-450.

80. Spurny, K. R., *Analytical Chemistry of Bioaerosols*. Lewis Publishers: Boca Raton, 1999.

81. Basile, F.; Beverly, M. B.; Abbas-Hawks, C.; Mowry, C. D.; Voorhees, K. J.; Hadfield, T. L., Direct Mass Spectrometric Analysis of in Situ Thermally Hydrolyzed and Methylated Lipids from Whole Bacterial Cells. *Anal. Chem.* **1998,** *70* (8), 1555-1562.

82. Basile, F.; Beverly, M. B.; Voorhees, K. J.; Hadfield, T. L., Pathogenic Bacteria: Their Detection and Differentiation by Rapid Lipid Profiling with Pyrolysis Mass Spectrometry. *TrAC-Trend. Anal. Chem.* **1998,** *17* (2), 95-109.

83. Voorhees, K. J.; Basile, F.; Beverly, M. B.; Abbas-Hawks, C.; Hendricker, A.; Cody, R. B.; Hadfield, T. L., The Use of Biomarker Compounds for the Identification of Bacteria by Pyrolysis Mass Spectrometry. *J. Anal. Appl. Pyrol.* **1997,** *40-1*, 111-134.

84. Sinha, M. P., Platz, R.M., Friedlander, S.K., Vilker, V.L., Characterization of Bacteria by Particle Beam Mass Spectrometry. *Appl. Environ. Microbiol.* **1985,** *49* (6), 1366-1373.

85. Snyder, A. P.; Dworzanski, J. P.; Tripathi, A.; Maswadeh, W. M.; Wick, C. H., Correlation of Mass Spectrometry Identified Bacterial Biomarkers from a Fielded Pyrolysis-Gas Chromatography-Ion Mobility Spectrometry Biodetector with the Microbiological Gram Stain Classification Scheme. *Anal. Chem.* **2004,** *76* (21), 6492-6499.

86. Voorhees, K. J.; Abbas-Hawks, C.; Miketova, P., Identification of Protein Biomarkers in the Pyrolysis Electron Ionization High-Resolution Mass Spectrum of Brucella Neotomae. *J. Anal. Appl. Pyrol.* **2006,** *75* (2), 90-96.

87. Wilkes, J. G.; Rafii, F.; Sutherland, J. B.; Rushing, L. G.; Buzatu, D. A., Pyrolysis Mass Spectrometry for Distinguishing Potential Hoax Materials from Bioterror Agentst. *Rapid. Commun. Mass Spectrom.* **2006,** *20* (16), 2383-2386.

88. Naumann, D., Infrared Spectroscopy in Microbiology. In *Encyclopedia of Analytical Chemistry*, Meyers, R. A., Ed. John Wiley & Sons Ltd: Chichester, 2000; pp 102-131.

89. Barber, M.; Bordoli, R. S.; Sedgwick, R. D.; Tyler, A. N., Fast Atom Bombardment of Solids (F.A.B.): A New Ion Source for Mass Spectrometry. *Chem. Commun.* **1981,** (7), 325-327.

90. Dass, C., *Fundamentals of Contemporary Mass Spectrometry*. John Wiley & Sons, Inc.: Hoboken, 2007.

91. Heller, D. N.; Cotter, R. J.; Fenselau, C.; Uy, O. M., Profiling of Bacteria by Fast Atom Bombardment Mass Spectrometry. *Anal. Chem.* **1987,** *59* (23), 2806-2809.

92. Heller, D. N.; Murphy, C. M.; Cotter, R. J.; Fenselau, C.; Uy, O. M., Constant Neutral Loss Scanning for the Characterization of Bacterial Phospholipids Desorbed by Fast Atom Bombardment. *Anal. Chem.* **1988,** *60* (24), 2787-2791.

93. Hillenkamp, F., Laser Desorption Techniques of Nonvolatile Organic Substances. *Int. J. Mass Spectrom. Ion Phys.* **1982,** *45*, 305-313.

94. Hercules, D. M.; Day, R. J.; Balasanmugam, K.; Dang, T. A.; Li, C. P., Laser Microprobe Mass Spectrometry. 2. Applications to Structural Analysis. *Anal. Chem.* **1982,** *54* (2), 280A-305A.

95. Graham, S. W.; Dowd, P.; Hercules, D. M., Laser Desorption Mass Spectrometry of Some Cobalamins. *Anal. Chem.* **1982,** *54* (4), 649-654.

96. Rousell, D. J.; Dutta, S. M.; Little, M. W.; Murray, K. K., Matrix-Free Infrared Soft Laser Desorption/Ionization. *J. Mass Spectrom.* **2004,** *39* (10), 1182-1189.

97. Ullom, J. N.; Frank, M.; Gard, E. E.; Horn, J. M.; Labov, S. E.; Langry, K.; Magnotta, F.; Stanion, K. A.; Hack, C. A.; Benner, W. H., Discrimination between Bacterial Spore Types Using Time-of-Flight Mass Spectrometry and Matrix-Free Infrared Laser Desorption and Ionization. *Anal. Chem.* **2001,** *73* (10), 2331-2337.

98. Heller, D. N.; Fenselau, C.; Cotter, R. J.; Demirev, P.; Olthoff, J. K.; Honovich, J.; Uy, M.; Tanaka, T.; Kishimoto, Y., Mass Spectral Analysis of Complex Lipids Desorbed Directly from Lyophilized Membranes and Cells. *Biochem. Biophys. Res. Commun.* **1987,** *142* (1), 194-199.

99. Ferreira, L.; Sánchez-Juanes, F.; Muñoz-Bellido, J. L.; González-Buitrago, J. M., Rapid Method for Direct Identification of Bacteria in Urine and Blood Culture Samples by Matrix-Assisted Laser Desorption Ionization Time-of-Flight Mass Spectrometry: Intact Cell Vs. Extraction Method. *Clin. Microbiol. Infect.* **2011,** *17* (7), 1007-1012.

100. Álvarez-Buylla, A.; Culebras, E.; Picazo, J. J., Identification of Acinetobacter Species: Is Bruker Biotyper MALDI-TOF Mass Spectrometry a Good Alternative to Molecular Techniques? *Infect. Genet. Evol.* **2012,** *12* (2), 345-349.

101. Szabados, F.; Woloszyn, J.; Richter, C.; Kaase, M.; Gatermann, S., Identification of Molecularly Defined Staphylococcus Aureus Strains Using Matrix-Assisted Laser Desorption/Ionization Time of Flight Mass Spectrometry and the Biotyper 2.0 Database. *J. Med. Microbiol.* **2010,** *59* (7), 787-790.

102. Fenselau, C.; Demirev, P. A., Characterization of Intact Microorganisms by MALDI Mass Spectrometry. *Mass Spectrom. Rev.* **2001,** *20* (4), 157-171.

103. What Makes Bacteria Pathogenic ? *The Lancet* **1972,** *300* (7771), 266.

104.   Arnold, R. J.; Reilly, J. P., Fingerprint Matching of E. Coli Strains with Matrix-Assisted Laser Desorption/Ionization Time-of-Flight Mass Spectrometry of Whole Cells Using a Modified Correlation Approach. *Rapid Commun. Mass Spectrom.* **1998,** *12* (10), 630-636.

105.   Valentine, N.; Wunschel, S.; Wunschel, D.; Petersen, C.; Wahl, K., Effect of Culture Conditions on Microorganism Identification by Matrix-Assisted Laser Desorption Ionization Mass Spectrometry. *Appl. Environ. Microbiol.* **2005,** *71* (1), 58-64.

106.   Freiwald, A.; Sauer, S., Phylogenetic Classification and Identification of Bacteria by Mass Spectrometry. *Nat. Protocols* **2009,** *4* (5), 732-742.

107.   Jarman, K. H.; Cebula, S. T.; Saenz, A. J.; Petersen, C. E.; Valentine, N. B.; Kingsley, M. T.; Wahl, K. L., An Algorithm for Automated Bacterial Identification Using Matrix-Assisted Laser Desorption/Ionization Mass Spectrometry. *Anal. Chem.* **2000,** *72* (6), 1217-1223.

108.   Giebel, R.; Worden, C.; Rust, S. M.; Kleinheinz, G. T.; Robbins, M.; Sandrin, T. R., Microbial Fingerprinting Using Matrix-Assisted Laser Desorption Ionization Time-of-Flight Mass Spectrometry (MALDI-TOF MS): Applications and Challenges. In *Advances in Applied Microbiology*, Laskin, A. I.; Sariaslani, S.; Gadd, G. M., Eds. Academic Press: 2010; Vol. Volume 71, pp 149-184.

109.   Mann, M.; Hojrup, P.; Roepstorff, P., Use of Mass Spectrometric Molecular Weight Information to Identify Proteins in Sequence Databases. *Biol. Mass. Spectrom.* **1993,** *22* (6), 338-345.

110.   Shadforth, I.; Crowther, D.; Bessant, C., Protein and Peptide Identification Algorithms Using Ms for Use in High-Throughput, Automated Pipelines. *Proteomics* **2005,** *5* (16), 4082-4095.

111.   Demirev, P. A.; Ho, Y. P.; Ryzhov, V.; Fenselau, C., Microorganism Identification by Mass Spectrometry and Protein Database Searches. *Anal. Chem.* **1999,** *71* (14), 2732-2738.

112.   Šedo, O.; Sedláček, I.; Zdráhal, Z., Sample Preparation Methods for MALDI-MS Profiling of Bacteria. *Mass Spectrom. Rev.* **2011,** *30* (3), 417-434.

113.   Ho, Y.-P.; Reddy, P. M., Identification of Pathogens by Mass Spectrometry. *Clin. Chem.* **2010,** *56* (4), 525-536.

114.   Fagerquist, C. K., Proteomics of Foodborne Bacterial Pathogens. In *Genomics of Foodborne Bacterial Pathogens*, Wiedmann, M.; Zhang, W., Eds. Springer New York: 2011; pp 343-402.

115.   Bessède, E.; Angla-gre, M.; Delagarde, Y.; Sep Hieng, S.; Ménard, A.; Mégraud, F., Matrix-Assisted Laser-Desorption/Ionization Biotyper: Experience in the Routine of a University Hospital. *Clin. Microbiol. Infect.* **2011,** *17* (4), 533-538.

116.   Buchan, B. W.; Riebe, K. M.; Ledeboer, N. A., Comparison of the MALDI Biotyper System Using Sepsityper Specimen Processing to Routine Microbiological Methods for Identification of Bacteria from Positive Blood Culture Bottles. *J. Clin. Microbiol.* **2012,** *50* (2), 346-352.

117. Maier, T.; Kostrzewa, M.; Gvozdyak, O.; Pusch, W.; Shi, G., The MALDI Biotyper: Identification and Classification of Microorganisms by MALDI-TOF Ms Profiling. *Mol. Cell. Proteomics* **2006,** *5* (10), 995.

118. Wimmer, J. L.; Long, S. W.; Cernoch, P.; Land, G. A.; Davis, J. R.; Musser, J. M.; Olsen, R. J., A Strategy for Rapid Identification and Antibiotic Susceptibility Testing of Gram-Negative Bacteria Directly Recovered from Positive Blood Cultures Using the Bruker MALDI Biotyper and Bd Phoenix. *J. Clin. Microbiol.* **2012**.

119. Huang, M.; Cheng, S.; Cho, Y.; Shiea, J., Ambient Ionization Mass Spectrometry: A Tutorial. *Anal. Chim. Acta* **2011,** *702* (1), 1-15.

120. Takats, Z.; Wiseman, J. M.; Gologan, B.; Cooks, R. G., Mass Spectrometry Sampling under Ambient Conditions with Desorption Electrospray Ionization. *Science* **2004,** *306* (5695), 471-473.

121. Cooks, R. G.; Ouyang, Z.; Takats, Z.; Wiseman, J. M., Ambient Mass Spectrometry. *Science* **2006,** *311* (5767), 1566-1570.

122. Weston, D. J., Ambient Ionization Mass Spectrometry: Current Understanding of Mechanistic Theory; Analytical Performance and Application Areas. *Analyst* **2010,** *135* (4), 661-668.

123. Gross, J., Ambient Mass Spectrometry. In *Mass Spectrometry a Textbook* 2nd ed.; Springer, Ed. Springer Berlin Heidelberg: 2011; pp 621-645.

124. Pirro, V.; Eberlin, L. S.; Oliveri, P.; Cooks, R. G., Interactive Hyperspectral Approach for Exploring and Interpreting Desi-Ms Images of Cancerous and Normal Tissue Sections. *Analyst* **2012,** *137* (10), 2374-80.

125. Wiseman, J. M.; Ifa, D. R.; Song, Q.; Cooks, R. G., Tissue Imaging at Atmospheric Pressure Using Desorption Electrospray Ionization (Desi) Mass Spectrometry. *Angew. Chem. Int. Edit.* **2006,** *45* (43), 7188-7192.

126. Campbell, I. S.; Ton, A. T.; Mulligan, C. C., Direct Detection of Pharmaceuticals and Personal Care Products from Aqueous Samples with Thermally-Assisted Desorption Electrospray Ionization Mass Spectrometry. *J. Am. Soc. Mass Spectrom.* **2011,** *22* (7), 1285-1293.

127. Lin, Z.; Zhao, M.; Zhang, S.; Yang, C.; Zhang, X., In Situ Arsenic Speciation on Solid Surfaces by Desorption Electrospray Ionization Tandem Mass Spectrometry. *Analyst* **2010,** *135* (6), 1268-1275.

128. Han, Y.; Levkin, P.; Abarientos, I.; Liu, H.; Svec, F.; Frechet, J. M. J., Monolithic Superhydrophobic Polymer Layer with Photopatterned Virtual Channel for the Separation of Peptides Using Two-Dimensional Thin Layer Chromatography-Desorption Electrospray Ionization Mass Spectrometry. *Anal. Chem.* **2010,** *82* (6), 2520-2528.

129. Paglia, G.; Ifa, D. R.; Wu, C.; Corso, G.; Cooks, R. G., Desorption Electrospray Ionization Mass Spectrometry Analysis of Lipids after Two-Dimensional High-Performance Thin-Layer Chromatography Partial Separation. *Anal. Chem.* **2010,** *82* (5), 1744-1750.

130.   Jackson, A. T.; Williams, J. P.; Scrivens, J. H., Desorption Electrospray Ionisation Mass Spectrometry and Tandem Mass Spectrometry of Low Molecular Weight Synthetic Polymers. *Rapid Commun. Mass Spectrom.* **2006,** *20* (18), 2717-2727.

131.   Cody, R. B.; Laramee, J. A.; Durst, H. D., Versatile New Ion Source for the Analysis of Materials in Open Air under Ambient Conditions. *Anal. Chem.* **2005,** *77* (8), 2297-2302.

132.   Jones, R., Dart Ms Makes Sense for Ink Forensics. *Trac-Trend. Anal. Chem.* **2007,** *26* (9), IV-V.

133.   Petucci, C.; Diffendal, J.; Kaufman, D.; Mekonnen, B.; Terefenko, G.; Musselman, B., Direct Analysis in Real Time for Reaction Monitoring in Drug Discovery. *Anal. Chem.* **2007,** *79* (13), 5064-5070.

134.   Pierce, C. Y.; Barr, J. R.; Cody, R. B.; Massung, R. F.; Woolfitt, A. R.; Moura, H.; Thompson, H. A.; Fernandez, F. M., Ambient Generation of Fatty Acid Methyl Ester Ions from Bacterial Whole Cells by Direct Analysis in Real Time (DART) Mass Spectrometry. *Chem. Commun.* **2007,** (8), 807-809.

135.   Song, Y.; Talaty, N.; Datsenko, K.; Wanner, B. L.; Cooks, R. G., In Vivo Recognition of Bacillus Subtilis by Desorption Electrospray Ionization Mass Spectrometry (DESI-MS). *Analyst* **2009,** *134* (5), 838-841.

136.   Song, Y. S.; Talaty, N.; Tao, W. A.; Pan, Z. Z.; Cooks, R. G., Rapid Ambient Mass Spectrometric Profiling of Intact, Untreated Bacteria Using Desorption Electrospray Ionization. *Chem. Commun.* **2007,** (1), 61-63.

137.   Zhang, J. I.; Talaty, N.; Costa, A. B.; Xia, Y.; Tao, W. A.; Bell, R.; Callahan, J. H.; Cooks, R. G., Rapid Direct Lipid Profiling of Bacteria Using Desorption Electrospray Ionization Mass Spectrometry. *Intern. J. Mass Spectrom.* **2011,** *301* (1-3), 37-44.

138.   Jackson, A. U.; Werner, S. R.; Talaty, N.; Song, Y.; Campbell, K.; Cooks, R. G.; Morgan, J. A., Targeted Metabolomic Analysis of Escherichia Coli by Desorption Electrospray Ionization and Extractive Electrospray Ionization Mass Spectrometry. *Anal. Biochem.* **2008,** *375* (2), 272-281.

139.   Caruana, D. J., Detection and Analysis of Airborne Particles of Biological Origin: Present and Future. *Analyst* **2011,** *136* (22), 4641-4652.

140.   Henningson, E. W.; Ahlberg, M. S., Evaluation of Microbiological Aerosol Samplers: A Review. *J. Aerosol Sci.* **1994,** *25* (8), 1459-1492.

141.   Nesa, D.; Lortholary, J.; Bouakline, A.; Bordes, M.; Chandenier, J.; Derouin, F.; Gangneux, J. P., Comparative Performance of Impactor Air Samplers for Quantification of Fungal Contamination. *J. Hosp. Infect.* **2001,** *47* (2), 149-155.

142.   Eduard, W.; Heederik, D., Methods for Quantitative Assessment of Airborne Levels of Noninfectious Microorganisms in Highly Contaminated Work Environments. *Am. Ind. Hyg. Assoc. J.* **1998,** *59* (2), 113-127.

143. Tsuji, K.; Steindler, K. A.; Harrison, S. J., Limulus Amoebocyte Lysate Assay for Detection and Quantitation of Endotoxin in a Small-Volume Parenteral Product. *Appl. Environ. Microbiol.* **1980,** *40* (3), 533-538.

144. Hussaini, S. N.; Hassanali, H. T., Limulus Amoebocyte Lysate Assay of Endotoxin: A Method for Visual Detection of the Positive Gel Reaction. *J. Med. Microbiol.* **1987,** *24* (1), 89-90.

145. Spaan, S.; Smit, L. A.; Eduard, W.; Larsson, L.; Arts, H. J.; Wouters, I. M.; Heederik, D. J., Endotoxin Exposure in Sewage Treatment Workers: Investigation of Exposure Variability and Comparison of Analytical Techniques. *Ann. Agr. Env. Med.* **2008,** *15* (2), 251-261.

146. McMurry, P. H., A Review of Atmospheric Aerosol Measurements. *Atmos. Environ.* **2000,** *34*, 1959-1999.

147. Sinha, M. P.; Platz, R. M.; Vilker, V. L.; Friedlander, S. K., Analysis of Individual Biological Particles by Mass Spectrometry. *Int. J. Mass Spectrom. Ion Processes* **1984,** *57* (1), 125-133.

148. McKeown, P. J.; Johnston, M. V.; Murphy, D. M., On-Line Single-Particle Analysis by Laser Desorption Mass Spectrometry. *Anal. Chem.* **1991,** *63* (18), 2069-2073.

149. Marijnissen, J.; Scarlett, B.; Verheijen, P., Proposed on-Line Aerosol Analysis Combining Size Determination, Laser-Induced Fragmentation and Time-of-Flight Mass Spectroscopy. *J. Aerosol Sci.* **1988,** *19* (7), 1307-1310.

150. Wuijckhuijse, A. L.; Baar, B. L. M., Recent Advances in Real-Time Mass Spectrometry Detection of Bacteria. In *Principles of Bacterial Detection: Biosensors, Recognition Receptors and Microsystems*, Zourob, M.; Elwary, S.; Turner, A., Eds. Springer New York: 2008; pp 929-954.

151. Prather, K. A.; Nordmeyer, T.; Salt, K., Real-Time Characterization of Individual Aerosol Particles Using Time-of-Flight Mass Spectrometry. *Anal. Chem.* **1994,** *66* (9), 1403-1407.

152. Srivastava, A.; Pitesky, M. E.; Steele, P. T.; Tobias, H. J.; Fergenson, D. P.; Horn, J. M.; Russell, S. C.; Czerwieniec, G. A.; Lebrilla, C. B.; Gard, E. E.; Frank, M., Comprehensive Assignment of Mass Spectral Signatures from Individual Bacillus Atrophaeus Spores in Matrix-Free Laser Desorption/Ionization Bioaerosol Mass Spectrometry. *Anal. Chem.* **2005,** *77* (10), 3315-3323.

153. Fergenson, D. P.; Pitesky, M. E.; Tobias, H. J.; Steele, P. T.; Czerwieniec, G. A.; Russell, S. C.; Lebrilla, C. B.; Horn, J. M.; Coffee, K. R.; Srivastava, A.; Pillai, S. P.; Shih, M.-T. P.; Hall, H. L.; Ramponi, A. J.; Chang, J. T.; Langlois, R. G.; Estacio, P. L.; Hadley, R. T.; Frank, M.; Gard, E. E., Reagentless Detection and Classification of Individual Bioaerosol Particles in Seconds. *Anal. Chem.* **2004,** *76* (2), 373-378.

154. Tobias, H. J.; Schafer, M. P.; Pitesky, M.; Fergenson, D. P.; Horn, J.; Frank, M.; Gard, E. E., Bioaerosol Mass Spectrometry for Rapid Detection of Individual Airborne Mycobacterium Tuberculosis H37ra Particles. *Appl. Environ. Microbiol.* **2005,** *71* (10), 6086-6095.

155. Murray, K. K.; Lewis, T. M.; Beeson, M. D.; Russell, D. H., Aerosol Matrix-Assisted Laser Desorption Ionization for Liquid Chromatography/Time-of-Flight Mass Spectrometry. *Anal. Chem.* **1994,** *66* (10), 1601-1609.

156. Murray, K. K.; Russell, D. H., Liquid Sample Introduction for Matrix-Assisted Laser Desorption Ionization. *Anal. Chem.* **1993,** *65* (18), 2534-2537.

157. Fei, X.; Wei, G.; Murray, K. K., Aerosol MALDI with a Reflectron Time-of-Flight Mass Spectrometer. *Anal. Chem.* **1996,** *68* (7), 1143-1147.

158. He, L.; Murray, K. K., 337 Nm Matrix-Assisted Laser Desorption/Ionization of Single Aerosol Particles. *J. Mass Spectrom.* **1999,** *34* (9), 909-914.

159. He, L.; Murray, K. K., A Laminar Flow Nebulizer for Aerosol MALDI. *Anal. Chem.* **1997,** *69* (17), 3613-3616.

160. Czerwieniec, G. A.; Russell, S. C.; Lebrilla, C. B.; Coffee, K. R.; Riot, V.; Steele, P. T.; Frank, M.; Gard, E. E., Improved Sensitivity and Mass Range in Time-of-Flight Bioaerosol Mass Spectrometry Using an Electrostatic Ion Guide. *J. Am. Soc. Mass. Spectrom.* **2005,** *16* (11), 1866-1875.

161. Stowers, M. A.; Wuijckhuijse, A. L. v.; Marijnissen, J. C. M.; Scarlett, B.; van Baar, B. L. M.; Kientz, C., E., Application of Matrix-Assisted Laser Desorption/Ionization to on-Line Aerosol Time-of-Flight Mass Spectrometry. *Rapid Commun. Mass Spectrom.* **2000,** *14* (10), 829-833.

162. Sullivan, R. C.; Prather, K. A., Recent Advances in Our Understanding of Atmospheric Chemistry and Climate Made Possible by on-Line Aerosol Analysis Instrumentation. *Anal. Chem.* **2005,** *77* (12), 3861-3886.

163. Fergenson, D. P.; Pitesky, M. E.; Tobias, H. J.; Steele, P. T.; Czerwieniec, G. A.; Russell, S. C.; Lebrilla, C. B.; Horn, J. M.; Coffee, K. R.; Srivastava, A.; Pillai, S. P.; Shih, M. T. P.; Hall, H. L.; Ramponi, A. J.; Chang, J. T.; Langlois, R. G.; Estacio, P. L.; Hadley, R. T.; Frank, M.; Gard, E. E., Reagentless Detection and Classification of Individual Bioaerosol Particles in Seconds. *Anal.Chem.* **2004,** *76* (2), 373-378.

164. St. Louis, R. H.; Hill, H. H., Ion Mobility Spectrometry in Analytical Chemistry. *Crit. Rev. Anal. Chem.* **1990,** *21* (5), 321-355.

165. Harvey, S. R.; MacPhee, C. E.; Barran, P. E., Ion Mobility Mass Spectrometry for Peptide Analysis. *Methods* **2011,** *54* (4), 454-461.

166. Fenn, L. S.; McLean, J. A., Biomolecular Structural Separations by Ion Mobility-Mass Spectrometry. *Anal. Bioanal. Chem.* **2008,** *391* (3), 905-909.

167. Karasek, F. W.; Hill, H. H.; Kim, S. H.; Rokushika, S., Gas Chromatographic Detection Modes for the Plasma Chromatograph. *J. Chromatogr. A* **1977,** *135* (2), 329-339.

168. Rokushika, S.; Hatano, H.; Hill, H. H., Ion Mobility Spectrometry in Carbon Dioxide. *Anal. Chem.* **1986,** *58* (2), 361-365.

169. Rokushika, S.; Hatano, H.; Hill, H. H., Ion Mobility Spectrometry after Supercritical Fluid Chromatography. *Anal. Chem.* **1987,** *59* (1), 8-12.

170. Karasek, F. W.; Keller, R. A., Gas Chromatograph/Plasma Chromatograph Interface and Its Performance in the Detection of Musk Ambrette. *J. Chromatogr. Sci.* **1972,** *10*, 626.

171. Karasek, F. W.; Denney, D. W., Evaluation of the Plasma Chromatograph as a Qualitative Detector for Liquid Chromatography. *Anal. Lett.* **1973,** *6* (11), 993.

172. Karasek, F. W.; Denney, D. W., Role of Nitric Oxide in Positive Reactant Ions in Plasma Chromatography. *Anal. Chem.* **1974,** *46* (6), 633-637.

173. Karasek, F. W.; Denney, D. W.; DeDecker, E. H., Plasma Chromatography of Normal Alkanes and Its Relation to Chemical Ionization Mass Spectrometry. *Anal. Chem.* **1974,** *46* (8), 970-973.

174. Karasek, F. W.; Kane, D. M., Plasma Chromatography of Isomeric Halogenated Nitrobenzenes. *Anal. Chem.* **1974,** *46* (6), 780-782.

175. Karasek, F. W.; Kim, S. H., Identification of the Isomeric Phthalic Acids by Mobility and Mass Spectra. *Anal. Chem.* **1975,** *47* (7), 1166-1168.

176. Karasek, F. W.; Kim, S. H.; Hill, H. H., Mass Identified Mobility Spectra of P-Nitrophenol and Reactant Ions in Plasma Chromatography. *Anal. Chem.* **1976,** *48* (8), 1133-1137.

177. Karasek, F. W.; Laub, R. J., Instrumental Determination of Molecular Weight by Gas Pressure. *Anal. Chem.* **1974,** *46* (9), 1349-1351.

178. Preston, J. M.; Karasek, F. W.; Kim, S. H., Plasma Chromatography of Phosphorus Esters. *Anal. Chem.* **1977,** *49* (12), 1746-1750.

179. Karpas, Z.; Eiceman, G. A., *Ion Mobility Spectrometry*. 2nd ed.; CRC Press: Boca Raton, 2005.

180. Snyder, A. P.; Shoff, D. B.; Eiceman, G. A.; Blyth, D. A.; Parsons, J. A., Detection of Bacteria by Ion Mobility Spectrometry. *Anal. Chem.* **1991,** *63* (5), 526-529.

181. Vinopal, R. T.; Jadamec, J. R.; deFur, P.; Demars, A. L.; Jakubielski, S.; Green, C.; Anderson, C. P.; Dugas, J. E.; DeBono, R. F., Fingerprinting Bacterial Strains Using Ion Mobility Spectrometry. *Anal. Chim. Acta* **2002,** *457* (1), 83-95.

182. Fernandez-Lima, F.; Kaplan, D.; Suetering, J.; Park, M., Gas-Phase Separation Using a Trapped Ion Mobility Spectrometer. *Int. J. Ion Mobil. Spectrom.* **2011,** *14* (2), 93-98.

183. Russell, D. H.; Gillig, K. J.; McLean, J. A.; Ruotolo, B. T., Ion Mobility-Mass Spectrometry: A New Paradigm for Proteomics. *Int. J. of Mass Spec.* **2005,** *240*, 301-315.

184. Myung, S.; Lee, Y. J.; Moon, M. H.; Taraszka, J.; Sowell, R.; Koeniger, S.; Hilderbrand, A. E.; Valentine, S. J.; Cherbas, L.; Cherbas, P.; Kaufmann, T. C.; Miller, D. F.; Mechref, Y.; Novotny, M. V.; Ewing, M. A.; Sporleder, C. R.; Clemmer, D. E., Development of High-Sensitivity Ion Trap Ion Mobility Spectrometry Time-of-Flight Techniques: A High-

Throughput Nano-LC-IMS-TOF Separation of Peptides Arising from a Drosophila Protein Extract. *Anal. Chem.* **2003,** *75* (19), 5137-5145.

185.   Merenbloom, S. I.; Koeniger, S. L.; Valentine, S. J.; Plasencia, M. D.; Clemmer, D. E., IMS − IMS and IMS − IMS − IMS /MS for Separating Peptide and Protein Fragment Ions. *Anal. Chem.* **2006,** *78* (8), 2802-2809.

186.   Tang, K.; Shvartsburg, A. A.; Lee, H.; Prior, D. C.; Buschbach, M. A.; Li, F.; Tolmachev, A. V.; Anderson, G. A.; Smith, R. D., High-Sensitivity Ion Mobility Spectrometry/Mass Spectrometry Using Electrodynamic Ion Funnel Interfaces. *Anal. Chem.* **2005,** *77* (10), 3330-3339.

187.   Merenbloom, S. I.; Koeniger, S. L.; Valentine, S. J.; Plasencia, M. D.; Clemmer, D. E., Ims-Ims and Ims-Ims-Ims/Ms for Separating Peptide and Protein Fragment Ions. *Anal. Chem.* **2006,** *78* (8), 2802-2809.

188.   Dwivedi, P.; Wu, P.; Klopsch, S.; Puzon, G.; Xun, L.; Hill, H., Metabolic Profiling by Ion Mobility Mass Spectrometry (Imms). *Metabolomics* **2008,** *4* (1), 63-80.

189.   Dwivedi, P.; Puzon, G.; Tam, M.; Langlais, D.; Jackson, S. N.; Kaplan, K.; Siems, W. F.; Schultz, A. J.; Xun, L.; Woods, A. S.; Hill, H. H., Metabolic Profiling of Escherichia Coli by Ion Mobility-Mass Spectrometry with MALDI Ion Source. *J. Mass Spectrom.* **2010,** *45* (12), 1383-1393.

190.   Dass, C., *Principles and Practice of Biological Mass Spectrometry*. 2001.

191.   Cotter, R. J., Time-of-Flight Mass Spectrometry. In *Time-of-Flight Mass Spectrometry*, Cotter, R. J., Ed. American Chemical Society: 1993; Vol. 549, p 35.

192.   Watson, J. T., *Introduction to Mass Spectrometry*. Raven Press: New York, 1985.

193.   Cotter, R. J., Time-of-Flight Mass Spectrometry. In *Time-of-Flight Mass Spectrometry*, Cotter, R. J., Ed. American Chemical Society: 1993; Vol. 549, pp 16-48.

194.   Cotter, R. J., Time-of-Flight Mass Spectrometry for the Structural Analysis of Biological Molecules. *Anal. Chem.* **1992,** *64* (21), 1027A-1039A.

195.   Vestal, M. L., Modern MALDI Time-of-Flight Mass Spectrometry. *J. Mass Spectrom.* **2009,** *44* (3), 303-317.

196.   Whittal, R. M.; Li, L., High-Resolution Matrix-Assisted Laser Desorption/Ionization in a Linear Time-of-Flight Mass Spectrometer. *Anal. Chem.* **1995,** *67* (13), 1950-1954.

197.   Gross, J. H., Instrumentation. In *Mass Spectrometry a Textbook*, Springer Berlin Heidelberg: 2011; pp 117-221.

198.   Brown, R. S.; Lennon, J., Mass Resolution Improvement by Incorporation of Pulsed Ion Extraction in a Matrix-Assisted Laser Desorption/Ionization Linear Time-of-Flight Mass Spectrometer. *Anal. Chem.* **1995,** *67* (13), 1998-2003.

199. Vestal, M. L.; Juhasz, P.; Martin, S. A., Delayed Extraction Matrix-Assisted Laser Desorption Time-of-Flight Mass Spectrometry. *Rapid Commun. Mass Spectrom.* **1995,** *9* (11), 1044-1050.

200. Olthoff, J. K.; Lys, I. A.; Cotter, R. J., A Pulsed Time-of-Flight Mass Spectrometer for Liquid Secondary Ion Mass Spectrometry. *Rapid Commun. Mass Spectrom.* **1988,** *2* (9), 171-175.

201. Cotter, R. J.; Griffith, W.; Jelinek, C., Tandem Time-of-Flight (Tof/Tof) Mass Spectrometry and the Curved-Field Reflectron. *J. Chromatogr.B* **2007,** *855* (1), 2-13.

202. Cornish, T. J.; Cotter, R. J., A Curved-Field Reflectron for Improved Energy Focusing of Product Ions in Time-of-Flight Mass Spectrometry. *Rapid Commun. Mass Spectrom.* **1993,** *7* (11), 1037-1040.

203. Guilhaus, M.; Selby, D.; Mlynski, V., Orthogonal Acceleration Time-of-Flight Mass Spectrometry. *Mass Spectrom. Rev.* **2000,** *19* (2), 65-107.

204. Gross, J. H., Tandem Mass Spectrometry. In *Mass Spectrometry a Textbook*, Springer Berlin Heidelberg: 2011; pp 415-478.

205. Johnson, J. V.; Yost, R. A.; Kelley, P. E.; Bradford, D. C., Tandem-in-Space and Tandem-in-Time Mass Spectrometry: Triple Quadrupoles and Quadrupole Ion Traps. *Anal. Chem.* **1990,** *62* (20), 2162-2172.

206. Bradbury, N. E.; Nielsen, R. A., Absolute Values of the Electron Mobility in Hydrogen. *Phys Rev.* **1936,** *49* (5), 0388-0393.

207. Holle, A.; Haase, A.; Kayser, M.; Höhndorf, J., Optimizing Uv Laser Focus Profiles for Improved MALDI Performance. *J. Mass Spectrom.* **2006,** *41* (6), 705-716.

208. Suckau, D.; Resemann, A.; Schuerenberg, M.; Hufnagel, P.; Franzen, J.; Holle, A., A Novel MALDI Lift-TOF/TOF Mass Spectrometer for Proteomics. *Anal. Bioanal.Chem.* **2003,** *376* (7), 952-965.

209. Go, E. P.; Apon, J. V.; Luo, G.; Saghatelian, A.; Daniels, R. H.; Sahi, V.; Dubrow, R.; Cravatt, B. F.; Vertes, A.; Siuzdak, G., Desorption/Ionization on Silicon Nanowires. *Anal. Chem.* **2005,** *77* (6), 1641-1646.

210. Savickas, P. J.; Moskovets, E.; Daniels, R. H.; Dubrow, R.; V., H.; Karger, B. L. Proceeding of the 53rd ASMS Cinference on Mass Spectrometry and Allied Topics, San Antonio, TX, San Antonio, TX, 2005.

211. Suckau, D.; Resemann, A., T3-Sequencing: Targeted Characterization of the N- and C-Termini of Undigested Proteins by Mass Spectrometry. *Anal. Chem.* **2003,** *75* (21), 5817-5824.

212. Gillig, K. J.; Ruotolo, B. T.; Stone, E. G.; Russell, D. H., An Electrostatic Focusing Ion Guide for Ion Mobility-Mass Spectrometry. *Int. J. Mass Spectrom.* **2004,** *239* (1), 43-49.

213. Russell, D. H.; Gillig, K. J.; Verbeck, G. F.; Ruotolo, B. T.; Sawyer, H. A., A Fundamental Introduction to Ion Mobility Mass Spectrometry Appliedto the Analysis of Biomolecules. *J. Biomol. Tech.* **2002,** *13* (2), 56-61.

214. Woods, A. S., Schultz, J. A., Ugarov, M., Egan, T., Koomen, J., Gillig, K. J., Fuhrer, K., Gonin, M., Lipid/Peptide/Nucleotide Separation with MALDI-Ion Mobility TOF Ms. *Anal. Chem.* **2004,** *76*, 2187-2195.

215. McLean, J. A.; Schultz, J. A.; Woods, A. S., *Ion Mobility-Mass Spectrometry*. 2nd ed.; Wiley: Hoboken, 2010; p 847.

216. Russell, D. H., Gillig, K.J., McLean, J.A., Ruotolo, B.T., , Peak Capacity of Ion Mobility Mass Spectrometry: The Utility of Varying Drift Gas Polarizability for the Separation of Tryptic Peptides. *J. Mass Spectrom.* **2004,** *39*, 361-367.

217. Russell, D. H.; McLean, J. A., Sub-Femtomole Peptide Detection in Ion-Mobility-Time-of-Flight. *J. Proteome Res.* **2003,** *2*, 427-430.

218. Monticelli, F.; Tutsch-Bauer, E.; Keller, A.; Keller, T., Application of Ion Mobility Spectrometry in Cases of Forensic Interest. *Forensic Sci. Int.* **2006,** *161*, 130 - 140.

219. Garofolo, F., Migliozzi, V., Roio, B., Application of Ion Mobility Spectrometry to the Identification of Trace Levels of Explosives in the Presence of Complex Matrices. *Rapid. Commun. Mass Spectrom.* **1994,** *8*, 527 - 532.

220. Woods, A. S.; Koomen, J. M.; Ruotolo, B. T.; Gillig, K. J.; Russel, D. H.; Fuhrer, K.; Gonin, M.; Egan, T. F.; Schultz, J. A., A Study of Peptide-Peptide Interactions Using MALDI Ion Mobility O-TOF and Esimass Spectrometry. *Journal of the American Society for Mass Spectrometry* **2002,** *13* (2), 166-169.

221. Ruotolo, B. T.; Gillig, K. J.; Stone, E. G.; Russell, D. H.; Fuhrer, K.; Gonin, M.; Schultz, J. A., Analysis of Protein Mixtures by Matrix-Assisted Laser Desorption Ionization-Ion Mobility-Orthogonal-Time-of-Flight Mass Spectrometry. *Int. J. of Mass Spec.* **2002,** *219* (1), 253-267.

222. Henderson, S. C.; Valentine, S. J.; Counterman, A. E.; Clemmer, D. E., Esi/Ion Trap/Ion Mobility/Time-of-Flight Mass Spectrometry for Rapid and Sensitive Analysis of Biomolecular Mixtures. *Anal. Chem.* **1999,** *71* (2), 291-301.

223. Gillig, K. J.; Ruotolo, B.; Stone, E. G.; Russell, D. H.; Fuhrer, K.; Gonin, M.; Schultz, A. J., Coupling High-Pressure MALDI with Ion Mobility/Orthogonal Time-of-Flight Mass Spectrometry. *Anal. Chem.* **2000,** *72* (17), 3965-3971.

224. Belov, M. E.; Buschbach, M. A.; Prior, D. C.; Tang, K., Multiplexed Ion Mobility Spectrometry-Orthogonal Time-of-Flight Mass Spectrometry. *Anal. Chem.* **2007,** *79*, 2451-2462.

225. Matz, L. M.; Asbury, G. R.; Hill, H. H., Two-Dimensional Separations with Electrospray Ionization Ambient Pressure High-Resolution Ion Mobility/Quadrupole Mass Spectrometry. *Rapid Commun. Mass Spectrom.* **2002,** *16*, 670-675.

226. Jackson, S. N.; Colsch, B.; Egan, T.; Lewis, E. K.; Schultz, J. A.; Woods, A. S., Gangliosides' Analysis by MALDI-Ion Mobility Ms. *Analyst* **2011,** *136* (3), 463-466.

227. Zhong, Y.; Hyung, S.; Ruotolo, B. T., Ion Mobility–Mass Spectrometry for Structural Proteomics. *Expert Rev. Proteomic.* **2012,** *9* (1), 47-58.

228. Ferreira, R.; Marchand, A.; Gabelica, V., Mass Spectrometry and Ion Mobility Spectrometry of G-Quadruplexes. A Study of Solvent Effects on Dimer Formation and Structural Transitions in the Telomeric DNA Sequence D(Tagggttagggt). *Methods* **2012,** *57* (1), 56-63.

229. Goodwin, C. R.; Fenn, L. S.; Derewacz, D. K.; Bachmann, B. O.; McLean, J. A., Structural Mass Spectrometry: Rapid Methods for Separation and Analysis of Peptide Natural Products. *J Nat. Prod.* **2012,** *75* (1), 48-53.

230. Wyttenbach, T.; Kemper, P. R.; Bowers, M. T., Design of a New Electrospray Ion Mobility Mass Spectrometer. *Int. J. Mass Spectrom.* **2001,** *212* (1-3), 13-23.

231. Karas, M.; Bahr, U.; Giessmann, U., Matrix-Assisted Laser Desorption Ionization Mass-Spectrometry. *Mass Spectrom. Rev.* **1991,** *10* (5), 335-357.

232. Hillenkamp, F.; Karas, M.; Beavis, R. C.; Chait, B. T., Matrix-Assisted Laser Desorption/Ionization Mass Spectrometry of Biopolymers. *Anal. Chem.* **1991,** *63* (24), 1193A-1203A.

233. Kang, M.-J.; Pyun, J.-C.; Lee, J.-C.; Choi, Y.-J.; Park, J.-H.; Park, J.-G.; Lee, J.-G.; Choi, H.-J., Nanowire-Assisted Laser Desorption and Ionization Mass Spectrometry for Quantitative Analysis of Small Molecules. *Rapid Commun. Mass Spectrom.* **2005,** *19* (21), 3166-3170.

234. Daniels, R. H.; Dikler, S.; Li, E.; Stacey, C., Break Free of the Matrix: Sensitive and Rapid Analysis of Small Molecules Using Nanostructured Surfaces and LDI-TOF Mass Spectrometry. *J. Assoc. Lab. Autom.* **2008,** *13* (6), 314-321.

235. Wyatt, M.; Ding, S.; Stein, B.; Brenton, A.; Daniels, R., Analysis of Various Organic and Organometallic Compounds Using Nanostructure-Assisted Laser Desorption/Ionization Time-of-Flight Mass Spectrometry (NALDI-TOF MS). *J. Am. Soc. Mass. Spectrom.* **2010,** *21* (7), 1256-1259.

236. Shenar, N.; Cantel, S.; Martinez, J.; Enjalbal, C., Comparison of Inert Supports in Laser Desorption/Ionization Mass Spectrometry of Peptides: Pencil Lead, Porous Silica Gel, Dios-Chip and NALDI Target. *Rapid Commun. Mass Spectrom.* **2009,** *23* (15), 2371-2379.

237. Akhmetov, A.; Moore, J. F.; Gasper, G. L.; Koin, P. J.; Hanley, L., Laser Desorption Postionization for Imaging Ms of Biological Material. *J. Mass Spectrom.* **2010,** *45* (2), 137-145.

238. Schultz, J. A.; Egan, T. F.; Waters, K. L.; Lewis, E. K. Post-Ionization of Neutrals for Ion Mobility Otofms Identification of Molecules and Elements Desorbed from Surfaces 2010.

239. Hanley, L.; Zimmermann, R., Light and Molecular Ions: The Emergence of Vacuum UV Single-Photon Ionization in Ms. *Anal. Chem.* **2009,** *81* (11), 4174-4182.

240.   Gasper, G. L.; Carlson, R.; Akhmetov, A.; Moore, J. F.; Hanley, L., Laser Desorption 7.87 eV Postionization Mass Spectrometry of Antibiotics in Staphylococcus Epidermidis Bacterial Biofilms. *Proteomics* **2008,** *8* (18), 3816-3821.

241.   Misra, P.; Dubinski, M. A., *Ultraviolet Spectroscopy and UV Laser: Practical Spectroscopy Series*. Marcel Dekker: New York 2002.

242.   Park, S.-G.; Murray, K. K., Infrared Laser Ablation Sample Transfer for MALDI and Electrospray. *J. Am. Soc. Mass Spectrom.* **2011,** *22* (8), 1352-1362.

243.   Rezenom, Y. H.; Dong, J.; Murray, K. K., Infrared Laser-Assisted Desorption Electrospray Ionization Mass Spectrometry. *Analyst* **2008,** *133* (2), 226-232.

244.   Sampson, J. S.; Murray, K. K.; Muddiman, D. C., Intact and Top-Down Characterization of Biomolecules and Direct Analysis Using Infrared Matrix-Assisted Laser Desorption Electrospray Ionization Coupled to Ft-Icr Mass Spectrometry. *J. Am. Soc. Mass Spectrom.* **2009,** *20* (4), 667-673.

245.   Bayat, A., Science, Medicine, and the Future - Bioinformatics. *Brit. Med. J.* **2002,** *324* (7344), 1018-1022.

246.   Edwards, N. J.; Pineda, F. In Proceedings of the 54th Conference of the Annual American Society of Mass Spectrometry; Seattle, WA, May 28-June 1, 2006.

247.   Salzberg, S. L.; Delcher, A. L.; Kasif, S.; White, O., Microbial Gene Identification Using Interpolated Markov Models. *Nucleic Acids Res.* **1998,** *26* (2), 544-548.

248.   Delcher, A. L.; Harmon, D.; Kasif, S.; White, O.; Salzberg, S. L., Improved Microbial Gene Identification with Glimmer. *Nucleic Acids Res.* **1999,** *27* (23), 4636-4641.

249.   Delcher, A. L.; Bratke, K. A.; Powers, E. C.; Salzberg, S. L., Identifying Bacterial Genes and Endosymbiont DNA with Glimmer. *Bioinformatics* **2007,** *23* (6), 673-679.

250.   Yergey, J.; Heller, D.; Hansen, G.; Cotter, R. J.; Fenselau, C., Isotopic Distributions in Mass Spectra of Large Molecules. *Anal. Chem.* **1983,** *55* (2), 353-356.

251.   Jackson, O. L., Jr., MALDI-TOF Mass Spectrometry of Bacteria. *Mass Spectrom. Rev.* **2001,** *20* (4), 172-194.

252.   Anhalt, J. P., Fenselau, C., Identification of Bacteria Using Mass Spectrometry. *Anal. Chem.* **1975,** *47* (2), 219-225.

253.   Krishnamurthy, T.; Rajamani, U.; Ross, P.; Jabbour, R.; Nair, H.; Eng, J.; Yates, J.; Davis, M.; Stahl, D.; Lee, T., Mass Spectral Investigations on Microoranisms. *J. Toxicol.–Toxin Rev.* **2000,** *19* (1), 95.

254.   Conway, G. C.; Smole, S. C.; Sarracino, D. A.; Arbeit, R. D.; Leopold, P. E., Phyloproteomics: Species Identification of Enterobacteriaceae Using Matrix-Assisted Laser Desorption/Ionization Time-of-Flight Mass Spectrometry. *J Mol Microbiol Biotechnol* **2001,** *3* (1), 103-112.

255. Ryzhov, V.; Hathout, Y.; Fenselau, C., Rapid Characterization of Spores of Bacillus Cereus Group Bacteria by Matrix-Assisted Laser Desorption-Ionization Time-of-Flight Mass Spectrometry. *Appl. Environ. Microbiol.* **2000,** *66* (9), 3828-3834.

256. Winkler, M. A.; Uher, J.; Cepa, S., Direct Analysis and Identification of Helicobacter and Campylobacter Species by MALDI-TOF Mass Spectrometry. *Anal. Chem.* **1999,** *71* (16), 3416-3419.

257. Krishnamurthy, T.; Ross, P. L.; Rajamani, U., Detection of Pathogenic and Non-Pathogenic Bacteria by Matrix-Assisted Laser Desorption/ Ionization Time-of-Flight Mass Spectrometry. *Rapid. Commun. Mass Spectrom.* **1996,** *10* (8), 883-888.

258. Carbonnelle, E.; Mesquita, C.; Bille, E.; Day, N.; Dauphin, B.; Beretti, J. L.; Ferroni, A.; Gutmann, L.; Nassif, X., MALDI-TOF Mass Spectrometry Tools for Bacterial Identification in Clinical Microbiology Laboratory. *Clin. Biochem.* **2011,** *44* (1), 104-9.

259. Yao, Z.-P.; Demirev, P. A.; Fenselau, C., Mass Spectrometry-Based Proteolytic Mapping for Rapid Virus Identification. *Anal. Chem.* **2002,** *74* (11), 2529-2534.

260. Claydon, M. A.; Davey, S. N.; EdwardsJones, V.; Gordon, D. B., The Rapid Identification of Intact Microorganisms Using Mass Spectrometry. *Nat. Biotechnol.* **1996,** *14* (11), 1584-1586.

261. Wahl, K. L.; Wunschel, S. C.; Jarman, K. H.; Valentine, N. B.; Petersen, C. E.; Kingsley, M. T.; Zartolas, K. A.; Saenz, A. J., Analysis of Microbial Mixtures by Matrix-Assisted Laser Desorption/Ionization Time-of-Flight Mass Spectrometry. *Anal. Chem.* **2002,** *74* (24), 6191-6199.

262. Koomen, J. M.; Routolo, B. T.; Gillig, K. J.; McClean, J. A.; Russell, D. H.; Kang, M.; Dunbar, K. R.; Fuhrer, K.; Gonin, M.; Schultz, J. A., Oligonucleotide Analysis with MALDI-Ion-Mobility-TOFMS. *Anal. Bioanal. Chem.* **2002,** *373*, 612-617.

263. Dwivedi, P.; Wu, P.; Klopsch, S. J.; Puzon, G. J.; Xun, L.; Hill, H. H., Metabolic Profiling by Ion Mobility Mass Spectrometry (Imms). *Metabolomics* **2008,** *4* (1), 63-80.

264. Leenders, F.; Stein, T. H.; Kablitz, B.; Franke, P.; Vater, J., Rapid Typing of *Bacillus Subtilis* Strains by Their Secondary Metabolites Using Matrix-Assisted Laser Desorption/Ionization Mass Spectrometry of Intact Cells. *Rapid. Commun. Mass Spectrom.* **1999,** *13* (10), 943-949.

265. Stein, T., Whole-Cell Matrix-Assisted Laser Desorption/Ionization Mass Spectrometry for Rapid Identification of Bacteriocin/Lantibiotic-Producing Bacteria. *Rapid. Commun. Mass Spectrom.* **2008,** *22* (8), 1146-1152.

266. Zhengping Wang; Larry Russon; Liang Li; Dennis C. Roser; Long, S. R., Investigation of Spectral Reproducibility in Direct Analysis of Bacteria Proteins by Matrix-Assisted Laser Desorption/Ionization Time-of-Flight Mass Spectrometry. *Rapid. Commun. Mass Spectrom.* **1998,** *12* (8), 456-464.

267. Jones, J. J.; Stump, M. J.; Fleming, R. C.; Lay, J. O.; Wilkins, C. L., Investigation of MALDI-TOF and FT-MS Techniques for Analysis of *Escherichia coli* Whole Cells. *Anal. Chem.* **2003,** *75* (6), 1340-1347.

268. Ryzhov, V.; Fenselau, C., Characterization of the Protein Subset Desorbed by MALDI from Whole Bacterial Cells. *Anal. Chem.* **2001,** *73* (4), 746-750.

269. Stein, T.; Borchert, S.; Conrad, B.; Feesche, J.; Hofemeister, B.; Hofemeister, J.; Entian, K., Two Different Lantibiotic-Like Peptides Originate from the Ericin Gene Cluster of Bacillus Subtilis A1/3. *J. Bacteriol.* **2002,** *184* (6), 1703-1711.

270. Stein, T.; Entian, K. D., Maturation of the Lantibiotic Subtilin: Matrix-Assisted Laser Desorption/Ionization Time-of-Flight Mass Spectrometry to Monitor Precursors and Their Proteolytic Processing in Crude Bacterial Cultures. *Rapid. Commun. Mass Spectrom.* **2002,** *16* (2), 103-110.

271. Madonna, A. J.; Voorhees, K. J.; Taranenko, N. I.; Laiko, V. V.; Doroshenko, V. M., Detection of Cyclic Lipopeptide Biomarkers from Bacillus Species Using Atmospheric Pressure Matrix-Assisted Laser Desorption/Ionization Mass Spectrometry. *Anal. Chem.* **2003,** *75* (7), 1628-1637.

272. Arnold, R. J.; Karty, J. A.; Ellington, A. D.; Reilly, J. P., Monitoring the Growth of a Bacteria Culture by MALDI-MS of Whole Cells. *Anal. Chem.* **1999,** *71* (10), 1990-1996.

273. Greenwood, D. P.; Jeys, T. H.; Johnson, B.; Richardson, J. M.; Shatz, M. P., Optical Techniques for Detecting and Identifying Biological-Warfare Agents. *Pr. Inst. Electr. Elect.* **2009,** *97* (6), 971-989.

274. Kim, J. K.; Jackson, S. N.; Murray, K. K., Matrix-Assisted Laser Desorption/Ionization Mass Spectrometry of Collected Bioaerosol Particles. *Rapid. Commun. Mass Spectrom.* **2005,** *19* (12), 1725-1729.

275. Dugas, A. J.; Murray, K. K., On-Target Digestion of Collected Bacteria for MALDI Mass Spectrometry. *Anal. Chim. Acta* **2008,** *627* (1), 154-161.

276. McBride, M. T.; Masquelier, D.; Hindson, B. J.; Makarewicz, A. J.; Brown, S.; Burris, K.; Metz, T.; Langlois, R. G.; Tsang, K. W.; Bryan, R.; Anderson, D. A.; Venkateswaran, K. S.; Milanovich, F. P.; Colston, B. W., Autonomous Detection of Aerosolized Bacillus Anthracis and Yersinia Pestis. *Anal. Chem.* **2003,** *75* (20), 5293-5299.

277. Linden, E. V., *Focus on Terrorism*. Nova Science Publisher: Hauppauge, 2002; Vol. 2.

278. Dowhan, W., Molecular Basis for Membrane Phospholipid Diversity:Why Are There So Many Lipids? *Annu. Rev. Biochem* **1997,** *66* (1), 199-232.

279. Bligh, E. G.; Dyer, W. J., A Rapid Method of Total Lipid Extraction and Purification. *Can. J. Biochem. Phys.* **1959,** *37* (8), 911-917.

280. Folch, J.; Lees, M.; Stanley, G. H. S., A Simple Method for the Isolation and Purification of Total Lipides from Animal Tissues *J. Biol. Chem.* **1957,** *226* (1), 497-509.

281. Gidden, J.; Denson, J.; Liyanage, R.; Ivey, D. M.; Lay Jr, J. O., Lipid Compositions in Escherichia Coli and Bacillus Subtilis During Growth as Determined by MALDI-TOF and TOF/TOF Mass Spectrometry. *Int. J. Mass Spectrom.* **2009,** *283* (1–3), 178-184.

282. Annesley, T. M., Ion Suppression in Mass Spectrometry. *Clin. Chem.* **2003,** *49* (7), 1041-1044.

283. Knochenmuss, R., Ion Formation Mechanisms in UV-MALDI. *Analyst* **2006,** *131* (9), 966-986.

284. Ho, Y. P.; Fenselau, C., Applications of 1.064 Mm Ir Laser Desorption on a Fourier Transform Mass Spectrometer. *Anal. Chem.* **1998,** *70* (23), 4890-4895.

285. Natali, B.; Jean-Claude, B.; Françoise, F.; Jean-Claude, T., Desorption/Ionization on Porous Silicon Mass Spectrometry (Dios) of Model Cationized Fatty Acids. *J. Mass Spectrom.* **2007,** *42* (1), 42-48.

286. Lewis, W. G.; Shen, Z. X.; Finn, M. G.; Siuzdak, G., Desorption/Ionization on Silicon (Dios) Mass Spectrometry: Background and Applications. *Int. J. Mass Spectrom.* **2003,** *226* (1), 107-116.

287. Thomas, J. J.; Shen, Z.; Crowell, J. E.; Finn, M. G.; Siuzdak, G., Desorption/Ionization on Silicon (Dios): A Diverse Mass Spectrometry Platform for Protein Characterization. *P. Natl. Acad. Sci. USA* **2001,** *98* (9), 4932-4937.

288. Wei, J.; Buriak, J. M.; Siuzdak, G., Desorption-Ionization Mass Spectrometry on Porous Silicon. *Nature* **1999,** *399* (6733), 243-246.

289. Kumar, P.; Huber, P., Effect of Etching Parameter on Pore Size and Porosity of Electrochemically Formed Nanoporous Silicon. *J. Nanomater.* **2007**.

290. Guenin, E.; Lecouvey, M.; Hardouin, J., Could a Nano-Assisted Laser Desorption/Ionization Target Improve the Study of Small Organic Molecules by Laser Desorption/Ionization Time-of-Flight Mass Spectrometry? *Rapid Commun. Mass Spectrom.* **2009,** *23* (9), 1395-1400.

291. Dowhan, W., Molecular Basis for Membrane Phospholipid Diversity: Why Are There So Many Lipids? *Annu. Rev. Biochem.* **1997,** *66*, 199-232.

292. Johnson, A. S.; van Horck, S.; Lewis, P. J., Dynamic Localization of Membrane Proteins in Bacillus Subtilis. *Microbiol.* **2004,** *150* (9), 2815-2824.

APPENDIX. LETTER OF PEMISSION

ACS Publications
High quality. High impact.

Book: Rapid Characterization of Microorganisms by Mass Spectrometry

Chapter: Matrix Assisted Laser Desorption Ionization Ion Mobility Time-of-Flight Mass Spectrometry of Bacteria

Author: Juaneka M. Hayes, Louis C. Anderson, J. Albert Schultz et al.

Publisher: American Chemical Society

Date: Jan 1, 2011

Copyright © 2011, American Chemical Society

Quick Price Estimate

I would like to... ❓   [▼]

Requestor Type ❓   [▼]

Portion ❓   [▼]

Format ❓   Print

Select your currency   [USD - $ ▼]

Quick Price   Click Quick Price

QUICK PRICE   CONTINUE

This service provides permission for reuse only. If you do not have a copy of the article you are using, you may copy and paste the content and reuse according to the terms of your agreement. Please be advised that obtaining the content you license is a separate transaction not involving Rightslink.

VITA

Juaneka M. Hayes was born in Montgomery, Alabama. She graduated with a Bachelor of Science degree in 2002 and a Master of Science degree in 2005 in chemistry from Florida Agricultural & Mechanical University (FAMU). During her tenure as a graduate student, at FAMU, Juaneka studied the electronic and protein structure of non-heme proteins using photoacoustic calorimetry and UV-vis absorption. She received the Florida-Georgia Alliance for Minority Participation Award and the Minority Biomedical Research Support Award while attending FAMU. Juaneka decided to pursue a terminal degree in Chemistry at Louisiana State University and selected Dr. Kermit K. Murray as her advisor. Her research involved the detection of microorganisms using MALDI and ion mobility mass spectrometry. While attending LSU, Juaneka was a member of the Chemistry Graduate Student Council, a student member of the American Chemical Society (ACS), American Society for Mass Spectrometry and the National Organization for the for the Advancement for the Black Chemists and Chemical Engineers, in which she served as parliamentarian. She has presented her research at several national conferences, including an invited talk at ACS. Juaneka is currently a candidate for Doctor of philosophy which will be awarded May 2013.